QUANTUM STATE RECONSTRUCTION IN QUANTUM OPTOMECHANICS

A Dissertation

by

SAEED MATER M ASIRI

Submitted to the Office of Graduate and Professional Studies of
Texas A&M University
in partial fulfillment of the requirements for the degree of

DOCTOR OF PHILOSOPHY

Chair of Committee,	M. Suhail Zubairy
Committee Members,	Philip Hemmer
	Olga Kocharovskaya
	Aleksei Zheltikov
Head of Department,	Grigory Rogachev

August 2018

Major Subject: Physics

ABSTRACT

The ability to perform mechanical states reconstruction is an essential task in quantum optomechanics to understand different quantum aspects of mechanical states of motion. Many interesting phenomena appear when the light and mechanical motion are coupled through the radiation-pressure coupling. Preparing, controlling, and measuring mechanical states are all very crucial in the study and development of quantum optomechanics. In this dissertation, we introduce a practical scheme for mechanical states reconstruction in the weak optomechancial coupling regime in which most optomechanical systems operates. The scheme relies on sending a beam of two-level atoms to pass through an optomechanical cavity where an oscillating mirror is coupled to a cavity field. The atoms interact resonantly with the cavity field as they pass through the cavity. As the oscillating mirror modifies the dynamics of the atoms, we show in this dissertation that by measuring the atomic population inversion of the atoms when they exit the optomechanical cavity, it is possible to obtain the mirror's state by analyzing the measured data of the population inversion.

In the first part of this dissertation, we study a hybrid system in which a two-level atom is placed inside a cavity field where one side of the cavity is free to move. The two-level atom is coupled to the cavity field through the well known Jaynes-Cummings coupling, whereas the mechanical mirror and the cavity field are coupled to each other via the radiation-pressure coupling. A complete analytical and numerical study is performed on this system, and it is shown that the mechanical mirror modifies the atomic population inversion in such a way that each mechanical state changes the signal of the population inversion of the atom differently. From the results in this part of the dissertation, we concluded that the population inversion can be analyzed and employed to extract the quantum state of the mechanical mirror.

Second, as each specific mechanical state affects the atomic population inversion differently, we developed the idea of using the atom as a tool to reconstruct the quantum state of the mechanical mirror. We first assumed that the two-level atom is initially in a superposition of its excited and ground states while both the cavity field and the mechanical mirror are in general superposi-

tion of Fock states with unknown coefficients. The derived general expression of the population inversion indicates that it is sufficient to initially prepare the atoms in the excited states before passing through the optomechancial cavity and the cavity field is in vacuum state. The population inversion of the atoms exiting the cavity can then be measured, and the collected data can be used to determine the full state of the mechanical mirror. The scheme in this part of the dissertation is only developed for measuring pure mechanical states.

Third, we extended the scheme of mechanical states reconstruction to the more practical states of the mirror in which the mirror is initially in a mixed state. We derived a general analytical solution of the population inversion allowing us to reconstruct more experimentally feasible states of the mechanical mirror such as thermal states.

DEDICATION

To my wife, my mother, and my father.

ACKNOWLEDGMENTS

First, I would like to thank my advisor Prof. M. Suhail Zubairy for his tremendous support, encouragement, and help during the years of working on my PhD at Texas A&M University. I also want to warmly thank him for making such a great and active research environment in his group. Knowledge and intuitive guidance of Prof. M. Suhail Zubairy made it possible for me to gain a great research experience in quantum optics. Following his valuable and wise advices, recommendations, and ideas while I was working under his supervision made the work presented in this dissertation possible to be accomplished.

Second, I would like to extend my thank and appreciation to my current and former colleagues and collaborators for their faithful discussions and collaboration. My thanks to my collaborators and colleagues Dr. Li-Gang Wang, Dr. M. Al-Amri, Dr. Jingping Xu, Dr. Wenchao Ge, Dr. Zeyang Liao, Dr. Xiaodong Zeng, and Dr. Longfei Fan.

Finally, I would like to thank my wife for her extraordinary support, encouragement, and patience during my PhD years. Her endless love, optimism, and dedication supported me toward this accomplishment. I should also not to forget to thank our son Haitham for all laughs and hugs I have been given form him during my PhD program.

CONTRIBUTORS AND FUNDING SOURCES

This work was supervised by a dissertation committee consisting of Prof. M. Suhail Zubairy [advisor] of the Department of Physics and Astronomy, Prof. Philip Hemmer of the Department of Electrical & Computer Engineering, Prof. Olga Kocharovskaya of the Department of Physics and Astronomy, and Prof. Aleksei Zheltikov of the Department of Physics and Astronomy. All work for the dissertation was conducted and completed independently by the student.

I would like to thank the government of the Kingdom of Saudi Arabia for giving me the opportunity to complete my PhD at Texas A&M University and for funding me during my stay in the United States. I also would like to thank King Abdulaziz City for Science and Technology (KACST) in Saudi Arabia and the Saudi Arabian Cultural Mission (SACM) in the United States for the financial support during the years of working on my PhD in the United States.

TABLE OF CONTENTS

Page

ABSTRACT ii

DEDICATION iv

ACKNOWLEDGMENTS v

CONTRIBUTORS AND FUNDING SOURCES vi

TABLE OF CONTENTS vii

LIST OF FIGURES ix

1. INTRODUCTION 1

    1.1 Quantum theory of atom-field interaction 3
    1.2 Cavity optomechanics 6

2. OPTOMECHANICALLY INDUCED ANOMALOUS POPULATION INVERSION IN A HYBRID SYSTEM 9

    2.1 Introduction 9
    2.2 The model 12
    2.3 Collapse and revival for an initial Fock state in the cavity 14
        2.3.1 Initial mechanical Fock states 14
            2.3.1.1 Zero atom-field detuning $\delta = 0$ 16
            2.3.1.2 Non-zero atom-field detuning $\delta \neq 0$ 18
        2.3.2 Initial mechanical coherent states 20
        2.3.3 Initial mechanical thermal states 23
    2.4 Collapse and revival for a coherent cavity field 26
    2.5 Conclusion 28

3. QUANTUM STATE RECONSTRUCTION OF A MECHANICAL MIRROR IN A HYBRID SYSTEM 30

    3.1 Introduction 30
    3.2 The model 32
    3.3 Excited state probability 34
    3.4 Quantum state reconstruction of the mechanical mirror 37
        3.4.1 Coherent state 40
        3.4.2 Arbitrary quantum state with phase 42

3.4.3 Squeezed vacuum state 44
3.4.4 Velocity fluctuation 46
3.4.5 Reconstruction of thermal state 46
3.5 Conclusion 50

4. QUANTUM STATE MEASUREMENT OF A MECHANICAL MIRROR 51

4.1 Introduction 51
4.2 Model 52
4.3 Population inversion of the atom 55
4.4 Reconstruction of mechanical mixed state 60
4.4.1 Reconstruction of mechanical pure state 61
4.4.2 Reconstruction of mechanical thermal state 63
4.4.3 Reconstruction of general density matrix 64
4.5 Conclusion 67

5. SUMMARY 68

REFERENCES 69

APPENDIX A. EFFECTIVE HAMILTONIAN 80

APPENDIX B. EQUATIONS OF MOTION FOR THE DENSITY MATRIX ELEMENTS 82

APPENDIX C. DERIVATION OF THE EXCITED STATE POPULATION WHEN THE MIRROR IS IN A THERMAL STATE 85

APPENDIX D. DERIVATION OF THE EXCITED STATE POPULATION FOR THE COHERENT CAVITY FIELD 88

APPENDIX E. DERIVATION OF THE EXCITED STATE POPULATION WHEN THE MIRROR IS IN A THERMAL STATE 90

LIST OF FIGURES

FIGURE Page

1.1 Atom-field interaction. 3

1.2 Population inversion as a function of time with $g_c = 1$ and $\delta = 0$. (a) Initial state of the cavity is a Fock state $|0\rangle$. (b) Initial state of the cavity is a coherent state with mean number of photons $< n >= 20$. 5

1.3 Schematic of an optomechanical system. 7

2.1 Schematic of the hybrid optomechanical system. 13

2.2 Population inversion as a function of time with $g_c = \omega_m/2$, $g_m = 0.04\omega_m$, and $\delta = 0$. (a) Analytical (solid) and numerical (without damping) (dashed) results with the initial state of the system $|e\rangle_a |0\rangle_c |0\rangle_m$. (b) Analytical (solid) and numerical (without damping) (dashed) results with the initial state of the system $|e\rangle_a |0\rangle_c |1\rangle_m$. (c) Numerical result with dissipation for otherwise the same situation as in (a). (d) Numerical result with dissipation for otherwise the same situation as in (b). The other parameters are $\gamma_a = 10^{-3}$, $\gamma_c = 10^{-3}\omega_m$, $\gamma_m = 10^{-5}\omega_m$, and $\bar{n}_{th} = 5$. 16

2.3 Population inversion as a function of time. (a) Analytical (solid) and numerical (without damping) (dashed) results with the initial state of the system $|e\rangle_a |0\rangle_c |2\rangle_m$. (b) Analytical (solid) and numerical (without damping) (dashed) results with the initial state of the system $|e\rangle_a |0\rangle_c |3\rangle_m$. (c) Numerical result with dissipation for otherwise the same situation as in (a). (d) Numerical result with dissipation for otherwise the same situation as in (b). The other parameters are the same as in Fig. 2.2. 17

2.4 Population inversion as a function of time for non-zero atom-field detuning $\delta = 0.95\omega_m$. (a) Analytical (solid) and numerical results with (dotted) and without (dashed) dissipation when the initial state of the system is $|e\rangle_a |0\rangle_c |0\rangle_m$. (b) Analytical (solid) and numerical results with (dotted) and without (dashed) dissipation when the initial state of the system is $|e\rangle_a |0\rangle_c |1\rangle_m$. The other parameters are $\gamma_a = \gamma_c = 10^{-3}\omega_m$, $\gamma_m = 10^{-5}\omega_m$, and $\bar{n}_{th} = 5$. 19

2.5 Population inversion as a function of time for non-zero atom-field detuning $\delta = 0.95\omega_m$ where the mechanical mirror is initially in a coherent state $|\gamma\rangle_m$. The initial state of the system is $|e\rangle_a |0\rangle_c |\gamma\rangle_m$. Mean number of phonons is (a) $|\gamma|^2 = 3$ and (b) $|\gamma|^2 = 6$. $\gamma_a = \gamma_c = 10^{-4}\omega_m$, $\gamma_m = 10^{-5}\omega_m$. The other parameters are the same as in Fig. 2.2. 21

2.6 Population inversion as a function of time where the mechanical mirror is initially in a mixed state. (a) Analytical (solid) and numerical (without damping) (dashed) results with mean number of thermal phonons $\bar{l} = 0.2$. (b) Analytical (solid) and numerical (without damping) (dashed) results with mean number of thermal phonons $\bar{l} = 0.6$. (c) Numerical result with dissipation for otherwise the same situation as in (a). (d) Numerical result with dissipation for otherwise the same situation as in (b). The other parameters are the same as in Fig. 2.2. 25

2.7 Population inversion as a function of time when the cavity field is initially in a coherent state $|\alpha\rangle_c$. Mean number of photons $|\alpha|^2 = 7$, $g_c = \omega_m/2\sqrt{s+1}$, $g_m = 0.02\omega_m$, $\delta = 0$, and $s = 7$. The initial state of the system is (a) $|e\rangle_a |\alpha\rangle_c |0\rangle_m$, (b) $|e\rangle_a |\alpha\rangle_c |1\rangle_m$, (c) $|e\rangle_a |\alpha\rangle_c |2\rangle_m$, and (d) $|e\rangle_a |\alpha\rangle_c |3\rangle_m$. The other parameters are the same as in Fig. 2.2. 27

3.1 Quantum state reconstruction using atom as detector in the hybrid optomechanical system..... 33

3.2 Reconstruction of initial mechanical coherent state. (a) Comparison between the exact and reconstructed probability distribution of phonons for two different values of l_{max} with $g_m/\omega_m = 0.07$. (b) Comparison between the exact and reconstructed probability distribution of phonons for two different coupling strength with $l_{max} = 12$. Mean number of phonons $\bar{l} = 3$. 41

3.3 Comparison between the exact and reconstructed probability distribution of phonons (a) and the phase difference $\Delta\varphi_{l+1}$ (b) where the initial state of the mechanical mirror is given by Eq. (3.21) for two different ratios between the optomechanical coupling g_m and the mechanical frequency ω_m..... 43

3.4 Comparison between the exact and reconstructed probability distribution of phonons (a) and the phase difference $\Delta\varphi_{l+2}$ (b) when the initial state of the mechanical mirror is squeezed vacuum for two different ratios between the optomechanical coupling g_m and the mechanical frequency ω_m. $r = 2$ and $\varphi = \pi/8$..... 45

3.5 Reconstruction of the initial state of the mechanical mirror when fluctuation in the interaction times between the atoms and the cavity field is considered. (a) Number of iterations is $N_{runs} = 10$. (b) Number of iterations is $N_{runs} = 30$. The average phonon number is $\bar{l} = 3$, $g_m/\omega_m = 0.9$, and the fluctuation in the interaction times is $\pm 2\%$. 47

3.6 Comparison between the exact and reconstructed phonon-number distributions for initially mechanical thermal state. (a) The comparison is made using $l_{max} = 6$ and $l_{max} = 10$ with $g_m/\omega_m = 0.07$. (b) The comparison is made for two different coupling strength ($g_m/\omega_m = 0.05$ and 0.09) with $l_{max} = 10$. (c) The comparison is made using two different values for the fluctuation in the interaction time, 4% and 2% with $g_m/\omega_m = 0.09$ and $l_{max} = 10$. Mean number of phonons is $\bar{l} = 2$. 49

4.1 Schematic of the mechanical state reconstruction model. Two level atoms in their excited states are sent to interact with the cavity field and the probability of finding the atoms in the excited state $P_e(t)$ is measured when the atoms are exciting the cavity. 53

4.2 Atomic population inversion as a function of time for initial mechanical Fock state (a) $\rho^m(0) = |0\rangle\langle 0|$ and (b) $\rho^m(0) = |2\rangle\langle 2|$. We considered resonant atom-field interaction ($\delta = 0$), $g_c = \omega_m/2$, and $g_m = 0.05\omega_m$. 58

4.3 Atomic population inversion as a function of time for initial mechanical thermal state for two different mean number of thermal phonons (a) $\bar{l} = 0.5$ and (b) $\bar{l} = 1.5$. We considered resonant atom-field interaction ($\delta = 0$), $g_c = \omega_m/2$, and $g_m = 0.05\omega_m$. 59

4.4 Reconstruction of the density matrix elements for initially pure mechanical states. (a-c) Initial mechanical state is $\psi(0) = |0\rangle$ state. (d-f) Initial mechanical state is $\psi(0) = 1/\sqrt{2}\big(|1\rangle + |2\rangle\big)$ state. (a) and (d) Exact density matrix elements. (b) and (e) The reconstructed density matrix elements when the interaction time has 2% fluctuation. (f) and (g) The reconstructed density matrix elements when the interaction time has 4% fluctuation. Other parameters are $g_m/\omega_m = 0.05$ and $N_{runs} = 30$. 62

4.5 Comparison between the exact and reconstructed phonon-number distributions for initially mechanical thermal state. (a) The comparison is made using $l_{max} = 10$ and $l_{max} = 14$ with $g_m/\omega_m = 0.06$. (b) The comparison is made using two different values for the fluctuation in the interaction time, 4% and 2% with $g_m/\omega_m = 0.09$ and $l_{max} = 15$. Mean number of phonons is $\bar{l} = 3$ in both subfigures. 65

4.6 Reconstruction of a general density matrix. (a) The exact density matrix elements to be reconstructed. (b) Reconstruction of the density matrix elements when the interaction time has 2% fluctuation. (c) Reconstruction of the density matrix elements when the interaction time has 4% fluctuation. 66

1. INTRODUCTION

The Jaynes-Cummings (JC) model [1, 2, 3, 4] describes the interaction between a single mode quantized field and a single two-level atom. The JC-model predicted the collapse and revival in the signal of the population inversion when the cavity field is prepared initially in a coherent state. Many extensions for this interesting model have been made since its development such as the study of the population inversion in a two-level atomic system interacting with a squeezed state electromagnetic field [5], a two-level atom initially prepared in a coherent superposition interacting with a quantized field [6], three-level atom interacting with a single mode quantized field [7], for time-dependent cavity frequency [8, 9].

In the recent years, the area of cavity optomechanics [10] in which the mechanical motion is coupled to electromagnetic fields through the radiation-pressure coupling has been extended and developed to many interesting areas of research. Applications in the area of cavity optomechanics are rapidly expanding for example to quantum information [11], high sensitivity displacement measurement [12], ground state cooling [13, 14, 15, 16, 17, 18, 19, 20, 21], macroscopic superposition [22, 23, 24, 25], and quantum entanglement [26, 27, 28, 29, 30, 31, 32, 33, 34, 35, 36, 37] in optomechanical systems.

In cavity optomechanics, mechanical state reconstruction refers to the ability to perform some series of measurements to determine the state of a mechanical oscillator. Mechanical state reconstruction allows for significant understand and characterization for different quantum properties in optomechanical systems. Few schemes for mechanical state reconstruction have recently been introduced [38, 39, 40, 41]. In [40], a mechanical oscillator is strongly coupled to a cavity light field where photons can leak outside. Measuring the emission and scattering spectra enables extracting the oscillator's state as the oscillator strongly imprints its state on the measured spectrum. The scheme introduced in [41] relies on creating a coupling between an atoms and a mechanical oscillator using a magnetic field. The Wigner function of the oscillator can then be measured by measuring the ground state population of the atom.

In this dissertation, we propose an atom-based measurement method to reconstruct the quantum state of a mechanical oscillator. We consider a cavity field weakly coupled to a mechanical mirror via the radiation-pressure force. We then consider a beam of two-level atoms initially prepared in the excited state to enter an optomechanical cavity and interact resonantly with a vacuum cavity field. The population inversion of the atoms can be measured after they exit the cavity. Due to the optomechanical coupling, the dynamics of the atoms are modified in such a way that each specific mechanical state leads to a distinct change in the atomic population inversion. Therefore the measured data of the population inversion can be used to extract the state of the mechanical mirror.

This dissertation is organized as follows: In Chapter 1, I give a brief review of the quantum theory of atom-field interaction followed by a general overview of the area of quantum optomechanics.

In Chapter 2, the atomic population inversion of a two-level atom placed inside an optomechanical cavity is studied analytically and numerically. We considered different initial conditions for the cavity field and the mechanical mirror. It is shown that the oscillating mirror significantly modifies the population inversion signal in comparison to the case of the Jaynes-Cummings model where the two-level atom is placed inside a cavity in which both of its sides are fixed. The results shown in this chapter motivate us to develop an atom-based scheme to measure the quantum state of the mechanical mirror.

In Chapter 3, a scheme for the reconstruction of pure mechanical states is introduced. The scheme contains a beam of initially excited two-level atoms sent to pass through an optomechanical cavity. The atoms interact with a vacuum cavity field as they pass through the optomechanical cavity, and the population inversion is measured upon exciting the atoms from the other side of the cavity. As different mechanical states result in different signals of the population inversion, it is shown that a mathematical data analysis of the population inversion can be used to reconstruct the full state of the mechanical mirror.

In Chapter 4, an extension of the work presented in the previous chapter to the general and more

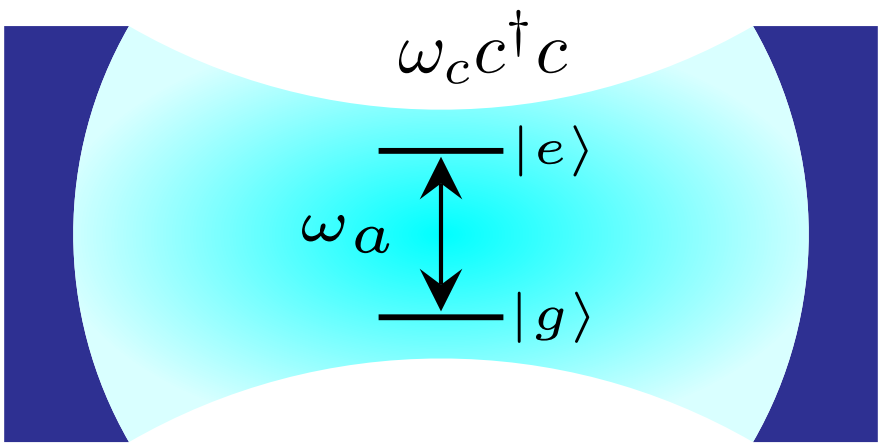

Figure 1.1: Atom-field interaction.

practical case where the mechanical mirror is initially considered in a mixed state. It is shown that the density matrix elements of the state of the mechanical mirror can be reconstructed using this scheme.

In Chapter 5, summaries and conclusions of the results and new findings in this dissertation are given.

1.1 Quantum theory of atom-field interaction

Here we provide brief description and derivation of the JC-model as it is related to the work presented in this dissertation. In the JC-model, a single two-level atom is set to interact with a single mode quantized electromagnetic field as shown in Fig. 1.1. $|e\rangle$ is the excited state of the two-level atom and $|g\rangle$ is the ground state with a transition frequency ω_a between both levels. The Hamiltonian of the system shown in Fig. 1.1 is explicitly given by [42]

$$\mathcal{H} = \hbar\omega_c c^\dagger c + \frac{1}{2}\hbar\omega_a\sigma_z + \hbar g_c(c^\dagger\sigma_- + \sigma_+ c) \tag{1.1}$$

where the first term in Eq. (1.1) describes the cavity field Hamiltonian with ω_c is the resonance frequency of the cavity and $c^\dagger$ (c) is the creation(annihilation) operator of the cavity field. The second term in Eq. (1.1) represents the two-level atom Hamiltonian with $\sigma_z = |e\rangle\langle e| - |g\rangle\langle g|$.

The third term in equation Eq. (1.1) describes the interaction energy between the two-level atom and the cavity field with coupling strength g_c. $\sigma_+ = |e\rangle\langle g|$ is the raising operator of the atom and $\sigma_- = |g\rangle\langle e|$ is the lowering operator of the atom.

In the interaction picture, the Hamiltonian Eq. (1.1) can be calculated from

$$\mathcal{V} = e^{i\mathcal{H}_0 t/\hbar}\, \mathcal{H}_{int}\, e^{-i\mathcal{H}_0 t/\hbar}, \tag{1.2}$$

where $\mathcal{H}_0 = \hbar\omega_c c^\dagger c + \frac{1}{2}\hbar\omega_a\sigma_z$ and $\mathcal{H}_{int} = \hbar g_c(c^\dagger\sigma_- + \sigma_+ c)$, are the free part and the interaction part of the system's Hamiltonian, respectively. Simple calculations of Eq. (1.2) gives the following expression for the interaction picture Hamiltonian

$$\mathcal{V} = \hbar g_c(\sigma_+ c\, e^{i\delta t} + c^\dagger\sigma_-\, e^{-i\delta t}), \tag{1.3}$$

where $\delta = \omega_a - \omega_c$.

The time-dependent state of the total system can be written as [42]

$$|\psi(t)\rangle = \sum_{n=0}^{\infty} c_{e,n}(t)\,|e,n\rangle + c_{g,n+1}(t)\,|g,n+1\rangle\,, \tag{1.4}$$

where $c_{e,n}(t)$ is the probability amplitude for the atom to be in its excited state with n photons in the cavity while $c_{g,n+1}(t)$ is the probability amplitude for the atom to be in the ground state with $n+1$ photons in the cavity. The system's dynamics can be studied using the time-dependent Schrödinger's equation which is given by

$$|\dot{\psi}\rangle = -\frac{i}{\hbar}\mathcal{V}\,|\psi\rangle\,. \tag{1.5}$$

Equations of motion for the probability amplitudes can be derived from Schrödinger's equation.

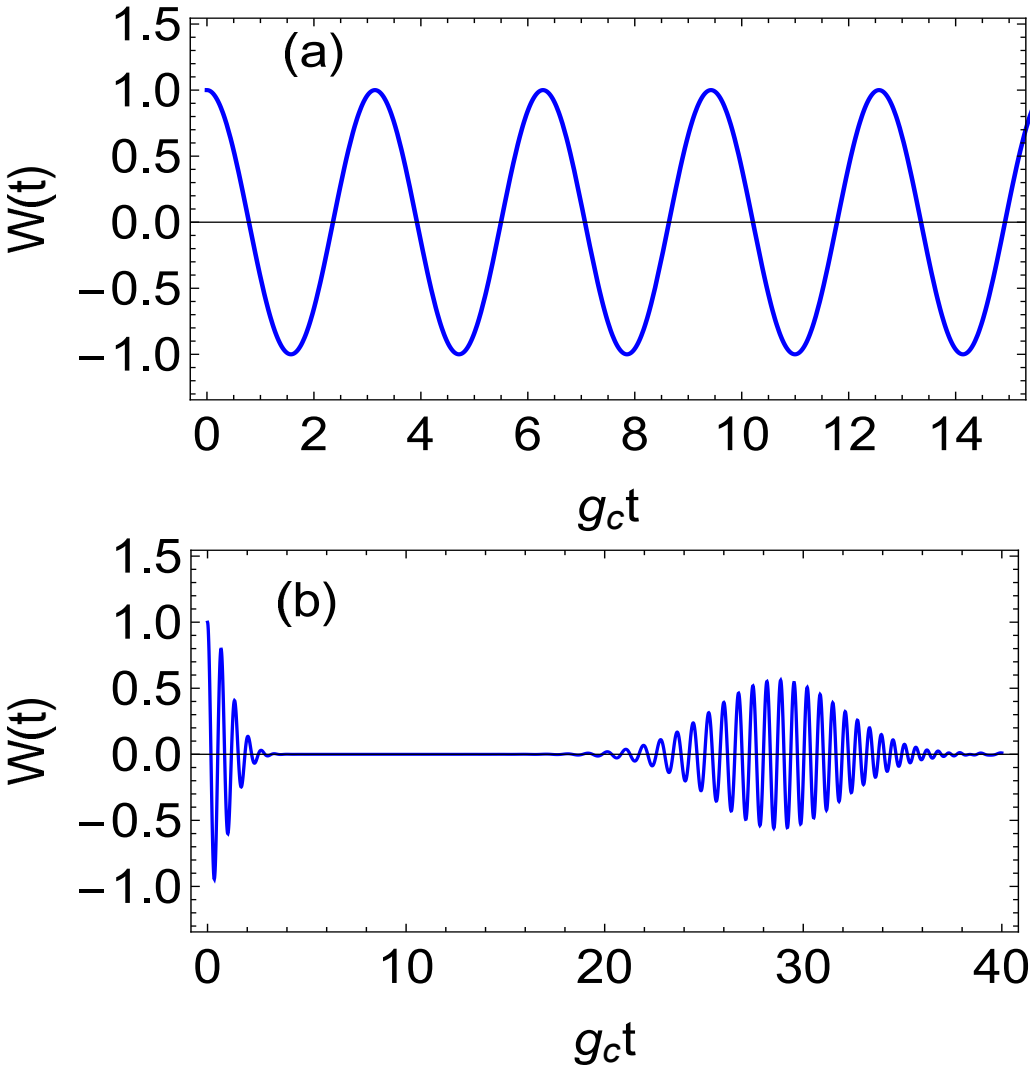

Figure 1.2: Population inversion as a function of time with $g_c = 1$ and $\delta = 0$. (a) Initial state of the cavity is a Fock state $|0\rangle$. (b) Initial state of the cavity is a coherent state with mean number of photons $< n >= 20$.

The equations of motion for the probability amplitudes are given by [42]

$$\dot{c}_{e,n}(t) = -ig_c\sqrt{n+1}\, e^{i\delta t} c_{g,n+1}(t), \tag{1.6a}$$

$$\dot{c}_{g,n+1}(t) = -ig_c\sqrt{n+1}\, e^{-i\delta t} c_{e,n}(t). \tag{1.6b}$$

Let us first consider the case when the cavity field is initially in a Fock state $|n\rangle$ while the two-level

atom is in the excited state. Subject to these initial conditions, Eqs. (1.6) can be solved and the resultant expression of the population inversion is given by

$$W(t) = |c_{e,n}(t)|^2 - |c_{g,n}(t)|^2 = \cos(\Omega_n t), \tag{1.7}$$

where $\Omega_n = 2g_c\sqrt{n+1}$. The population inversion in this case is obviously oscillating periodically as seen in Fig. 1.2(a).

When the cavity field is initially in a coherent state while the atom is in the excited state, the population inversion is given by

$$W(t) = \sum_{n=0}^{\infty} \left[|c_{e,n}(t)|^2 - |c_{g,n}(t)|^2 \right] = \sum_{n=0}^{\infty} p_n \cos(\Omega_n t), \tag{1.8}$$

where

$$p_n = \frac{\langle n \rangle^n e^{-\langle n \rangle}}{n!}, \tag{1.9}$$

is the coherent state distribution of the photons with $\langle n \rangle$ being the mean number of photons. As shown in Fig. 1.2(b), the population inversion collapses for certain time and then starts to revives. This can be understood from having the summation in Eq. (1.8) over many terms where each term has a different oscillation frequency and this leads to constructive and destructive interference between these terms.

1.2 Cavity optomechanics

The fundamental optomechanical system in cavity optomechanics consists of a cavity with one mirror fixed at one end and an oscillating mirror at the other end of the cavity as shown in Fig. 1.3. The cavity field is coupled to the mechanical mirror via the radiation-pressure force [10].

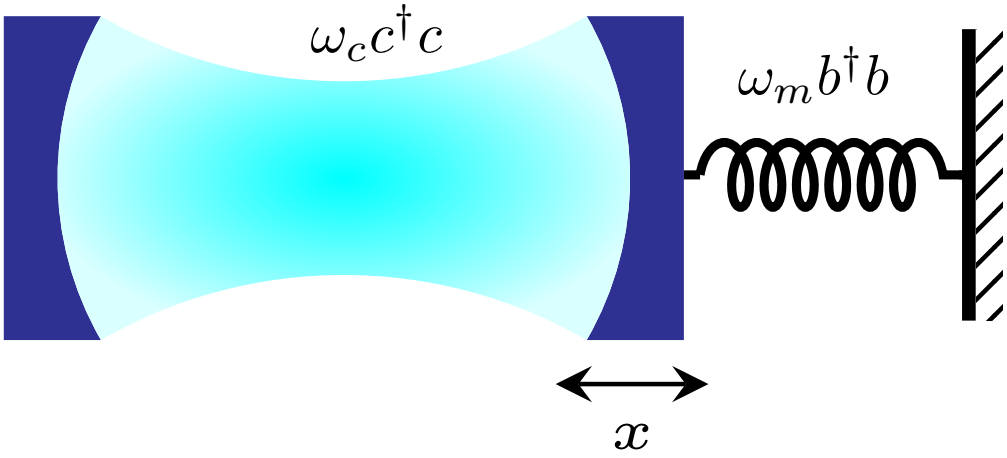

Figure 1.3: Schematic of an optomechanical system.

We consider that the length of the cavity in Fig. 1.3 is L and its resonance frequency is ω_c. Let's also consider the mechanical mirror is oscillating at frequency ω_m and its mass is denoted as m. Due to the oscillation of the mechanical mirror, length of the cavity field changes accordingly and becomes position dependent, i.e. $\omega_c(x)$. Position of the mechanical mirror is defined as $x = x_0(b + b^\dagger)$ where $b^\dagger(b)$ is the creation (annihilation) operator of the mechanical mirror. x_0 represents the zero-point motion or fluctuation of the oscillating mirror and in terms of the mass and frequency of the mechanical mirror, it is defined as $x_0 = \sqrt{\hbar/2m\omega_m}$. With all these definitions, the Hamiltonian of the optomechanical system depicted in Fig. 1.3 can be written as

$$\mathcal{H} = \hbar\omega_c(x)c^\dagger c + \hbar\omega_m b^\dagger b, \tag{1.10}$$

where the first term in Eq. (1.10) describes the cavity field Hamiltonian while the second term describes the Hamiltonian of the oscillating mirror. $c^\dagger(c)$ is the cavity field creation (annihilation) operator. Taylor expansion of the frequency of the cavity gives

$$\omega_c(x) = n\frac{\pi c}{L + x} = \omega_c + \frac{\partial\omega_c}{\partial x}x + ... = \omega_c - \omega_c\frac{x}{L} + ... \tag{1.11}$$

As the change of the cavity length is very small, the first and second terms in the previous equation can be kept and the higher order terms can be neglected. By using the expansion of the cavity field frequency in Eq. (1.11), the Hamiltonian of the optomechanical system Eq. (1.10) can be rewritten as

$$\mathcal{H} = \hbar\omega_c c^\dagger c + \hbar\omega_m b^\dagger b - \hbar g_m c^\dagger c(b^\dagger + b), \tag{1.12}$$

where

$$g_m = \frac{\omega_c}{L}\sqrt{\frac{\hbar}{2m\omega_m}}. \tag{1.13}$$

is optomechanical coupling strength defined in terms of the cavity and mechanical mirror variables.

2. OPTOMECHANICALLY INDUCED ANOMALOUS POPULATION INVERSION IN A HYBRID SYSTEM*

2.1 Introduction

The quantum mechanical description of the interaction between a two-level atom and a single mode field is known as the Jaynes-Cummings (JC) model [1]. Collapse and revival of the atomic population inversion, a pure quantum effect, was predicted theoretically [2] and demonstrated experimentally [3, 4] using the JC model.

The atomic population inversion in the JC model has been extended to a variety of schemes. For example, for a three-level atom interacting with a quantized field [7], for a time dependent atom-field coupling strength [43], for a time-varying cavity frequency with [8] and without [9] the rotating wave approximation, and for double two-level atoms that interact with a two-mode quantized field [44]. Effects of amplitude dissipation and phase dissipation on the population inversion have also been investigated [45, 46, 47, 48].

Recently, cavity optomechanics [10], which describes the radiation-pressure interaction between electromagnetic fields and mechanical motions, has developed into a promising area of research. Motivated by quantum information processing [11], testing quantum mechanics [49], and sensitive measurements [12], quantum state engineering of a mechanical oscillator, such as ground state [13, 14, 15, 16, 17], Fock state [15, 19], and squeezed state [50, 51, 52, 53, 54], have been proposed theoretically and achieved experimentally.

More recently, hybrid optomechanical systems have been studied, aiming at harnessing the advantages of different quantum systems to novel quantum technologies [55]. Specifically, cavity optomechanics with atomic ensembles have been investigated for macroscopic entanglement [30, 56, 31], ground-state cooling [57, 58, 59, 60], and optomechanical coupling enhancement [61]. For a cavity optomechanical system with a single atom, atom-field-mirror tripartite coupling [62],

*Reprinted with permission from "Optomechanically induced anomalous population inversion in a hybrid system" by S. Asiri, W. Ge, and M. S. Zubairy, 2018. J. Phys. A: Mathematical and Theoretical, Accepted Manuscript online 4 April 2018, copyright [2018] IOP Publishing. Reproduced with permission. All rights reserved.

strong atom-mirror coupling [63], atom-assisted strong coupling [64], atom-assisted cooling [65], and nonlinear coherent state preparation [66] have been explored.

In this chapter, we present a study on the atomic population inversion of a single two-level atom that is coupled to an optomechanical cavity, extending the JC model in the newly developed area of hybrid optomechanics. The Hamiltonian of the hybrid optomechanical system has been studied recently [67] on the phonon number statistics of a mechanical mirror in the presence of an artificial two-level atom. Here we are interested in the opposite effect where the atomic population is affected by the mechanical mirror.

Recently, there is a related work [68] on suppression of Rabi oscillations in a hybrid optomechanical system using the same initial Hamiltonian as in this manuscript. In comparison to [68], our work has the following differences: (i) On the contrary to Ref. [68], where single-photon strong coupling is required for exotic features, we focus on the experimental accessible regime of single-photon weak coupling, i. e., $\omega_m \gg g_m$. (ii) In Ref. [68], the study is mostly focused on the initial state $|e\rangle_a |0\rangle_c |0\rangle_m$, while in this work we consider a variety of different initial states, both pure and mixed. (iii) In the current work, the population inversion exhibits different features than suppression of Rabi oscillations reported in [68]. For example, we have observed both optomechanically induced collapses and oscillations in the population inversion. (iv) We present both analytical derivations and numerical calculations to explore different features, while in Ref. [68] the study on suppression of Rabi oscillations is only carried out with numerical calculations.

In the classical limit, the radiation-pressure coupling between a cavity field and a mechanical mirror results in a time-dependent cavity frequency [8]. Here we investigate the effect of optomechanical coupling on the population inversion when the mechanical mirror is in a quantum state. Our results may be useful for identifying the initial state of a mechanical mirror from different characteristics in the population invesion [69].

We study the anomalous effects in two different cases. In the first case, we study the interaction between initially excited two-level atom and a Fock state cavity field coupled to a mechanical mirror. For the resonant atom-field interaction, we show that the atomic population inversion can

exhibit collapses and revivals induced by the mechanical mirror when it is initially in a Fock state. This is drastically different from the JC model which predicts Rabi oscillations for a Fock state cavity field. The first collapse region becomes more apparent when the mirror is in a higher number state. For the far-detuned atom-field interaction, we first show that the atomic population inversion can undergo full Rabi oscillations between the excited state and the ground state of the atom by coupling to a Fock state of the mechanical mirror. Under this situation, the atom couples effectively to the mirror via the resonant JC interaction with the help of the cavity field. We further investigate this effective interaction by considering an initial coherent state of the mechanical mirror, and we find that collapse and revival feature similar to the JC model is observed. For a more realistic situation, we consider the case when the mechanical mirror is initially in a mixed state and we find that the mixture of the mechanical states induces slower collapse and reduced revival amplitude in the population inversion. In the second case, we consider the population inversion when the cavity field is in a coherent state and the mechanical mirror is in a Fock state. We show that the first collapse region in the JC model displays non-collapsed behavior induced by the mechanical mirror and the revival amplitude is reduced as well.

Our model is quite generic, therefore it can be implemented in different hybrid optomechanical systems, such as a superconducting qubit coupled to superconducting circuits [70]. With recent developments in preparing quantum states of a mechanical oscillator [13, 14, 15, 16, 17, 19, 50, 51, 52, 53, 54] and demonstrations on long cavity and atomic coherence time [10, 71], our predications in a hybrid optomechanical system may be possible with experimental demonstration.

This chapter is organized as follows: In Sec. 2.2, we introduce the model. In Sec. 2.3, we investigate the collapse-revival phenomena when the cavity field is initially in a Fock state, while the mechanical mirror is in a Fock state or a coherent state. In Sec. 2.4, we present an analytical and numerical solutions for the hybrid optomechanical system when the cavity field is initially in a coherent state and the mechanical mirror is in a Fock state. In Sec. 2.5, we summarize our results.

2.2 The model

We consider a hybrid optomechanical system that consists of a two-level atom and a cavity with a mechanical mirror at one end, as illustrated in Fig. (2.1). The cavity field is coupled to the two-level atom and the mechanical mirror via Jaynes-Cummings coupling and radiation-pressure coupling, respectively. In our model, the atom is prepared in the excited state $|e\rangle_a$ initially and passed through the cavity to interact with the cavity field for a certain amount of time. We are interested in the population inversion of the atom as a function of time in the presence of the mechanical mirror for different initial states of the cavity and the mirror.

The Hamiltonian of the hybrid system is given by [67]

$$\mathcal{H}_s = \mathcal{H}_0 + \mathcal{H}_1, \tag{2.1}$$

where $\mathcal{H}_0$ is the free Hamiltonian and $\mathcal{H}_1$ is the interaction Hamiltonian of the system. The free Hamiltonian is explicitly given by

$$\mathcal{H}_0 = \hbar\omega_c c^\dagger c + \hbar\frac{\omega_a}{2}\sigma_z + \hbar\omega_m b^\dagger b, \tag{2.2}$$

where ω_c is the cavity resonant frequency, ω_a is the atomic transition frequency, and ω_m is the oscillation frequency of the mechanical mirror. The operator b (c) is the annihilation operator of the phonon (photon) number, and $\sigma_z = |e\rangle_{a\,a}\langle e| - |g\rangle_{a\,a}\langle g|$ is the population inversion operator of the two-level atom. Here $|g\rangle_a$ is the ground state of the atom. The interaction Hamiltonian is written as

$$\mathcal{H}_1 = -i\hbar g_c(\sigma_+ c - c^\dagger\sigma_-) - \hbar g_m c^\dagger c(b^\dagger + b), \tag{2.3}$$

where the first term describes the Jaynes-Cummings coupling between the cavity field and the two-level atom [42] while the second term is the radiation-pressure coupling between the cavity field and the mechanical mirror [72]. The atom-field (mirror-field) coupling strength is g_c (g_m).

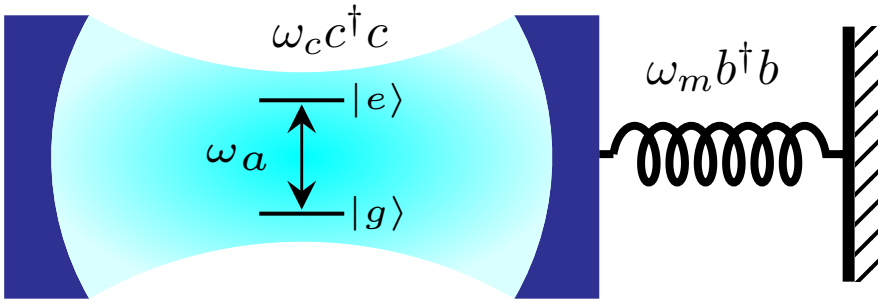

Figure 2.1: Schematic of the hybrid optomechanical system.

The mirror-field coupling strength is defined as $g_m = \frac{\omega_c}{L}\sqrt{\frac{\hbar}{2m\omega_m}}$ where L is the cavity length. $\sigma_+ = |e\rangle_{a\,a}\langle g|$ and $\sigma_- = |g\rangle_{a\,a}\langle e|$ are the atomic transition operators.

According to the time-dependent Shrödinger's equation, the state vector of the hybrid system, $|\psi_s\rangle$, evolves as

$$|\dot{\psi}_s\rangle = -\frac{i}{\hbar}\mathcal{H}_s\,|\psi_s\rangle\,. \tag{2.4}$$

Here we neglect the decoherence of the system for simplicity. The dissipation of the system will be considered in the numerical simulation using the master equation approach (see Appendix B).

To study the evolution of the system in a simpler way, we apply some mathematical procedures [25]. Recently, a different operator approach was presented in Ref. [73]. Here our method is more suitable for analyzing the population inversion in the atom-field polariton basis as discussed below.

As presented in Appendix A, we obtain an effective Hamiltonian of the hybrid system in the transformed picture given by $\mathcal{T} = e^{-\beta c^\dagger c(b^\dagger - b)}$ with $\beta = g_m/\omega_m$. After some procedures, the effective Hamiltonian is then given by

$$\mathcal{H}_\mathcal{T} = \sum_{n=1}^{\infty}\left(\hbar\frac{\Omega_n}{2}\sigma_z^{(n)} + \hbar g_{pn}(\sigma_-^{(n)} - \sigma_+^{(n)})(b^\dagger - b)\right) + \hbar\omega_m b^\dagger b, \tag{2.5}$$

where $\sigma_z^{(n)}$ and $\sigma_\mp^{(n)}$ are the polariton Pauli matrices for the polariton states $|\pm, n\rangle$ of the atom and the cavity field (see Appendix A), and $\Omega_n = \sqrt{\delta^2 + 4g_c^2(n+1)}$ is the polariton energy with $\delta = \omega_a - \omega_c$, and $g_{pn} = \beta g_c\sqrt{n+1}$ is the effective polariton-phonon coupling strength. This

effective Hamiltonian will be used throughout this chapter for the interactions among the tripartite. Therefore, it is clear from the effective Hamiltonian that for a particular polariton state $|\pm, n\rangle$, the mechanical mirror couples to these states similar to the JC model.

In the absence of the mechanical mirror, the Hamiltonian is reduced to the JC coupling in the atom-photon dressed state by taking $g_m = 0$, i. e., $g_{pn} = 0$. In the presence of the mechanical mirror, we will show in this chapter interesting results for the atomic population inversion even if $g_{pn} \ll \Omega_n$. Under the condition $\omega_m + \Omega_n \gg g_{pn} \gg |\omega_m - \Omega_n|$, we apply rotating-wave approximation and the transformed Hamiltonian is reduced to

$$\mathcal{H}_{\mathcal{T}} = \sum_{n=1}^{\infty} \left[\hbar \frac{\Omega_n}{2} \sigma_z^{(n)} + \hbar g_{pn} (\sigma_-^{(n)} b^\dagger + \sigma_+^{(n)} b) \right] + \hbar \omega_m b^\dagger b. \tag{2.6}$$

Under the effective Hamiltonian $\mathcal{H}_{\mathcal{T}}$, the transformed state vector is defined as $|\psi_T\rangle = \mathcal{T} |\psi_s\rangle$ where

$$|\dot{\psi}_T\rangle = -\frac{i}{\hbar} \mathcal{H}_{\mathcal{T}} |\psi_T\rangle . \tag{2.7}$$

is the time-dependent Schrodinger's equation.

2.3 Collapse and revival for an initial Fock state in the cavity

2.3.1 Initial mechanical Fock states

We first consider the cavity field is initially in a Fock state $|n\rangle_c$, and the mechanical mirror is in a Fock state $|l\rangle_m$, namely $|\psi_s(0)\rangle = |e\rangle_a |n\rangle_c |l\rangle_m$. In the transformed picture, the initial state is given by

$$\begin{aligned} |\psi_T(0)\rangle &= e^{-\beta n (b^\dagger - b)} |e\rangle_a |n\rangle_c |l\rangle_m \\ &\approx |e\rangle_a |n\rangle_c \left(|l\rangle_m - \beta n \sqrt{l+1} |l+1\rangle_m + \beta n \sqrt{l} |l-1\rangle_m \right) \\ &= \left[\cos\left(\frac{\alpha_n}{2}\right) |+, n\rangle + \sin\left(\frac{\alpha_n}{2}\right) |-, n\rangle \right] \left(|l\rangle_m - \beta n \sqrt{l+1} |l+1\rangle_m + \beta n \sqrt{l} |l-1\rangle_m \right) . \end{aligned} \tag{2.8}$$

From Eq. (2.6), we see that the effective Hamiltonian $\mathcal{H}_{\mathcal{T}}$ transfers one phonon between the polariton state, therefore the time-dependent state vector is given by

$$|\psi_T(t)\rangle = \sum_{k=l-2}^{l+1} c_k^+ |+,n\rangle |k\rangle + \sum_{k=l-1}^{l+2} c_k^- |-,n\rangle |k\rangle , \tag{2.9}$$

where $c_{l-2}^+(0) = 0$, $c_{l-1}^+(0) = \cos\left(\frac{\alpha_n}{2}\right)\beta n\sqrt{l}$, $c_{l-1}^-(0) = \sin\left(\frac{\alpha_n}{2}\right)\beta n\sqrt{l}$, $c_l^-(0) = \sin\left(\frac{\alpha_n}{2}\right)$, $c_l^+(0) = \cos\left(\frac{\alpha_n}{2}\right)$, $c_{l+1}^-(0) = -\sin\left(\frac{\alpha_n}{2}\right)\beta n\sqrt{l+1}$, $c_{l+1}^+(0) = -\cos\left(\frac{\alpha_n}{2}\right)\beta n\sqrt{l+1}$, and $c_{l+2}^-(0) = 0$. We derive from Schrödinger's equation (2.7) the time-dependent solutions of the coefficients as

$$c_k^+(t) = e^{-i\omega_m(k+\frac{1}{2})t}\Big[c_k^+(0)\cos\Big(g_{pn}\sqrt{k+1}t\Big) - ic_{k+1}^-(0)\sin\Big(g_{pn}\sqrt{k+1}t\Big)\Big], \tag{2.10a}$$

$$c_{k+1}^-(t) = e^{-i\omega_m(k+\frac{1}{2})t}\Big[c_{k+1}^-(0)\cos\Big(g_{pn}\sqrt{k+1}t\Big) - ic_k^+(0)\sin\Big(g_{pn}\sqrt{k+1}t\Big)\Big], \tag{2.10b}$$

where we consider $\Omega_n = \omega_m$ for simplicity. The excited state population of the atom is given by

$$P_e(t) = \sum_{k=l-2}^{l+2} \left| c_k^+(t)\cos\left(\frac{\alpha_n}{2}\right) + c_k^-(t)\sin\left(\frac{\alpha_n}{2}\right)\right|^2. \tag{2.11}$$

By substituting the expression of $c_k^+(t)$ and $c_k^-(t)$ from Eqs. (2.10), we find the population of the excited state $|e\rangle_a$ is

$$\begin{aligned} P_e(t) \approx & \sin^2\left(\frac{\alpha_n}{2}\right)\left[\cos^2\left(\frac{\alpha_n}{2}\right)\sin^2\left(g_{pn}\sqrt{l}t\right) + \sin^2\left(\frac{\alpha_n}{2}\right)\cos^2\left(g_{pn}\sqrt{l}t\right)\right] \\ & + \cos^2\left(\frac{\alpha_n}{2}\right)\left[\cos^2\left(\frac{\alpha_n}{2}\right)\cos^2\left(g_{pn}\sqrt{l+1}t\right) + \sin^2\left(\frac{\alpha_n}{2}\right)\sin^2\left(g_{pn}\sqrt{l+1}t\right)\right] \\ & + 2\cos(\omega_m t)\sin^2\left(\frac{\alpha_n}{2}\right)\cos^2\left(\frac{\alpha_n}{2}\right)\cos\left(g_{pn}\sqrt{l}t\right)\cos\left(g_{pn}\sqrt{l+1}t\right), \end{aligned} \tag{2.12}$$

where we have omitted higher-order terms $\mathcal{O}(\beta n)$ for $\beta n \ll 1$. The expression of $P_e(t)$ shows the feature of polariton interference represented by the cross product $\sin^2\left(\frac{\alpha_n}{2}\right)\cos^2\left(\frac{\alpha_n}{2}\right)$ in the last

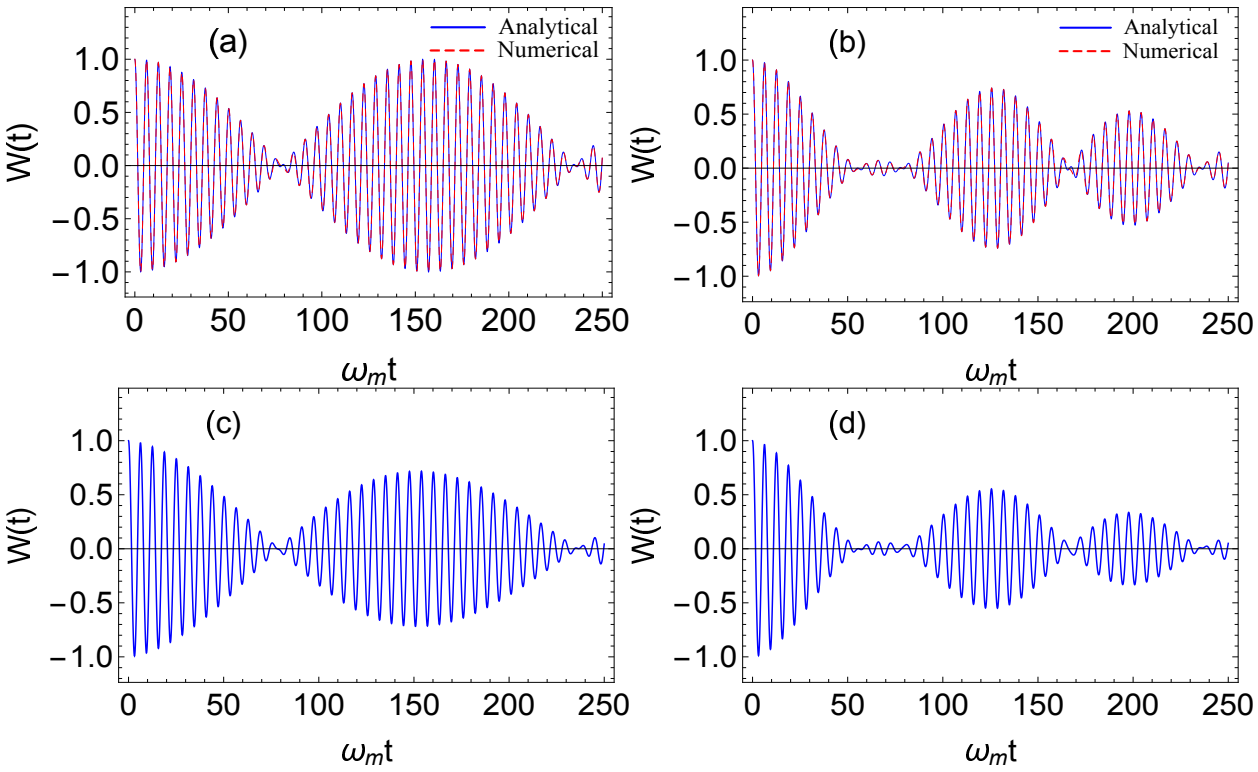

Figure 2.2: Population inversion as a function of time with $g_c = \omega_m/2$, $g_m = 0.04\omega_m$, and $\delta = 0$. (a) Analytical (solid) and numerical (without damping) (dashed) results with the initial state of the system $|e\rangle_a |0\rangle_c |0\rangle_m$. (b) Analytical (solid) and numerical (without damping) (dashed) results with the initial state of the system $|e\rangle_a |0\rangle_c |1\rangle_m$. (c) Numerical result with dissipation for otherwise the same situation as in (a). (d) Numerical result with dissipation for otherwise the same situation as in (b). The other parameters are $\gamma_a = 10^{-3}$, $\gamma_c = 10^{-3}\omega_m$, $\gamma_m = 10^{-5}\omega_m$, and $\bar{n}_{th} = 5$.

line in Eq. (2.12).

Since we have the expression of the population in the excited state, the population inversion is given by $W(t) = 2P_e(t) - 1$. Now we consider two limiting cases for our model.

2.3.1.1 Zero atom-field detuning $\delta = 0$

When $\delta = 0$, $\sin\left(\frac{\alpha_n}{2}\right) = \cos\left(\frac{\alpha_n}{2}\right) = \frac{1}{\sqrt{2}}$. Therefore, the population is reduced to

$$P_e(t) = \frac{1}{2} + \frac{1}{2}\cos(\omega_m t)\cos\left(g_{pn}\sqrt{l}t\right)\cos\left(g_{pn}\sqrt{l+1}t\right). \tag{2.13}$$

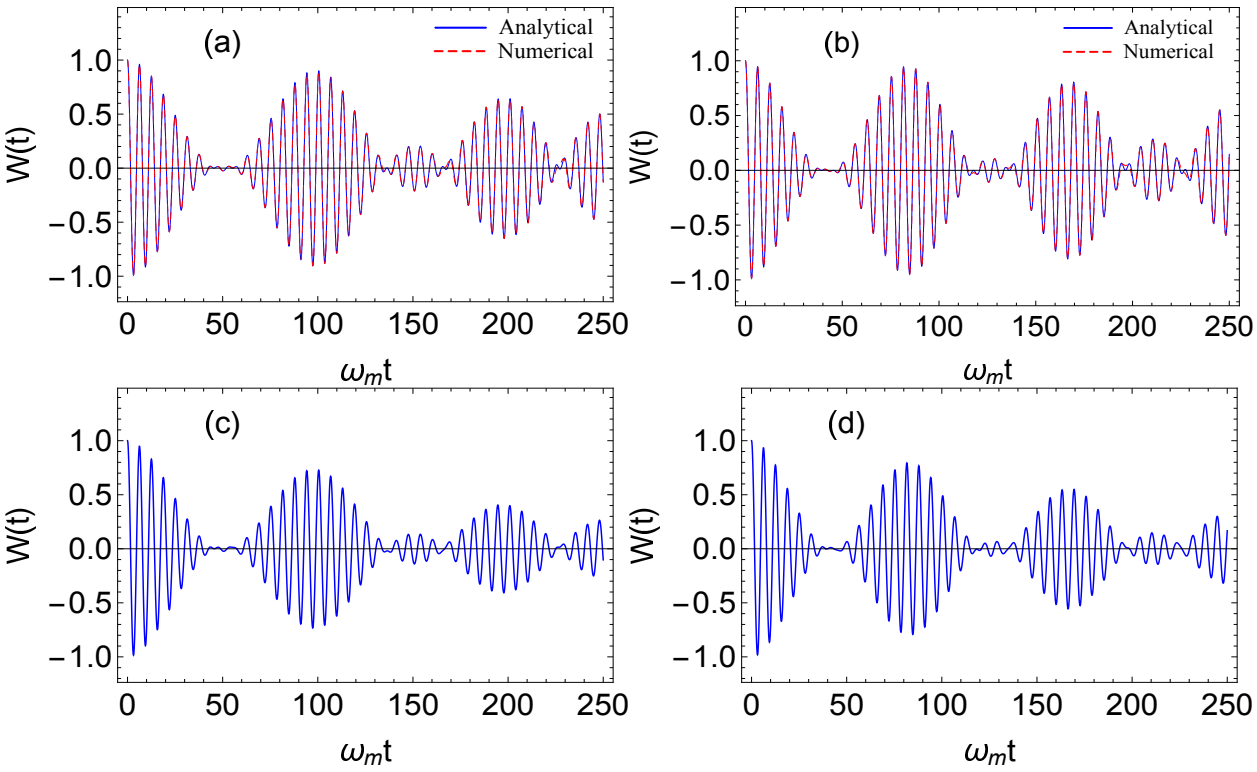

Figure 2.3: Population inversion as a function of time. (a) Analytical (solid) and numerical (without damping) (dashed) results with the initial state of the system $|e\rangle_a |0\rangle_c |2\rangle_m$. (b) Analytical (solid) and numerical (without damping) (dashed) results with the initial state of the system $|e\rangle_a |0\rangle_c |3\rangle_m$. (c) Numerical result with dissipation for otherwise the same situation as in (a). (d) Numerical result with dissipation for otherwise the same situation as in (b). The other parameters are the same as in Fig. 2.2.

First, we observe that when $g_m = 0$ ($g_{pn} = 0$), $P_e(t) = \frac{1}{2} + \frac{1}{2}\cos(\omega_m t)$, exhibiting Rabi oscillations in the case of an atom interacting resonantly with a field in a Fock state described by the original JC model [42].

Second, when the mechanical mirror is initially in the vacuum state, i. e., $l = 0$, the result reduces to $P_e(t) = \frac{1}{2} + \frac{1}{2}\cos(\omega_m t)\cos\left(\beta g_c\sqrt{n+1}t\right)$ which is presented in the previous work [68, 74] and also shown in Fig. 2.2(a). In Ref. [68], suppression of Rabi oscillations of the atomic population has been shown in a hybrid optomechanical system in the single photon strong-coupling regime ($g_m \sim \omega_m$). Here we present a general expression given by Eq. (2.13) for different mechanical states in the single-photon weak coupling regime ($g_m \ll \omega_m$). We see from Eq. (2.13) that

the Rabi oscillations are modified by two cosine functions due to the optomechanical interaction. This can be understood as the interference of the two polariton states modulated by the mechanical state. Since $g_{pn}\sqrt{l} \ll \omega_m$, the product of the two cosine functions $\cos\left(g_{pn}\sqrt{l}t\right)\cos\left(g_{pn}\sqrt{l+1}t\right)$ determines the profile of the population inversion. The first collapse time is when the cosine function with the faster oscillation reaches zero, i.e., $t_c \approx \frac{\pi}{2g_{pn}\sqrt{l+1}}$. The population inversion starts to have the first revival when the cosine function with the slower oscillation has a zero value, i.e., $t_r \approx \frac{\pi}{2g_{pn}\sqrt{l}}$.

To confirm our analytical result, we plot the population inversion using Eq. (2.13) along with the numerical results (see Appendix B) in Figs. 2.2(a), 2.2(b) and Figs. 2.3(a), 2.3(b). We observe a quantitative agreement (both plots are overlapped on each other in the figures) between the two methods. Moreover, we see collapses and revivals of the population inversion for $l > 0$ Fock state of the mechanical mirror when the atom is interacting with a cavity Fock state. The collapse is due to the interference between two polariton states interacting with the mechanical Fock state for $l > 0$. The first collapse and revival times are also in good agreement with our analytical results. For example, when $l = 2$, $t_c \approx 45/\omega_m$ and $t_r \approx 56/\omega_m$. Whereas for $l = 0$ no such an interference occurs because $|0\rangle_m$ only interacts with the upper-level polariton state $|+, n\rangle$. We also consider the population inversion when the dissipation of the system is included as shown in Figs. 2.2(c), 2.2(d), and Figs. 2.3(c), 2.3(d). It is shown that the predicted anomalous collapses and revivals are also apparent with suppressed amplitudes. The details of the dissipation mechanism are presented in Appendix B.

2.3.1.2 Non-zero atom-field detuning $\delta \neq 0$

Now we consider the situation when $\delta \neq 0$ that the atom-field coupling is non-resonant. First, when the field-mirror coupling is zero, i. e., $g_m = 0$, then we obtain

$$P_e(t) = 1 - \frac{1}{2}\sin^2(\alpha_n)\left(1 - \cos(\omega_m t)\right), \tag{2.14}$$

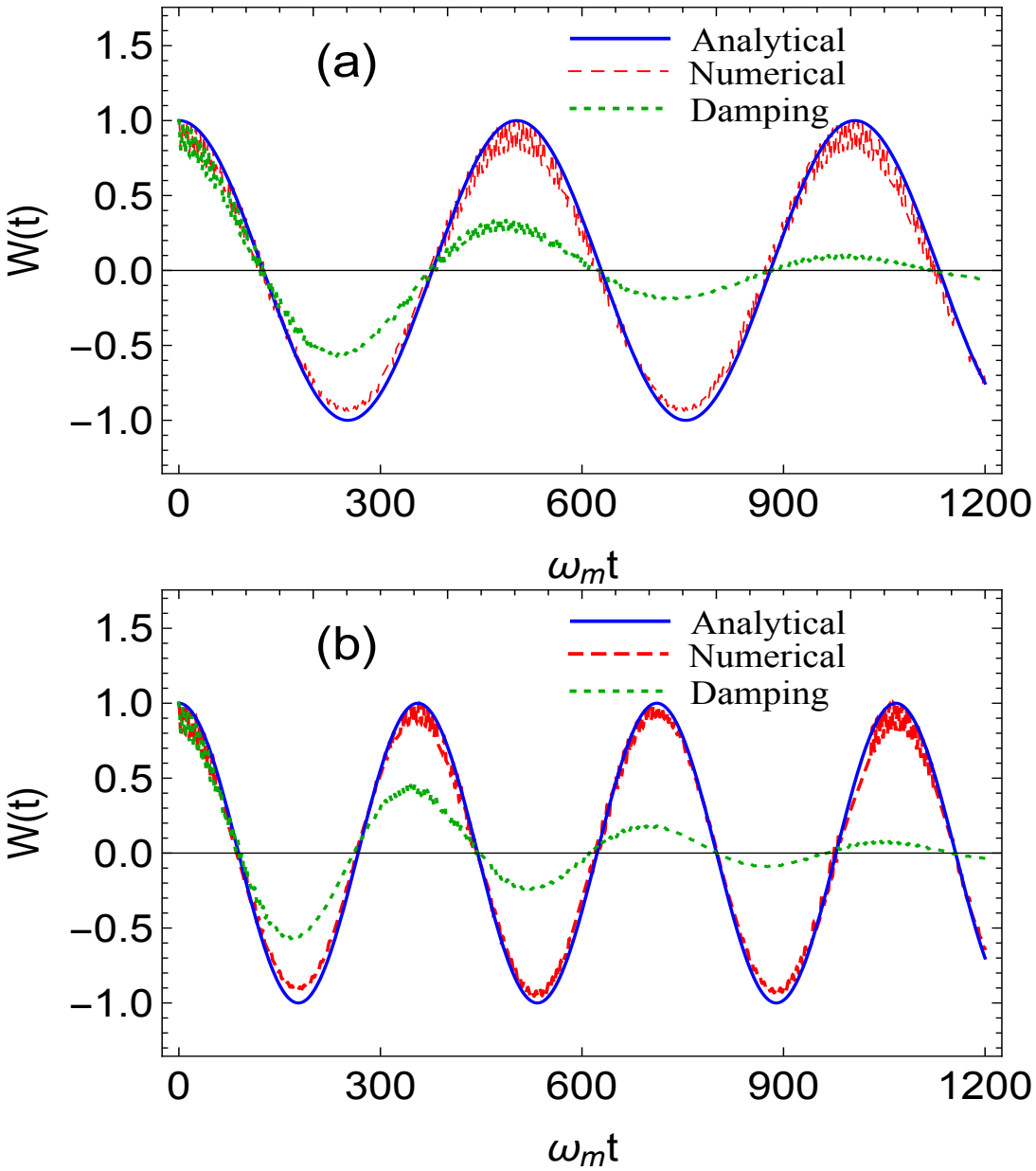

Figure 2.4: Population inversion as a function of time for non-zero atom-field detuning $\delta = 0.95\omega_m$. (a) Analytical (solid) and numerical results with (dotted) and without (dashed) dissipation when the initial state of the system is $|e\rangle_a |0\rangle_c |0\rangle_m$. (b) Analytical (solid) and numerical results with (dotted) and without (dashed) dissipation when the initial state of the system is $|e\rangle_a |0\rangle_c |1\rangle_m$. The other parameters are $\gamma_a = \gamma_c = 10^{-3}\omega_m$, $\gamma_m = 10^{-5}\omega_m$, and $\bar{n}_{th} = 5$.

which recovers the original JC model for a single atom interacting nonresonantly with a Fock state in a cavity [42]. We see from this expression that for $\alpha_n \approx 0$ or π, $P_e \approx 1$, i. e., the atomic

population will mostly stay in the excited state. Second, when we consider $g_{pn} \neq 0$ and the atom-field interaction is far-detuned from the atomic transition frequency such that $\delta \gg 2g_c\sqrt{n+1}$, then for $\delta > 0$, we have $\alpha_n \approx 0$, and for $\delta < 0$, we have $\alpha_n \approx \pi$. In these situations, the mechanical mirror couples to the two-level atom through an effective JC interaction since the polariton states are approximately equivalent to the atomic states. In the former situation, we have

$$P_e(t) \approx 1 - \sin^2\left(g_{pn}\sqrt{l+1}t\right). \tag{2.15}$$

This result is not trivial since in the far-detuned case of a JC model without a mechanical mirror, the population of the excited state will mostly stay in that state as shown in Eq. (2.14). However, with the assistance of the mechanical mirror, the atom can undergo Rabi oscillations resonantly from level $|e\rangle_a$ to level $|g\rangle_a$ by creating a photon into the cavity and a phonon into the mechanical mirror, i. e. $|e\rangle_a |0\rangle_c |l\rangle_m \rightarrow |g\rangle_a |1\rangle_c |l+1\rangle_m$. In the latter case, we have

$$P_e(t) \approx 1 - \sin^2\left(g_{pn}\sqrt{l}t\right). \tag{2.16}$$

Similarly, the atom is able to oscillate between the excited state $|e\rangle_a$ and the ground state $|g\rangle_a$ with the field coupled to the mechanical mirror. In this case, the atom will create a photon and destroy a phonon by going from $|e\rangle_a$ to $|g\rangle_a$ due to the energy conservation, i. e. $|e\rangle_a |0\rangle_c |l\rangle_m \rightarrow |g\rangle_a |1\rangle_c |l-1\rangle_m$. In Fig. (2.4), we show the population inversion using the analytical expression Eq. (2.15)and the numerical results with and without dissipation. These plots show good agreement between the analytical and numerical results and it can be seen that the optomechanically-induced Rabi oscillation is persistent in the presence of dissipation.

2.3.2 Initial mechanical coherent states

In this subsection, we consider the case when the mechanical mirror is in a coherent state $|\gamma\rangle_m$ in which the other initial conditions are the same as in the previous subsection.

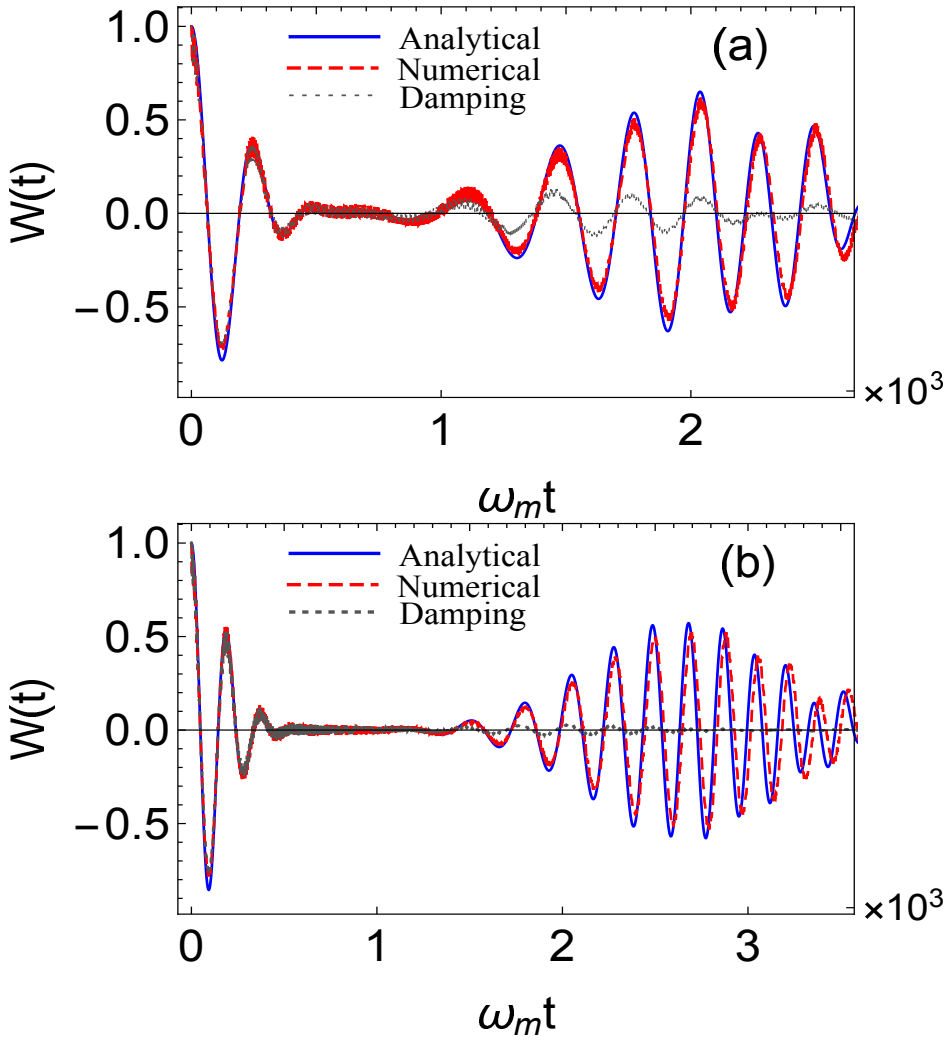

Figure 2.5: Population inversion as a function of time for non-zero atom-field detuning $\delta = 0.95\omega_m$ where the mechanical mirror is initially in a coherent state $|\gamma\rangle_m$. The initial state of the system is $|e\rangle_a |0\rangle_c |\gamma\rangle_m$. Mean number of phonons is (a) $|\gamma|^2 = 3$ and (b) $|\gamma|^2 = 6$. $\gamma_a = \gamma_c = 10^{-4}\omega_m$, $\gamma_m = 10^{-5}\omega_m$. The other parameters are the same as in Fig. 2.2.

In the transformed picture, the initial state of the system is

$$\begin{aligned} |\psi_T(0)\rangle &= e^{-\beta n(b^\dagger - b)} |e\rangle_a |n\rangle_c |\gamma\rangle_m \\ &\approx \sum_{l=0}^{\infty} C_l^m \left[\cos\left(\frac{\alpha_n}{2}\right)|+,n\rangle + \sin\left(\frac{\alpha_n}{2}\right)|-,n\rangle\right] \\ &\times \left[|l\rangle_m - \beta n\sqrt{l+1}\,|l+1\rangle_m + \beta n\sqrt{l}\,|l-1\rangle_m\right], \end{aligned} \tag{2.17}$$

where $C_l^m = e^{-|\gamma|^2/2}\gamma^l/\sqrt{l!}$ is the coefficient of the coherent state of the mechanical mirror. The time-dependent state vector is

$$|\psi_T(t)\rangle = \sum_{l=0}^{\infty} c_l^+(t)\,|+,n\rangle\,|l\rangle + c_l^-(t)\,|-,n\rangle\,|l\rangle\,, \tag{2.18}$$

where $c_{l-2}^+(0) = 0$, $c_{l-1}^+(0) = C_l^m \cos\left(\frac{\alpha_n}{2}\right)\beta n\sqrt{l}$, $c_{l-1}^-(0) = C_l^m \sin\left(\frac{\alpha_n}{2}\right)\beta n\sqrt{l}$, $c_l^-(0) = C_l^m \sin\left(\frac{\alpha_n}{2}\right)$, $c_l^+(0) = C_l^m \cos\left(\frac{\alpha_n}{2}\right)$, $c_{l+1}^-(0) = -C_l^m \sin\left(\frac{\alpha_n}{2}\right)\beta n\sqrt{l+1}$, $c_{l+1}^+(0) = -C_l^m \cos\left(\frac{\alpha_n}{2}\right)\beta n\sqrt{l+1}$, and $c_{l+2}^-(0) = 0$.

The general analytical expression of the population of the excited state is quite cumbersome. Therefore, we study the case of far-detuned atom-cavity interaction.

When the cavity field is far-detuned from the atomic transition frequency in the hybrid system, the mechanical mirror can couple to the two-level atom through an effective JC interaction if the mechanical frequency is close to the polariton frequency as discussed in Sec. 2. 3. 1. 2. Therefore, for an initial coherent state of the mechanical mirror, we expect the atomic population inversion to exhibit collapse and revival in an exact manner as the original JC model. For $\delta > 0$, the excited state population in this case is given by

$$P_e(t) \approx \sum_{l=0}^{\infty} p_l^m \left[1 - \sin^2\left(g_{pn}\sqrt{l+1}t\right)\right], \tag{2.19}$$

where $p_l^m = |C_l^m|^2$ is the initial probability of the mechanical mirror in the phonon number state $|l\rangle_m$. For the case when $\delta < 0$, the excited state population is

$$P_e(t) \approx \sum_{l=0}^{\infty} p_l^m \left[1 - \sin^2\left(g_{pn}\sqrt{l}t\right)\right]. \tag{2.20}$$

These expressions of the excited state population are similar to that in the original JC model [42]. In Figs. 2.5(a) and (b), we compare the analytical solution of the population inversion Eq. (2.20) to the numerical solutions with and without dissipation for two different mean number of phonons of the mechanical mirror. Figs. 5(a) and 5(b) show good agreements between the analytical and

the numerical results.

We conclude in this section that for an atom interacting with a Fock state cavity field, anomalous population inversion of the atom can be induced by coupling the field to a mechanical mirror. Our treatment can be extended to any other initial states of the mechanical mirror.

2.3.3 Initial mechanical thermal states

In order to make our model more relevant to experiments [13, 14, 15, 16, 17, 19], we consider that the mechanical mirror is initially in a mixture of different Fock states. The initial state of the mechanical mirror in this case can be represented by the density operator $\rho^m(0)$ and we assume that the atom is initially in its excited state and the cavity field is in a Fock state. The initial state of the total system can be described by the following density operator

$$\rho(0) = \rho^p(0) \otimes \rho^m(0), \tag{2.21}$$

where $\rho^p(0)$ is the initial state of the atom-field subsystem. The evolution of the system is described by the master equation

$$\dot{\rho} = -\frac{i}{\hbar}[\mathcal{V}, \rho], \tag{2.22}$$

where $\mathcal{V}$ is the Hamiltonian of the system in the interaction picture (see Appendix C). The formal solution of this equation can be written as

$$\rho(t) = U(t)\rho(0)U^{\dagger}(t), \tag{2.23}$$

where $U(t)$ is the time evolution operator of the system (see Appendix C). After getting the density operator of the total system $\rho(t)$, the density operator of polariton state can be found by tracing over the mirror states as

$$\rho^p(t) = Tr_m\rho(t) = \sum_{k=0}^{\infty} \langle k| \rho(t) |k\rangle . \tag{2.24}$$

From the above equation, the density matrix elements of the polariton state can then be calculated from the following equation

$$\rho_{ij}^{p}(t) = \sum_{k=0}^{\infty} \langle k, n, i| \, \rho(t) \, |j, n, k\rangle \,, \tag{2.25}$$

where $i, j \equiv +, -$.

By transforming the state $|e, n\rangle$ to the interaction picture as

$$|e, n\rangle_I = U_0^{\dagger}(t) \, |e, n\rangle \,, \tag{2.26}$$

it is straightforward to show that $P_e(t)$ when $\delta = 0$ and $\Omega_n = \omega_m$ can be calculated using the following equation

$$P_e(t) = \frac{1}{2}\Big[\rho_{++}^{p}(t) + \rho_{--}^{p}(t) + e^{i\omega_m t} \, \rho_{+-}^{p}(t) + e^{-i\omega_m t} \, \rho_{-+}^{p}(t)\Big]. \tag{2.27}$$

By calculating the density matrix elements of the polariton state (see Appendix C), it follows that the excited state population when the mirror is initially in a mixed state is given by

$$P_e(t) = \sum_{l=0}^{\infty} p_l \left[\frac{1}{2} + \frac{1}{2}\cos(\omega_m t)\cos\Big(g_{pn}\sqrt{l}t\Big)\cos\Big(g_{pn}\sqrt{l+1}\Big)\right], \tag{2.28}$$

where p_l is the phonon distribution. In Figs. 2.6(a)-(c), we show the analytical (Eq. (2.28)) and numerical (Eq. (B.3)) solutions of the population inversion without dissipation for an initial thermal mechanical state, where the mean phonon number is $\bar{l}$ and $p_l = \frac{\bar{l}^l}{(\bar{l}+1)^{l+1}}$. It can be seen from Figs. 2.6(a)-2.6(c) that the population inversion behavior converges to the same case when the mechanical mirror is in its ground state $|0\rangle_m$ as mean number of thermal phonons becomes very small i. e., $\bar{l} \ll 1$. For finite mean thermal phonon number, the population inversion collapses slower and the revival amplitude becomes smaller due the mixture of different contributions in Eq. (2.28)).

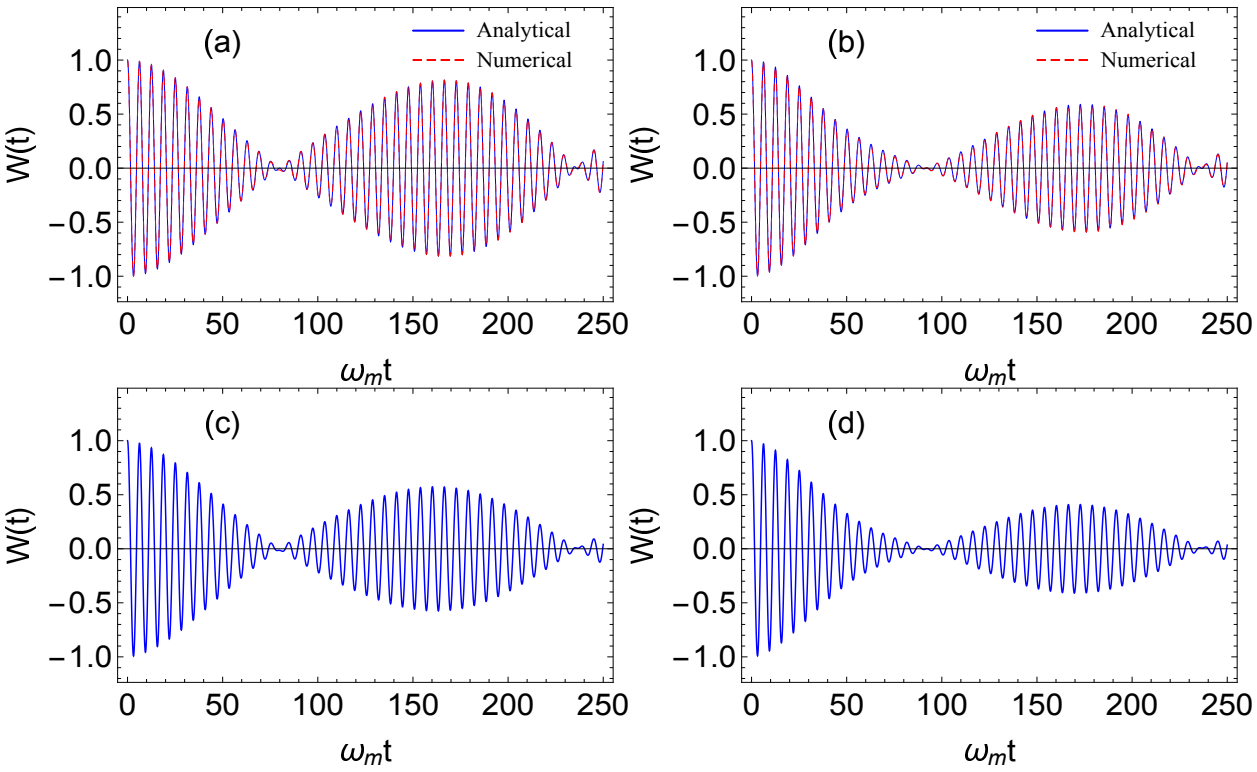

Figure 2.6: Population inversion as a function of time where the mechanical mirror is initially in a mixed state. (a) Analytical (solid) and numerical (without damping) (dashed) results with mean number of thermal phonons $\bar{l} = 0.2$. (b) Analytical (solid) and numerical (without damping) (dashed) results with mean number of thermal phonons $\bar{l} = 0.6$. (c) Numerical result with dissipation for otherwise the same situation as in (a). (d) Numerical result with dissipation for otherwise the same situation as in (b). The other parameters are the same as in Fig. 2.2.

Another interesting situation appears when $\bar{l} \ll 1$, which has been realized in recent experiments [13, 14, 15, 16, 17, 19]. We approximate the initial thermal state of the mechanical mirror as

$$\rho^m(0) \simeq p_0 \left|0\right\rangle \left\langle 0\right| + p_1 \left|1\right\rangle \left\langle 1\right|, \tag{2.29}$$

where $p_0 + p_1 \simeq 1$. If we consider a single phonon excitation on this state, then the resultant initial state of the mechanical mirror becomes

$$\rho^m(0) \simeq \frac{1}{N}\Big(p_0 \left|1\right\rangle \left\langle 1\right| + 2\, p_1 \left|2\right\rangle \left\langle 2\right| \Big), \tag{2.30}$$

where $N = p_0 + 2p_1$ is a normalization constant. The above state approximates to $|1\rangle_m$ when p_1 approaches zero. Using the initial state (2.30), the excited state population in this case becomes

$$\begin{aligned} P_e(t) = \frac{1}{N}\Bigg[\frac{p_0}{2}\Big(1+\cos(\omega_m t)\cos(g_{pn}t)\cos(g_{pn}\sqrt{2}t)\Big) \\ + p_1\Big(1+\cos(\omega_m t)\cos(g_{pn}\sqrt{2}t)\cos(g_{pn}\sqrt{3}t)\Big)\Bigg]. \end{aligned} \tag{2.31}$$

In the limit of very small mean number of phonons $\bar{l} \ll 1$, the result (2.31) becomes very close to the result shown in Fig. 2.2(b) where the initial state of the mechanical mirror is $|1\rangle_m$. Therefore, anomalous features on the population inversion in the presence of an optomechanical mirror may still be observable even if the initial mechanical state is in a mixed state.

2.4 Collapse and revival for a coherent cavity field

We now consider the case when initially the cavity field is in a coherent state $|\alpha\rangle_c$, and the mechanical mirror is in a Fock state $|l\rangle_m$. Similar to the treatment in the previous section, the initial state vector in the transformed picture is given by

$$\begin{aligned} |\psi_T(0)\rangle &= e^{-\beta c^\dagger c(b^\dagger - b)}\,|e\rangle_a\,|\alpha\rangle_c\,|l\rangle_m \\ &\approx |e\rangle_a\,|\alpha\rangle_c\,|l\rangle_m \\ &= \sum_{n=0}^{\infty} C_n^c\left[\cos\left(\frac{\alpha_n}{2}\right)|+,n\rangle + \sin\left(\frac{\alpha_n}{2}\right)|-,n\rangle\right]|l\rangle_m \end{aligned} \tag{2.32}$$

where we consider $|\alpha|\beta \ll 1$ such that the mean displacement of the mirror due to the coherent state is negligible. $C_n^c = e^{-|\alpha|^2/2}\alpha^n/\sqrt{n!}$ is the coefficient of the coherent state of the field $|\alpha\rangle_c$.

In this situation, we consider the mechanical mirror interacts resonantly with one of the polariton states $|\pm, s\rangle$ such that $\omega_m = \Omega_s$. It also interacts nonresonantly with the other polariton states $|\pm, n\rangle$ with $n \neq s$. When the mechanical mirror is in a Fock state and interacts resonantly with a polariton state, the excited state population is given by Eq. (2.12). For the nonresonant interaction case, we provide the derivation of the excited state population for the atom in Appendix C.

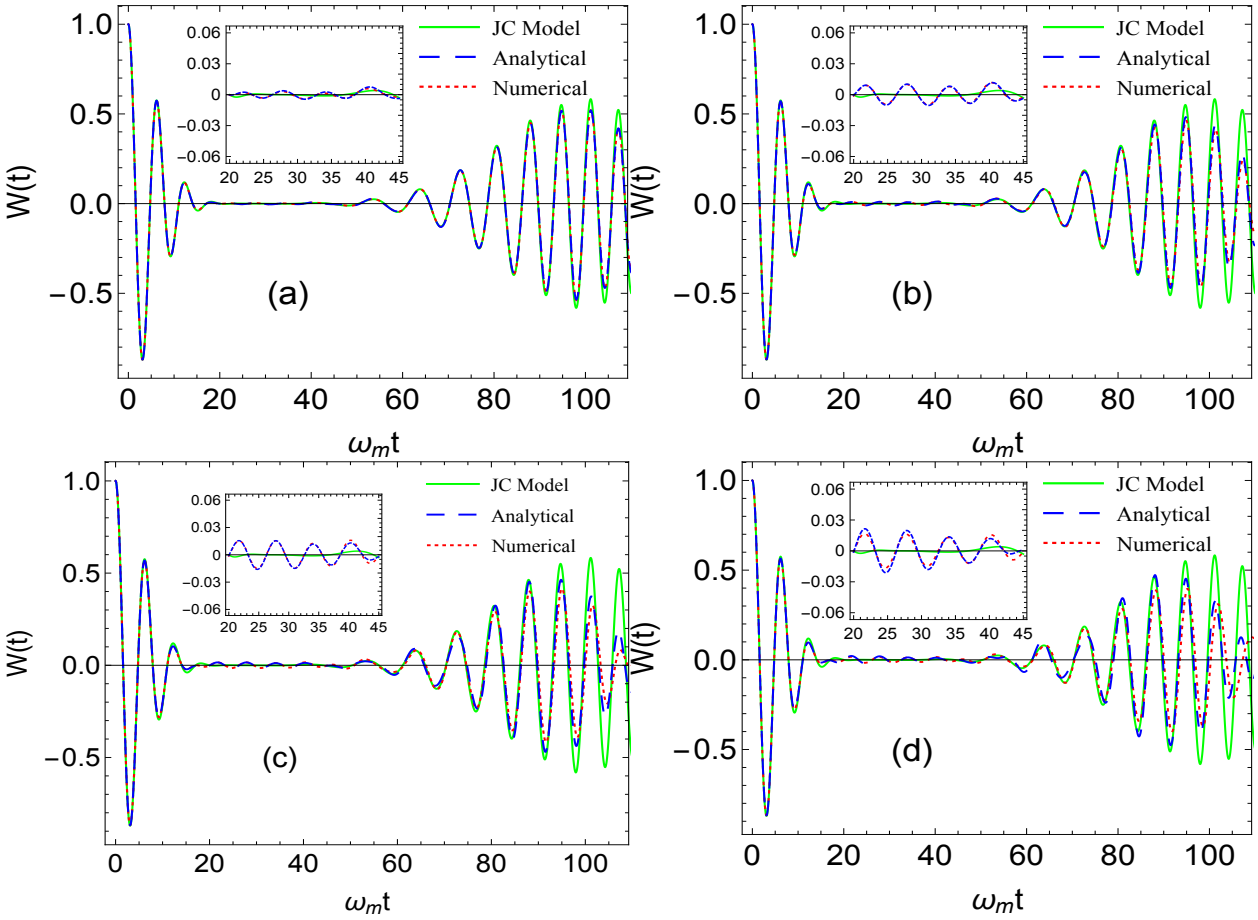

Figure 2.7: Population inversion as a function of time when the cavity field is initially in a coherent state $|\alpha\rangle_c$. Mean number of photons $|\alpha|^2 = 7$, $g_c = \omega_m/2\sqrt{s+1}$, $g_m = 0.02\omega_m$, $\delta = 0$, and $s = 7$. The initial state of the system is (a) $|e\rangle_a |\alpha\rangle_c |0\rangle_m$, (b) $|e\rangle_a |\alpha\rangle_c |1\rangle_m$, (c) $|e\rangle_a |\alpha\rangle_c |2\rangle_m$, and (d) $|e\rangle_a |\alpha\rangle_c |3\rangle_m$. The other parameters are the same as in Fig. 2.2.

Since different polariton states do not couple to each other, the excited state population can be given as a sum of these contributions, i. e.,

$$P_e(t) = p_s^c \; P_e^s(t) + \sum_{\substack{n=0 \\ n\neq s}}^{\infty} p_n^c \; P_e^n(t), \tag{2.33}$$

where $p_n^c = |C_n^c|^2$ is photon number distribution of the cavity field. The first term in $P_e(t)$ is the contribution due to the resonant interaction between the mechanical mirror and the polariton states $|\pm, s\rangle$, while the second term is the contribution due to the non-resonant interaction between

the mechanical mirror and the other atom-field polariton states $|\pm, n \neq s\rangle$. For the nonresonant contributions, we can check two interesting limits. First, when $\Delta_n = 0$, P_e^n in Eq. (2.33) reduces to the resonant case given by Eq. (2.13). Second, when the mirror frequency is far out of resonance to the polariton states, i. e. $\Delta_n \gg g_{pn}$, the expression of P_e^n reduces to $1 + \cos(\Omega_n t)$ which is the result of original JC model. We note that, in general, the result of Eq. (2.33) can be extended for an arbitrary initial photon number distribution.

In Fig. 2.7, we show the atomic population inversion for an initial excited state of the atom, initial coherent cavity field with mean number of photons $|\alpha|^2 = 7$, and different initial Fock states of the mechanical mirror. We consider the parameters such that the mechanical mirror is interacting resonantly with the polariton states $|\pm, s = 7\rangle$, the most populated initial polariton states. In order to see the effect of the mechanical mirror being in various Fock states, we compare both the analytical result Eq. (2.33) and the numerical results to the original JC model without a mechanical mirror. It can be seen that the mechanical mirror induces oscillations in the collapse region predicted by the original JC model and the amplitude of these oscillations increases as the mechanical mirror is initially in a larger Fock state. We also observe that the mechanical mirror reduces the amplitude of the revival oscillations compared to the original JC model. Therefore, we conclude that due to the optomechanical coupling, the population inversion shows anomalous oscillations.

2.5 Conclusion

In this chapter, we have studied the atomic population inversion for an initially excited two-level atom in an optomechanical cavity for different initial states of the cavity field and the mechanical mirror. We have derived analytical expressions for the population inversion in various cases and compared them with the numerical calculations with and without dissipation. Our results showed that the population inversion exhibits anomalous oscillations induced by the mechanical mirror. In general, the population inversion can display the collapse-and-revival feature induced by the mechanical mirror even if the cavity field is initially prepared in a Fock state. While for a coherent state cavity field, the population inversion can present small oscillations in the first collapse

region in the original JC model. The amplitude of these oscillations increases as the mechanical mirror is in a larger Fock state. We also considered the case of having the mechanical mirror initially in different mixed states. We showed that the population inversion approaches the case of initial mechanical Fock states when the initial mean thermal phonon number is much smaller than one. As the mean thermal phonon number increases, the population inversion exhibits slower collapse and smaller revival amplitudes.

Our findings may be useful for distinguishing different quantum states of a mechanical mirror in a cavity, which may deserve a further study in the future.

3. QUANTUM STATE RECONSTRUCTION OF A MECHANICAL MIRROR IN A HYBRID SYSTEM

3.1 Introduction

Cavity optomechanics is a rapidly developing area of research [10] which explores the interaction between electromagnetic fields and mechanical states of motion via radiation-pressure forces [72, 75, 76]. Numerous research studies in cavity optomechanics cover a wide variety of problems such as ground state cooling [12, 16, 18, 15, 13, 14, 19, 20, 21], generation of macroscopic quantum superposition in optomechancial systems [22, 23, 24, 25], and creation and verification of quantum entanglement [26, 27, 28, 29, 30, 31, 32, 33, 34, 35, 36, 37].

Quantum state reconstruction of the mechanical states of motion plays a very crucial role in revealing and understanding various non-classical properties and aspects in different cavity optomechanical systems [77]. Recently, several reconstruction schemes have been introduced to reconstruct motional mechanical states in cavity optomechanics. A mechanical state tomography scheme [38] is based on sending short optical pulse to enter an optomechanical cavity. The accumulated phase of the output pulse is measured to obtain information about the oscillator quadratures. Mechanical state tomography based on a back-action-evading interaction has been experimentally demonstracted to accurately measure the position of the mechanical oscillator [39].

Another interesting reconstruction scheme was introduced in which an optomechanical cavity is coupled to an outside continuous field [40]. Detection of a single photon emission and scattering spectrum [78] is used to measure the quantum state of the mechanical mirror in the system. Due to the large coupling strength between the cavity field and the mechanical mirror, effect of the mechanical motion strongly affects the detected emission and scattering spectra of the photon, and thus enabling an extraction of accurate information about the initial state of the mechanical mirror. However, this method works well only when the optomechanical coupling strength is strong, but fails in the weak coupling regime.

A number of researches investigate using atoms as a measurement tool for the quantum states of cavity fields[79, 80, 81, 82, 83, 84, 85, 86, 87, 88, 89, 90, 91]. A measurement scheme [80] was introduced to reconstruct the quantum state of a light field using a beam of two-level atoms initially prepared in a coherent superposition of their excited and ground states. In this scheme, a beam of two-level atoms is sent in an optical cavity to interact with a quantized electromagnetic field inside and the probability of detecting the atoms in the excited states is measured after the atoms exit the cavity. By controlling the phase difference between the two states of the atom and varying the interaction time, the complete quantum state of the cavity field can be reconstructed by solving a system of linear equations. Similarily, using atom as a detector, one can also measure the quantum state of a nanomechanical oscillator in an optomichanical system [41]. The atom is coupled to an optical field via a Raman transition and to the nanomechanical oscillator via a magneticsublevel-phonon interaction [41]. Since the atom is directly coupled to the nanomechanical oscillator, measurement of the probability of the atom to be in its ground state directly gives the Wigner function of the nanomechanical oscillator. This method is an interesting extension of the idea of nonlinear atom homodyne [81] which was developed to measure the quantum state of a single mode field.

In this chapter, we propose a scheme to detect the full quantum state of a mechanical oscillator in a hybrid optomechanical system. Our method is also based on the use of a beam of two-level atoms as detector for the state of the mechancial oscillator. Instead of using direct magneticsublevel-phonon coupling as in Ref. [41], the atoms can indirectly couple to the mechanical mirror in our system via the polariton-phonon coupling. In our method, the atom is initially considered in the excited state while the cavity field is in vacuum state. We show that by measuring the probability of the atoms being in the excited state for different interaction times after passing through the cavity, it is possible to reconstruct the initial state of the mechanical mirror by inverting a simple system of linear equations. Although stronger optomechanical coupling strength can have better reconstruction quality, our method does not require the coupling strength to be ultrastrong.

This chapter is organized as follows: In Sec. 3.2, we introduce the suggested model to measure

the state of the mechanical mirror. In Sec. 3.3, we derive the excited state probability of the atom when the atom passes through the optomechanical cavity. In Sec. 3.4, we show how to measure the full quantum state of the mechanical mirror. Finally, we summarize the results.

3.2 The model

We consider an optomechanical system consisting of an optical cavity with a fixed mirror on one side and a mechanical mirror on the other side of the cavity. The position of the mechanical mirror is described by $x = x_0(b + b^\dagger)$ where x_0 is the zero point position of the mechanical mirror and it is given by $x_0 = \sqrt{\hbar/2m\omega_m}$. Here $b(b^\dagger)$ is the mechanical mirror annihilation (creation) operator and m and ω_m are the mass and frequency of the mechanical mirror, respectively. The cavity field is weakly coupled to the mechanical mirror via the radiation pressure coupling. To detect the quantum state of the mechanical mirror, we consider a beam of two level atoms entering the cavity to interact with the quantized field inside the cavity and the probability of finding the atom in the excited state is measured for different interaction times.

The total Hamiltonian describing the system depicted in Fig. 3.1 is

$$\mathcal{H} = \mathcal{H}_0 + \mathcal{H}_I, \tag{3.1}$$

where $\mathcal{H}_0$ and $\mathcal{H}_I$ are the free and interaction parts of the system's Hamiltonian, respectively. The free part of the Hamiltonian can be written as

$$\mathcal{H}_0 = \hbar\omega_c c^\dagger c + \hbar\frac{\omega_a}{2}\sigma_z + \hbar\omega_m b^\dagger b, \tag{3.2}$$

where the first term in Eq. (3.2) describes the Hamiltonian of the cavity field with frequency ω_c. The second and third terms in Eq. (3.2) represent the Hamiltonian of the two-level atom with transition frequency ω_a and the mechanical mirror with fundamental oscillation frequency ω_m, respectively. Here $c(c^\dagger)$ is the annihilation (creation) operator of the cavity field. The interaction

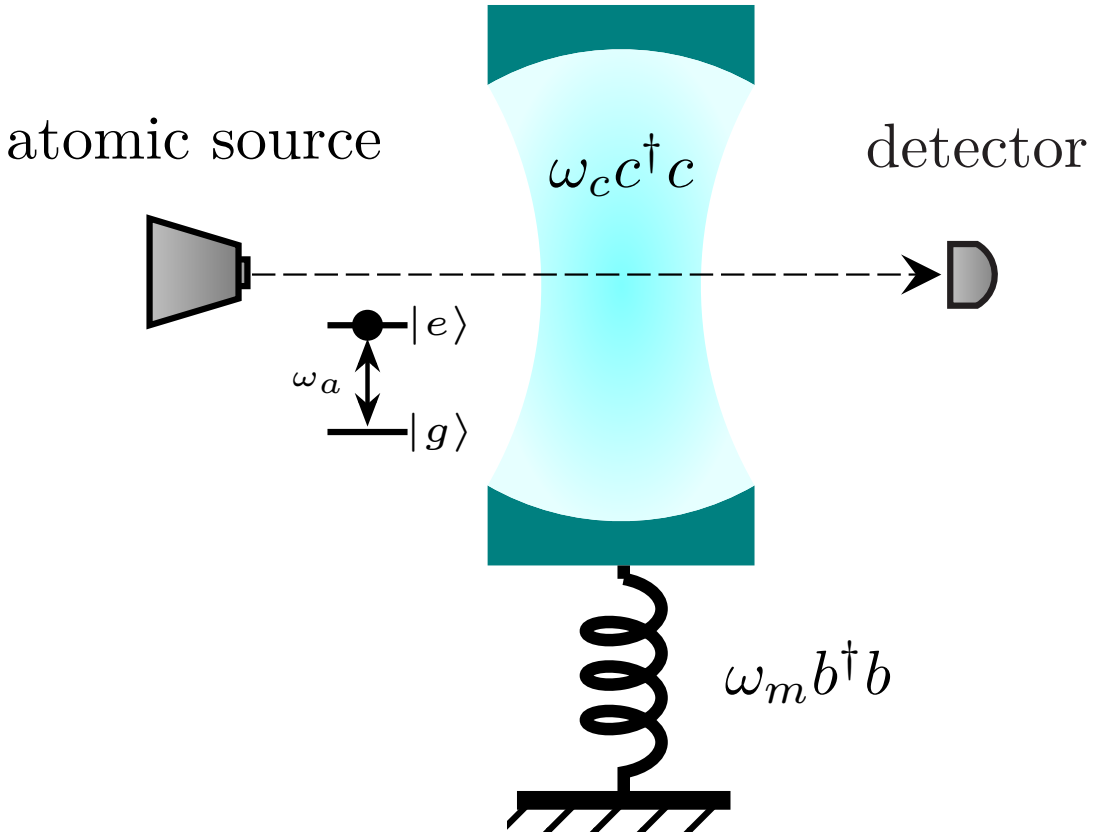

Figure 3.1: Quantum state reconstruction using atom as detector in the hybrid optomechanical system.

part of the Hamiltonian in Eq. (3.1) is given by [67, 92]

$$\mathcal{H}_I = -i\hbar g_c(\sigma_+ c - c^\dagger \sigma_-) - \hbar g_m c^\dagger c(b^\dagger + b). \tag{3.3}$$

The first term in Eq. (3.3) describes the interaction between the two-level atom and the cavity field. The second term describes the interaction between the cavity field and the mechanical mirror via the radiation pressure coupling. The coefficients g_c and g_m are the coupling strengths of the atom-field and the cavity field-mechanical mirror interaction, respectively. The coefficient g_m is defined as $g_m = (\omega_c/L)\sqrt{\hbar/2m\omega_m}$ where L is the length of the cavity and $\sigma_+ = |e\rangle\langle g|$ and $\sigma_- = |g\rangle\langle e|$ are the atomic raising and lowering operators, respectively.

In the weak mechanical coupling limit, the Hamiltonian of the system can be simplified [67,

92] so that the system's dynamics can be treated analytically. The Hamiltonian is reduced in such a way that the mechanical mirror is coupled to a specific polariton state $|\pm, n\rangle$ in a Jaynes-Cummings (JC)-like coupling where $|+, n\rangle = \cos(\alpha_n/2)|e, n\rangle + i\sin(\alpha_n/2)|g, n+1\rangle$ and $|-, n\rangle = \sin(\alpha_n/2)|e, n\rangle - i\cos(\alpha_n/2)|g, n+1\rangle$ with $\tan\alpha_n = 2g_c\sqrt{n+1}/\delta$ and $\delta = \omega_a - \omega_c$ is the detuning between the transition frequency of the two-level atom and the frequency of the cavity field. The rotating-wave approximation under the condition $\omega_m + \Omega_n \gg g_{pn} \gg |\omega_m - \Omega_n|$ can be applied. Therefore transformed Hamiltonian in the linear approximation is reduced to [67, 92]

$$\mathcal{H}_{\mathcal{T}} = \sum_{n=1}^{\infty}\left[\hbar\frac{\Omega_n}{2}\sigma_z^{(n)} + \hbar g_{pn}\left(\sigma_-^{(n)}b^\dagger + \sigma_+^{(n)}b\right)\right] + \hbar\omega_m b^\dagger b, \tag{3.4}$$

where $\Omega_n = \sqrt{\delta^2 + 4g_c^2(n+1)}$ describes the energy of the polariton with photon number n, and $g_{pn} = \beta g_c\sqrt{n+1}$ is the effective coupling between the polariton and the mechanical mirror. $\sigma_z^{(n)}$ and $\sigma_\mp^{(n)}$ are the polariton Pauli matrices for the polariton states $|\pm, n\rangle$. It is clearly seen that in the dressed state picture the polariton effectively couples to the phonons. Using the effective Hamiltonian shown in Eq. (3.4), we can solve the dynamics of the system using the time-dependent Schrödinger's equation

$$|\dot{\psi}_T\rangle = -\frac{i}{\hbar}\mathcal{H}_{\mathcal{T}}|\psi_T\rangle, \tag{3.5}$$

where $|\psi_T\rangle = \mathcal{T}|\psi_s\rangle$ is the transformed state of the total system with $\mathcal{T} = e^{-\beta c^\dagger c(b^\dagger - b)}$ and $|\psi_s\rangle$ the untransformed state of the system. By solving Eq. (3.5), we can obtain the population dynamics of the atom which encodes the information of the mechanical mirror. Therefore, it is possible to reconstruct the quantum state of the mechanical mirror by measuring the atomic population.

3.3 Excited state probability

When the atoms pass through the cavity, the population in the excited state can be modified by the cavity field and the mechanical mirror phonon. It is therefore possible to measure the quantum state of the mechanical mirror from the atomic excited state probability. In this section,

we calculate the evolution of the excited state probability and show how we can measure the quantum state of the mechanical mirror.

We assume that the mechanical mirror is in an unknown superposition state $|\psi_{mirror}\rangle = \sum_{l=0}^{\infty} u_l|l\rangle$ where u_l is unknown amplitude to be determined and it satisfies that $\sum_{l=0}^{\infty} |u_l|^2 = 1$. We first consider the general case where the two-level atom is initially in a superposition of the excited state $|e\rangle$ and the ground state $|g\rangle$, i.e., $|\psi_{atom}(0)\rangle = c_e\,|e\rangle + c_g\,|g\rangle$ with $|c_g|^2 + |c_e|^2 = 1$, and the cavity field is in the state $|\psi_{cavity}(0)\rangle = \sum_{n=0}^{\infty} w_n|n\rangle$ with $\sum_{n=0}^{\infty} |w_n|^2 = 1$. The initial state of the total system can then be written as

$$|\psi_s(0)\rangle = \sum_{n=0}^{\infty}\sum_{l=0}^{\infty} w_n u_l \Big(c_e\,|e,n\rangle + c_g\,|g,n\rangle \Big)\,|l\rangle\,. \tag{3.6}$$

The initial state (3.6) in the transformed picture is given as $|\psi_T(0)\rangle = e^{-\beta n\,(b^\dagger - b)}\,|\psi_s(0)\rangle$. For $\beta n \ll 1$, the initial state $|\psi_T(0)\rangle \approx |\psi_s(0)\rangle$. Using the dressed state bases of the atom-field subsystem, the system's initial state can be rewritten as

$$\begin{aligned} |\psi(0)\rangle = {} & w_0 c_g \sum_{l=0}^{\infty} u_l\,|g,0\rangle\,|l\rangle \\ & + \sum_{n=0}^{\infty}\sum_{l=0}^{\infty} u_l \Bigg[\left(c_e w_n \cos\left(\frac{\alpha_n}{2}\right) - i c_g w_{n+1} \sin\left(\frac{\alpha_n}{2}\right) \right) |+,n\rangle \\ & + \left(c_e w_n \sin\left(\frac{\alpha_n}{2}\right) + i c_g w_{n+1} \cos\left(\frac{\alpha_n}{2}\right) \right) |-,n\rangle \Bigg]\,|l\rangle\,. \end{aligned} \tag{3.7}$$

It is clear that the effective Hamiltonian (3.4) can lead to transitions such that $|+,n\rangle\,|l\rangle \longleftrightarrow |-,n\rangle\,|l+1\rangle$. The state of the system at time t is therefore given by

$$\begin{aligned} |\psi(t)\rangle = {} & \sum_{l=0}^{\infty} C^{g}_{0,l}(t)\,|g,0\rangle\,|l\rangle + \sum_{n=0}^{\infty} C^{-}_{n,0}(t)\,|-,n\rangle\,|0\rangle \\ & + \sum_{n=0}^{\infty}\sum_{l=0}^{\infty} \Big[C^{+}_{n,l}(t)\,|+,n\rangle\,|l\rangle + C^{-}_{n,l+1}(t)\,|-,n\rangle\,|l+1\rangle \Big]. \end{aligned} \tag{3.8}$$

where $C^{g}_{0,l}(t)$ is the probability amplitude that the atom is in the ground state and the field is

in the vacuum state with the mechanical mirror being in the state $|l\rangle$, and $C^{+}_{n,l}(t)$ ($C^{-}_{n,l}(t)$) is the probability amplitude that the polariton being in the state $|+,n\rangle$ ($|-,n\rangle$) and the mechanical mirror being in the state $|l\rangle$. The equations of motion for the probability amplitudes can be derived from the time-dependent Schrödinger's equation. A solution of these coupled equations can give the following expressions

$$C^{g}_{0,l}(t) = 0, \tag{3.9a}$$

$$C^{+}_{n,l}(t) = e^{-i\omega_m(l+\frac{1}{2})t}\left[C^{+}_{n,l}(0)\cos\left(\frac{\omega_{nl}}{2}t\right) - i\frac{\Delta_n}{\omega_{nl}}C^{+}_{n,l}(0)\sin\left(\frac{\omega_{nl}}{2}t\right) - 2i\frac{g_{pn}\sqrt{l+1}}{\omega_{nl}}C^{-}_{n,l+1}(0)\sin\left(\frac{\omega_{nl}}{2}t\right)\right], \tag{3.9b}$$

$$C^{-}_{n,l+1}(t) = e^{-i\omega_m(l+\frac{1}{2})t}\left[C^{-}_{n,l+1}(0)\cos\left(\frac{\omega_{nl}}{2}t\right) + i\frac{\Delta_n}{\omega_{nl}}C^{-}_{n,l+1}(0)\sin\left(\frac{\omega_{nl}}{2}t\right) - 2i\frac{g_{pn}\sqrt{l+1}}{\omega_{nl}}C^{+}_{n,l}(0)\sin\left(\frac{\omega_{nl}}{2}t\right)\right] \tag{3.9c}$$

$$C^{-}_{n,0}(t) = e^{\frac{i\Omega_n}{2}t}C^{-}_{n,0}(0), \tag{3.9d}$$

where $\Delta_n = \Omega_n - \omega_m$ and $\omega_{nl} = \sqrt{\Delta_n^2 + 4g_{pn}^2(l+1)}$. For resonant atom-field interaction ($\delta = 0$), $\sin\left(\alpha_n/2\right) = \cos\left(\alpha_n/2\right) = 1/\sqrt{2}$. In this case, the probability to find the atom in the excited state can be calculated from the following equation

$$P_e(t) = \frac{1}{2}\sum_{n=0}^{\infty}\sum_{l=0}^{\infty}\left|C^{+}_{n,l}(t) + C^{-}_{n,l}(t)\right|^2. \tag{3.10}$$

If we consider the atom to be initially prepared in the excited state, i. e., $c_e = 1$ and $c_g = 0$, and the cavity field is in the vacuum state, i. e., $w_0 = 1$ and $w_n = 0$ for $n \neq 0$. The atomic population inversion defined by $W(t) = 2P_e(t) - 1$ follows directly by substituting the solutions of the probability amplitudes from Eqs. (3a)-(3d) into Eq. (3.10). The resulting expression for

$W(t)$ is

$$
\begin{aligned}
W(t) = \sum_{l=0}^{\infty} \Bigg[& \cos\left(g_{p0}\sqrt{l}t\right) \cos\left(g_{p0}\sqrt{l+1}t\right) \cos\left(\omega_m t\right)\, a_l \\
& + \sin\left(g_{p0}\sqrt{l+1}t\right) \sin\left(g_{p0}\sqrt{l+2}t\right) \Big(\mathrm{Re}\left(b_l\right)\cos(\omega_m t) - \mathrm{Im}\left(b_l\right)\sin\left(\omega_m t\right)\Big) \\
& + \left(\cos\left(g_{p0}\sqrt{l+2}t\right) - \cos\left(g_{p0}\sqrt{l}t\right) \right) \sin\left(g_{p0}\sqrt{l+1}t\right) \\
& \times \Big(\mathrm{Re}\left(c_l\right)\sin(\omega_m t) + \mathrm{Im}\left(c_l\right)\cos(\omega_m t)\Big) \Bigg],
\end{aligned}
\tag{3.11}
$$

where for simplicity sake, we considered $\Omega_0 = 2g_c = \omega_m$. The coefficients a_l, b_l, and c_l are given by

$$
a_l = \left|u_l\right|^2,\ b_l = u_l u_{l+2}^*,\ c_l = u_l u_{l+1}^*. \tag{3.12}
$$

The coefficient a_l gives the probability distribution of the initial state of the mechanical mirror while the phase information of the mirror's state is contained in either b_l or c_l depending on what the mirror's initial state is. In the next section, we show how the initial state of the mechanical mirror can be reconstructed using Eq. (3.11).

3.4 Quantum state reconstruction of the mechanical mirror

In order to reconstruct the full initial state of the mechanical mirror, we need to find the coefficients a_l, b_l and c_l in Eq. (3.11). From Eq. (3.11), we see that we have an infinite number of the coefficients a_l, b_l, and c_l. We can truncate the infinite summation over the number of phonons l in Eq. (3.11) to a maximum number l_{max} such that $l_{max} \gg \bar{l}$, where $\bar{l}$ is the average number of phonons. Since a_l is a real number but both b_l and c_l are complex number, the unknown variables for each l is 5 ($a_l, \mathrm{Re}[b_l], \mathrm{Im}[b_l], \mathrm{Re}[c_l], \mathrm{Im}[c_l]$). For a cutoff l_{max}, the total number of unknown variables is $5(l_{max}+1)$. Therefore, to determine all the unknown variables, we need to measure $W(t)$ for at least $5(l_{max}+1)$ interaction times. For each value of t_k ($k = 1, 2, \cdots, 5(l_{max}+1)$),

the expression for the inversion is given by

$$W(t_k) = \sum_{l=0}^{l_{max}} \Big[A_l(t_k)\, a_l + B_l(t_k)\, \mathrm{Re}\,(b_l) + C_l(t_k)\, \mathrm{Im}\,(b_l) + D_l(t_k)\, \mathrm{Re}\,(c_l) + E_l(t_k)\, \mathrm{Im}\,(c_l) \Big], \tag{3.13}$$

where $a_l, \mathrm{Re}[b_l], \mathrm{Im}[b_l], \mathrm{Re}[c_l], \mathrm{Im}[c_l]$ are unknown variables to be determined and

$$A_l(t_k) = \cos\left(g_{p0}\sqrt{l}t_k\right) \cos\left(g_{p0}\sqrt{l+1}t_k\right) \cos\left(\omega_m t_k\right) \tag{3.14a}$$

$$B_l(t_k) = \sin\left(g_{p0}\sqrt{l+1}t_k\right) \sin\left(g_{p0}\sqrt{l+2}t_k\right) \cos(\omega_m t_k) \tag{3.14b}$$

$$C_l(t_k) = -\sin\left(g_{p0}\sqrt{l+1}t_k\right) \sin\left(g_{p0}\sqrt{l+2}t_k\right) \sin(\omega_m t_k) \tag{3.14c}$$

$$D_l(t_k) = \left[\cos\left(g_{p0}\sqrt{l+2}t_k\right) - \cos\left(g_{p0}\sqrt{l}t_k\right)\right] \sin\left(g_{p0}\sqrt{l+1}t_k\right) \sin(\omega_m t_k) \tag{3.14d}$$

$$E_l(t_k) = \left[\cos\left(g_{p0}\sqrt{l+2}t_k\right) - \cos\left(g_{p0}\sqrt{l}t_k\right)\right] \sin\left(g_{p0}\sqrt{l+1}t_k\right) \cos(\omega_m t_k). \tag{3.14e}$$

Eq. (3.13) can be further written as the matrix form

$$\mathbf{W} = \mathbf{M}\,\mathbf{X}, \tag{3.15}$$

where $\mathbf{W}$ is a $5(l_{max}+1)$-dimensional vector which contains the experimental data of the population inversion, i.e., $\mathbf{W} = (W(t_1), W(t_2), \cdots, W(t_{5(l_{max}+1)})^T$. The vector $\mathbf{X}$ contains the unknown coefficients which need to be determined to reconstruct the initial state of the mechanical mirror and it is defined as $\mathbf{X} \equiv (\mathbf{X_0}, \mathbf{X_1}, \cdots, \mathbf{X_{5(l_{max}+1)}})^{\mathbf{T}}$ with $\mathbf{X_l} = \Big(a_l, \mathrm{Re}\,(b_l), \mathrm{Im}\,(b_l), \mathrm{Re}\,(c_l), \mathrm{Im}\,(c_l)\Big)^T$. The matrix $\mathbf{M}$ is preknown and it is given by

$$\mathbf{M}_{k\,l} = A_l(t_k) + B_l(t_k) + C_l(t_k) + D_l(t_k) + E_l(t_k), \tag{3.16}$$

where the elements of this matrix are defined in Eqs. (13a)-(13d), and $k, l = 1, 2, ..., 5(l_{max}+1)$. Having $\mathbf{W}$ and $\mathbf{M}$ we can either use matrix inversion or least Square fitting method to obtain the

solutions for $\mathbf{X}$ which contains both the probability and phase information of the mirror's state.

Extracting the values of a_l from the vector $\mathbf{X}$ directly yields the phonon probability distribution of the mechanical mirror. The phase of the mechanical mirror can be obtained from other elements of the vector $\mathbf{X}$. In what follows we explain the procedure of reconstructing the phase of the mirror's state. When we look at Eq. (3.11), we see that it contains terms of the product of different amplitudes, i.e., $u_l u_{l+1}^*$ and $u_l u_{l+2}^*$. These terms contain the phase of the amplitude from which we can reconstruct the phase of the quantum state of the mechanical mirror. Since $a_l = |u_l|^2$ and $c_l = u_l u_{l+1}^*$, we have $c_l = \sqrt{a_l a_{l+1}} e^{-i(\varphi_{l+1}-\varphi_l)}$ where the amplitude $u_l = |u_l| e^{i\phi_l}$. Therefore, the phase difference between the probability amplitude u_l and its first neighbor u_{l+1} is given by

$$\Delta\varphi_{l+1} = \varphi_{l+1} - \varphi_l = \arctan\Big[\frac{-\mathrm{Im}\big(c_l\big)}{\mathrm{Re}\big(c_l\big)}\Big]. \tag{3.17}$$

Hence, the phase can be determined from c_l. In certain cases some elements may be missing and the phase difference between neighboring elements is undefined. For example, in the squeezed vacuum, only even photon number has nonzero amplitude. In this case, $c_l = 0$ and the phase can not be reconstructed. Fortunately, we can use a_l and b_l to determine the phase difference between the next-nearest-neighbor elements. We have $b_l = u_l u_{l+2}^* = \sqrt{a_l a_{l+2}} e^{-i(\varphi_{l+2}-\varphi_l)}$. Then the phase difference between two neighboring bases is given by

$$\Delta\varphi_{l+2} = \varphi_{l+2} - \varphi_l = \arctan\Big[\frac{-\mathrm{Im}\big(b_l\big)}{\mathrm{Re}\big(b_l\big)}\Big]. \tag{3.18}$$

By solving b_l, one can reconstruct the phase of squeezed vacuum.

In the following, we apply our scheme to three examples of the mechanical state and examine different conditions in which this scheme can work to reconstruct the initial state of the mechanical mirror.

3.4.1 Coherent state

Supposing that the initial state of the mechanical mirror is a coherent state and it can be written as

$$|\psi_{mirror}(0)\rangle = e^{-\bar{l}/2} \sum_{l=0}^{\infty} \frac{\bar{l}^{l/2}}{\sqrt{l!}} |l\rangle \,, \tag{3.19}$$

where $\bar{l}$ is the average phonon number. The exact probability distribution of phonons is given by

$$P(l) = \frac{\bar{l}^{\,l}\, e^{-\bar{l}}}{l!} \tag{3.20}$$

which is a Poisson distribution. From Eq. (3.19), we know that $u_l = e^{-\bar{l}/2}\, \bar{l}^{\,l/2}/\sqrt{l!}$ and the population inversion can be calculated from Eq. (3.11) for an arbitrary time. To reconstruct the quantum state of the mechanical mirror, we need to choose a value of the cutoff l_{max} and measure $W(t)$ for $5(l_{max}+1)$ discrete times. Then we use the least square method to fit the unknown variables $\mathbf{X}$ from Eq. (3.15). In Fig. 3.2(a), we compare the reconstructed probability distribution of phonons with the exact distribution Eq. (3.20) with $\bar{l} = 3$ for two different cutoffs ($l_{max} = 8$ and 15). In this example, we fix the coupling ratio to be $g_m/\omega_m = 0.07$. The solid curve represents the exact probability distribution of phonons, the triangles correspond to the reconstructed probability distribution when $l_{max} = 8$, and the points correspond to the reconstructed probability distribution when $l_{max} = 15$. It is clearly seen that in both cases ($l_{max} = 8$ and 15) the reconstructed results of the probability distribution of phonons are close to the exact distribution. More importantly, when the the cutoff l_{max} is increased, the quality of reconstruction apparently improves. In pratice, the cutoff l_{max} is chosen such that the phonon distribution is negligible when $l > l_{max}$.

Fig. 3.2(b) shows the effect of increasing the optomechanical coupling strength g_m on the quality of reconstruction while l_{max} is fixed. Here, the averge phonon number is $\bar{l} = 3$ and l_{max} is set to be 12. When $g_m/\omega_m = 0.06$, the reconstructed probability distribution is close to the exact distribution but most points are still deviating from the exact probability distribution (the solid curve).

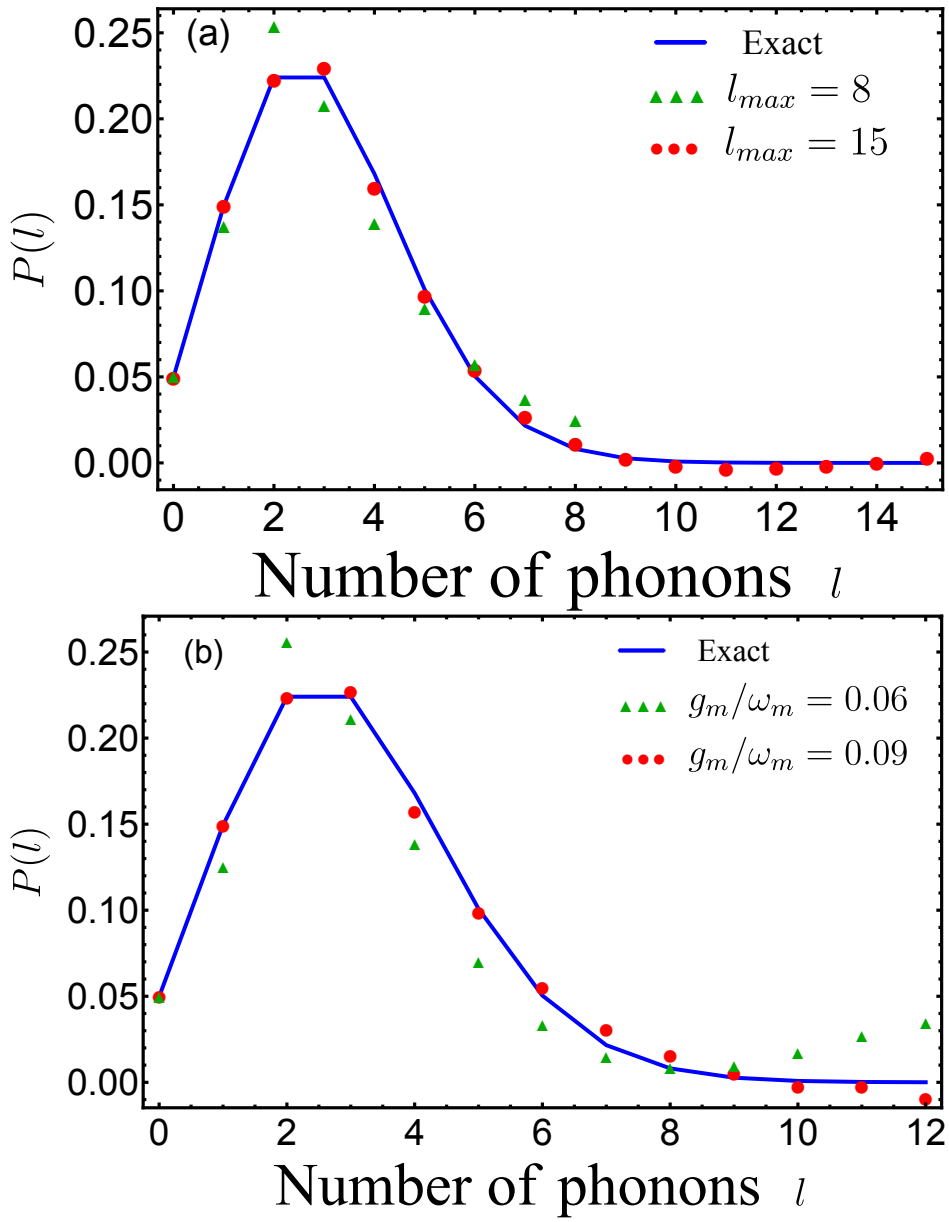

Figure 3.2: Reconstruction of initial mechanical coherent state. (a) Comparison between the exact and reconstructed probability distribution of phonons for two different values of l_{max} with $g_m/\omega_m = 0.07$. (b) Comparison between the exact and reconstructed probability distribution of phonons for two different coupling strength with $l_{max} = 12$. Mean number of phonons $\bar{l} = 3$.

However, when the optomechanical coupling is increased to $g_m/\omega_m = 0.09$, the result of reconstruction is clearly approaching the exact probability distribution. Therefore, increasing the optomechanical coupling strength leads to extracting a more accurate information about the initial

state of the mechanical mirror. We should emphasize that the optomechanical coupling strengths in the considered examples are in the weak coupling regime. This is different from the method presented in [40] where strong optomechanical coupling is needed to reconstruct the initial state of the mechanical mirror, i.e., $g_m/\omega_m > 1$.

3.4.2 Arbitrary quantum state with phase

In the previous subsection, we considered that the initial state has real amplitudes. In this subsection we show how to reconstruct a general quantum state when both probability and phase are included. A general quantum state can be expanded as a superposition of Fock state. Here, as an example, we consider that the initial state of the mechanical mirror is a superposition of four Fock states $|0\rangle$, $|1\rangle$, $|2\rangle$, and $|3\rangle$ with a phase difference between neighboring Fock states.

$$|\psi_{mirror}(0)\rangle = \frac{1}{\sqrt{10}}\Big(\sqrt{3}\ |0\rangle + e^{i\pi/5}\,|1\rangle + \sqrt{5}\,e^{i\pi/3}\,|2\rangle + e^{i\pi/4}\,|3\rangle\Big) \tag{3.21}$$

In order to extract the full quantum state of the mechanical mirror, we solve Eq. (3.15) for a truncated maximum number of phonons l_{max}. In this example, we chose $l_{max} = 4$ which means the atomic population inversion is measured for $5(l_{max}+1) = 25$ discrete interaction times. From Eq. (3.15), we can construct a linear system of equations using the measured data of the atomic population inversion $W(t_k)$ along with Eqs. (3.14a)-(3.14d). We solve this system of linear equations by simple matrix inversion to reconstruct the initial state of the mechanical mirror. The values of a_l which are contained in the vector $\mathbf{X}$ yields the probability of the mirror's quantum state while the real and imaginary parts of c_l can be used to reconstruct the phase difference between the neighboring Fock states.

In Fig. 3.3(a), we compare the exact values of the phonon number distribution of the initial state of the mirror $1/10\big(3,1,5,1\big)^T$ with the reconstructed values for two different values of the ratio between the optomechanical coupling and the oscillation frequency of the mechanical mirror, i.e., $g_m/\omega_m = 0.02$ and 0.05. The reconstructed values of the probability clearly converges to the exact values as g_m/ω_m increases.

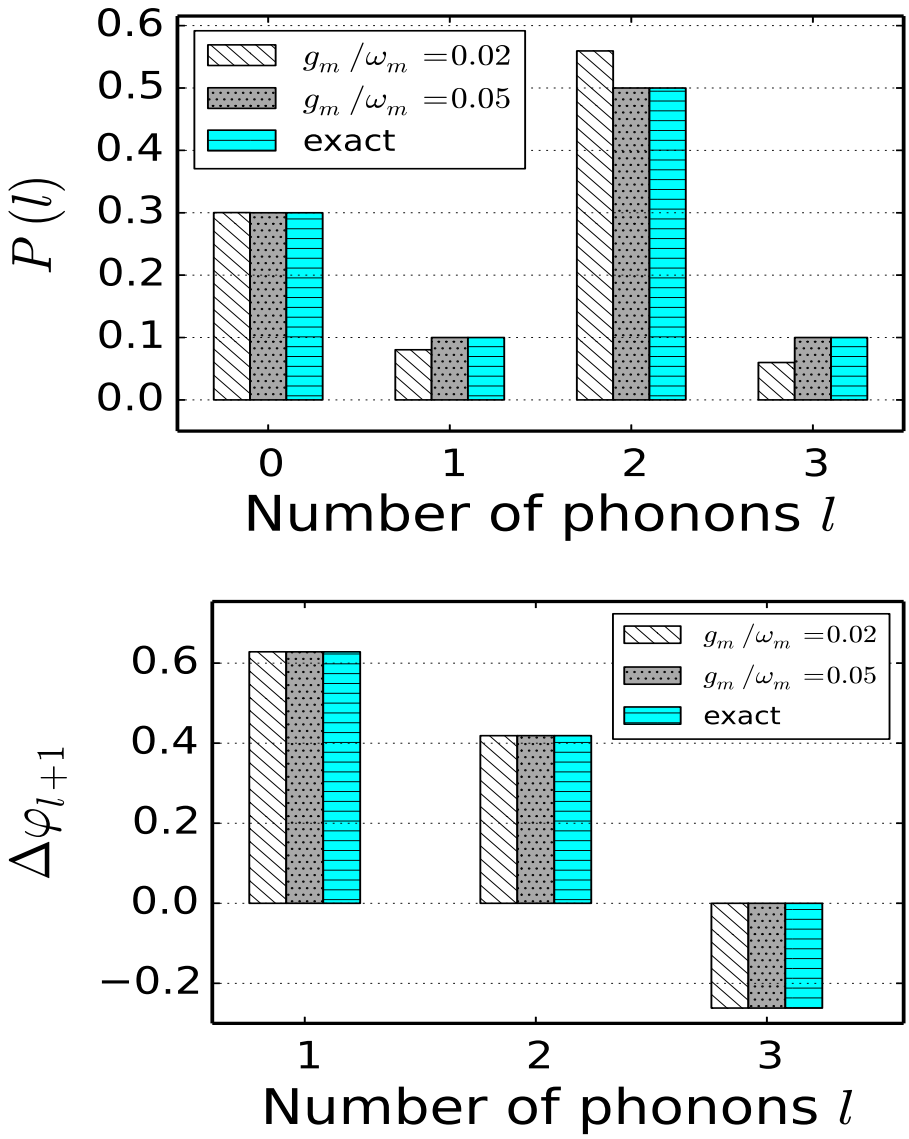

Figure 3.3: Comparison between the exact and reconstructed probability distribution of phonons (a) and the phase difference $\Delta\varphi_{l+1}$ (b) where the initial state of the mechanical mirror is given by Eq. (3.21) for two different ratios between the optomechanical coupling g_m and the mechanical frequency ω_m.

This is similar to the reconstruction of the coherent state and it is because stronger coupling strength can project more information from the mechanical mirror to the atom. The phase reconstruction is shown in Fig. 3.3(b) where we can see that the reconstructed values of the phase difference between two successive phonon numbers agrees very well with the exact values for

both coupling strengths. This indicates that the reconstruction of phase is not very sensitive to the fluctuation.

3.4.3 Squeezed vacuum state

The reconstruction method for the phase shown in subsection (3.4.2) fails when certain coefficients vanish. For example, in the squeezed vacuum state only the coefficients with even Fock number are nonzero. Then $c_l = u_l u_{l+1}^*$ is always zero and the reconstruction of phase is impossible. Fortunately, in our reconstruction method, we have the terms like $b_l = u_l u_{l+2}^*$ in addition to c_l (see Eq. (3.11)). In the squeezed vacuum state, although c_l is zero, b_l is not equal to zero from which we can still extract the phase information of the squeezed vacuum state.

The initial state of the mechanical mirror in a squeezed vacuum state can be written as

$$|\psi_{mirror}(0)\rangle = \sum_{l=0}^{\infty} C_{2l} \, |2l\rangle \, , \tag{3.22}$$

where the coefficients $C_{2\,l}$ are given by [42]

$$C_{2l} = \frac{(-1)^l}{\sqrt{\cosh r}} \frac{\sqrt{(2l)!}}{2^l \, l!} \left(e^{i\varphi} \tanh r\right)^l, \tag{3.23}$$

with r being the squeezing parameter. By solving a_l and b_l in Eq. (3.11), we can in principle reconstruct both the phonon number distribution and the phase of the squeezed vacuum state.

In Fig. 3.4(a), we plot the exact probability distribution of the mechanical mirror $P(2l) = \left|C_{2l}\right|^2$ along with the reconstructed distributions using two different values of g_m/ω_m. The reconstruction values are very close to the exact values and the quality of the probability distribution reconstruction improves as the mechanical coupling strength g_m is larger as in the previous example. In Fig. 3.4(b), we compare the exact phase differences $\Delta\varphi_{l+2}$ with the reconstructed ones using Eq. (3.18). Different from the phase reconstruction based on c_l, the reconstruction based on b_l is more sensitive to the coupling strength. Stronger coupling strength can give better phase reconstruction.

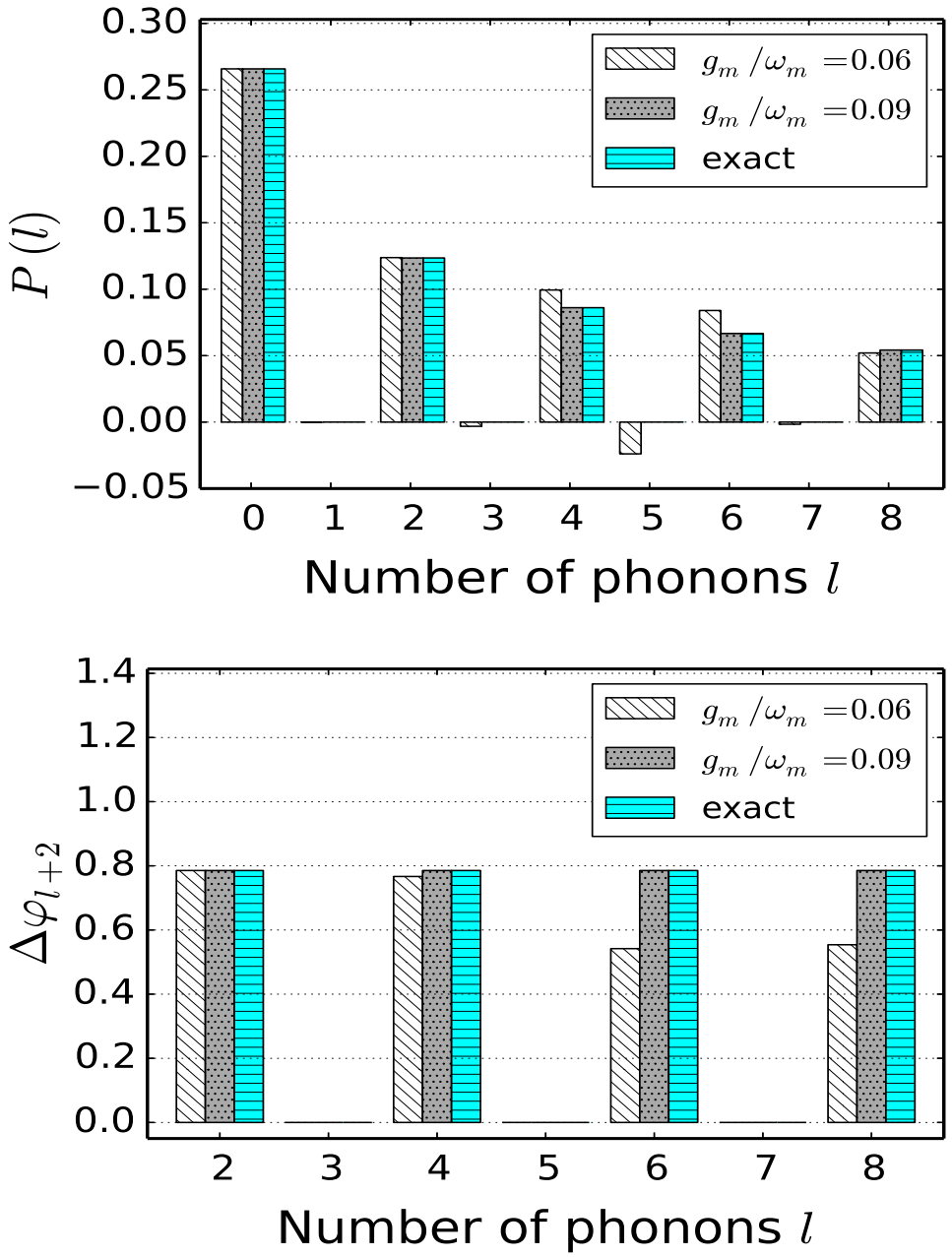

Figure 3.4: Comparison between the exact and reconstructed probability distribution of phonons (a) and the phase difference $\Delta\varphi_{l+2}$ (b) when the initial state of the mechanical mirror is squeezed vacuum for two different ratios between the optomechanical coupling g_m and the mechanical frequency ω_m. $r = 2$ and $\varphi = \pi/8$.

3.4.4 Velocity fluctuation

In the previous subsections, we assume that interaction times are precisely determined. However, in practice the interaction times can vary a bit due to the uncertainty in the velocity of atoms. In this subsection, we show that even if the interaction times have small fluctuations, our method still works very well.

Suppose that each interaction time has an uncertainty. To reconstruct the quantum state of the mechanical mirror, we measure $W(t_k)$ for N_{runs} times for each t_k and their average $\overline{W}(t_k)$ is treated as $W(t_k)$ in Eq. (3.15). Then we reconstruct the quantum state of the mechanical mirror by using the same method presented in the previous section. We consider the case when the mechanical mirror is initially prepared in a coherent state with average number of phonons $\bar{l} = 3$ and each atom velocity has 4% uncertainty. In the numerical simulation, the sampling time is randomly chosen between $t_k - 0.02\Delta t$ and $t_k + 0.02\Delta t$ for each t_k and Δt is the gap between two successive interaction times (i.e., $\Delta t = t_{k+1} - t_k$). Using the least square fitting method with 10^{-3} tolerance, we can obtain a solution for $\mathbf{X}$. The reconstructed results for two different iteration times are shown in Fig. 3.5 where Fig. 3.5(a) is the result of reconstruction using $N_{runs} = 10$ while Fig. 3.5(b) is the result of reconstruction using $N_{runs} = 30$. We see from both figures that when $N_{runs} = 10$, the reconstructed probability distribution of phonons is deviating significantly from the exact distribution of phonons. However, when the iteration times is increased to $N_{runs} = 30$, the reconstructed probability distribution of phonons converges to the exact distribution very well.

3.4.5 Reconstruction of thermal state

So far we considered quantum state reconstruction of pure states of the mirror. Next we address the question about the reconstruction of mixed states. It turns out that, for arbitrary mixed states described by a density operator ρ, our proposed method can be applied to reconstruct only the diagonal elements ρ_{ll} and the off diagonal elements $\rho_{l,l+1}$ and $\rho_{l,l+2}$. It can be shown that, for mixed states, Eq. (3.11) can be obtained with a_l, b_l and c_l replaced by ρ_{ll}, $\rho_{l,l+2}$ and $\rho_{l,l+1}$, respectively.

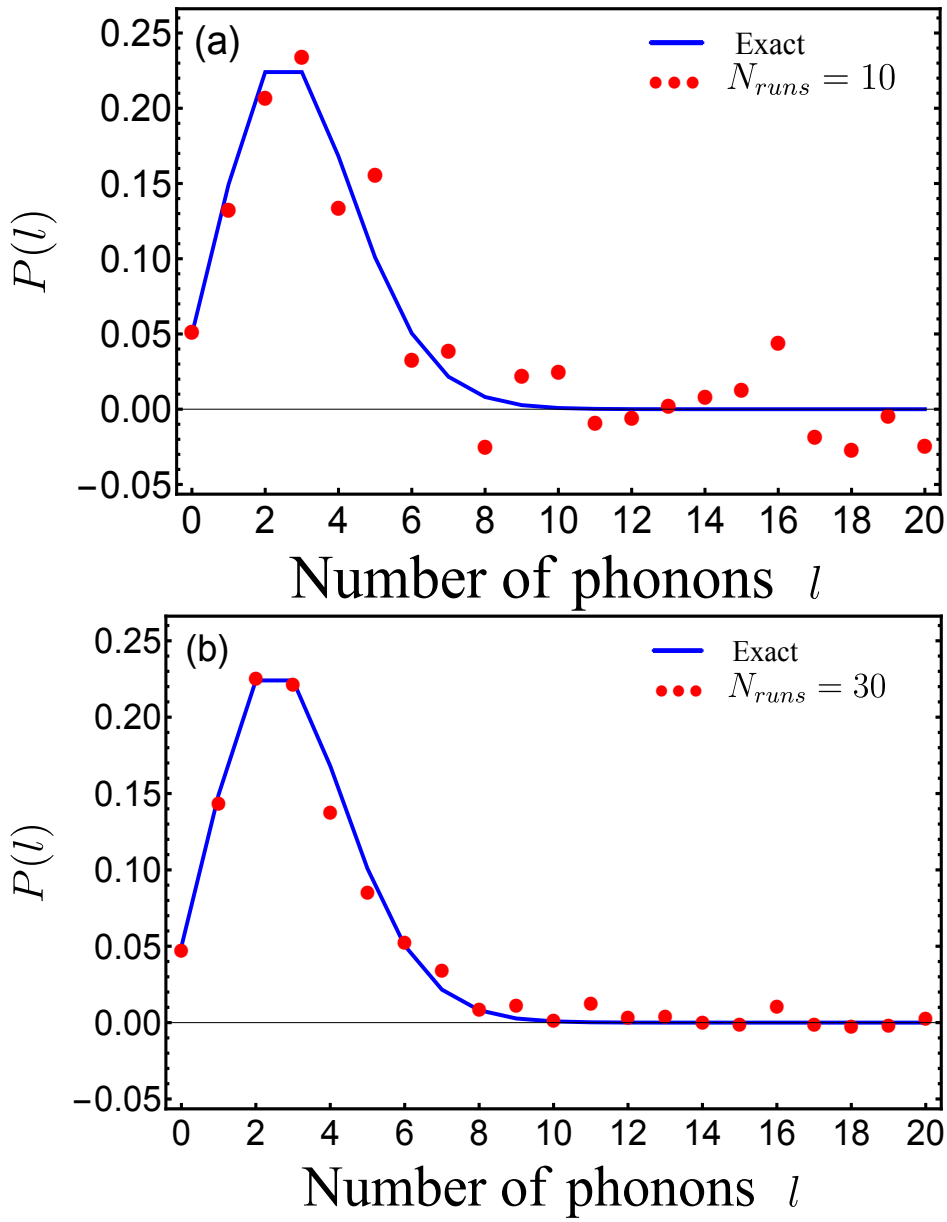

Figure 3.5: Reconstruction of the initial state of the mechanical mirror when fluctuation in the interaction times between the atoms and the cavity field is considered. (a) Number of iterations is $N_{runs} = 10$. (b) Number of iterations is $N_{runs} = 30$. The average phonon number is $\bar{l} = 3$, $g_m/\omega_m = 0.9$, and the fluctuation in the interaction times is $\pm 2\%$.

We can then use the reconstruction method discussed in previous sections to obtain the partial information of the density matrix of the mechanical mirror.

One important state of the mirror that we can reconstruct using our method is the thermal state

for which only the diagonal density matrix elements are non-vanishing. The state is given by

$$\rho^m(0) = \sum_{l=0}^{\infty} \rho_{ll} \left|l\right\rangle \left\langle l\right|, \tag{3.24}$$

where $\rho_{ll} = \frac{\bar{l}^l}{(\bar{l}+1)^{l+1}}$ is the phonon-number distribution with $\bar{l}$ being the average number of phonons. Since the thermal state has only the diagonal terms, the coefficients shown in Eq. (3.11) are $a_l = \rho_{ll}$ and $b_l = c_l = 0$. Therefore, the population inversion $W(t)$ for the thermal state is given by

$$W(t) = \sum_{l=0}^{\infty} \cos\left(g_{p0}\sqrt{l}t\right) \cos\left(g_{p0}\sqrt{l+1}t\right) \cos\left(\omega_m t\right) \rho_{ll}. \tag{3.25}$$

Using the same method discussed above, we can reconstruct the phonon-distribution for the thermal state.

The numerical results are shown in Fig. 3.6 where we assume the average phonon number $\bar{l} = 2$. In Fig. 3.6(a) we compare the reconstruction results for two different cutoffs with the exact thermal distribution. We can see that when l_{max} is not large enough, the reconstruction deviates from the exact distribution significantly. However, if we increase the cutoff l_{max}, the reconstruction result matches the exact thermal distribution very well. In Fig. 3.6(b), we show the reconstruction results for two different coupling strengths. It shows that larger coupling strength can give better reconstruction result. In Fig. 3.6(c), we consider the case when the velocity of the atoms has certain uncertainty. In the figure, we compare the reconstruction results for two different velocity uncertainties, i.e., 2% and 4%. It is shown that smaller uncertainty can have better reconstruction results. Even if the uncertainty is 4%, the reconstructed phonon distribution cans still be very close to the exact thermal phonon distribution.

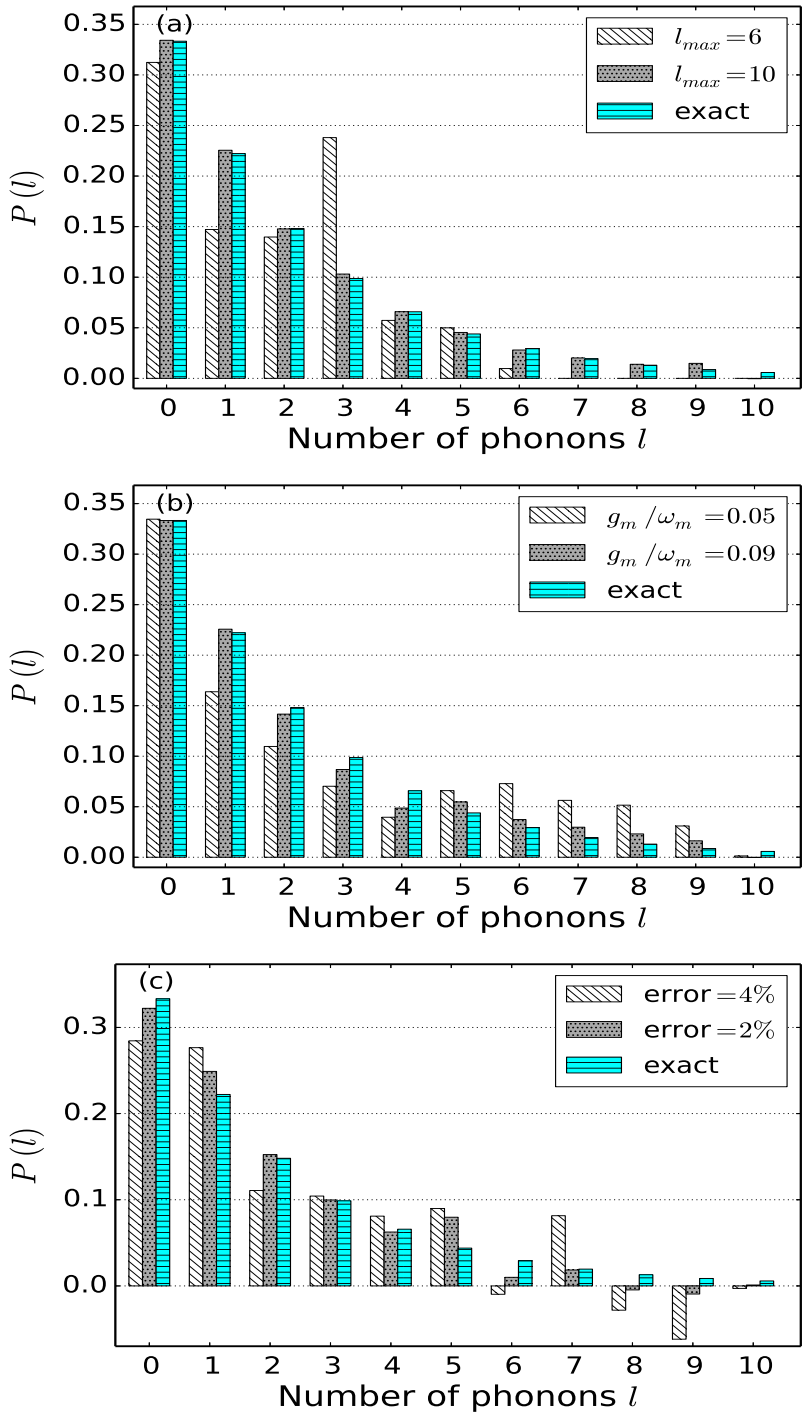

Figure 3.6: Comparison between the exact and reconstructed phonon-number distributions for initially mechanical thermal state. (a) The comparison is made using $l_{max} = 6$ and $l_{max} = 10$ with $g_m/\omega_m = 0.07$. (b) The comparison is made for two different coupling strength ($g_m/\omega_m = 0.05$ and 0.09) with $l_{max} = 10$. (c) The comparison is made using two different values for the fluctuation in the interaction time, 4% and 2% with $g_m/\omega_m = 0.09$ and $l_{max} = 10$. Mean number of phonons is $\bar{l} = 2$.

3.5 Conclusion

In this chapter, we proposed a scheme to detect the quantum state of the mechanical mirror. In this scheme, a beam of two-level atoms initially prepared in the excited state are sent through an optomechanical cavity to interact with the cavity field. The polariton formed by the atom and the cavity field can effectively couple to the phonon of the mechanical mirror. From this coupling, the quantum state of the mechanical mirror can imprint to the dynamics of the atom. By measuring the probability of the atoms to be in the excited state when exciting the optomechanical cavity, it is possible to reconstruct the full quantum state of the mechanical mirror including both the phonon number distribution and the phase even if the interaction times have a certain amount of uncertainty. We also show that mechanical thermal state can be reconstructed with high fidelity. Our method does not require a strong optomechanical coupling and it may provide a useful tool in the quantum information processing based on optomechanical systems.

4. QUANTUM STATE MEASUREMENT OF A MECHANICAL MIRROR

4.1 Introduction

Cavity optomechanics [10, 93, 75] which explores the interaction between electromagnetic fields and mechanical states of motion has recently been developed and dramatically extended to investigate different phenomena in quantum physics. Mechanical motion of nanomechanical or micromechanical oscillators can be effectively coupled to a cavity field via the radiation-pressure force. A number of interesting phenomena has been demonstrated in the area of optomechanics such as cooling of mechanical motion near its ground state [14, 94, 95, 41, 18, 15, 96, 12, 16, 19, 21], macroscopic quantum superposition [23, 49, 97, 25, 24], quantum entanglement between light and mechanical motion [28, 98, 99, 100] and between mechanical oscillators [26, 101, 31, 32, 33, 102, 103]. Quantum systems such as optomechanical systems could therefore be exploited to explain some fundamental questions in modern physics. An important task for these purposes is the ability to measure the quantum state of mechanical motion in optomechanical systems.

Reconstruction of quantum state is very important in many quantum optics experiments as it allows to characterize full information of the quantum system. In cavity optomechanics, few schemes [38, 39, 40, 41] have been proposed for the measurement of mechanical states of motion. In [41], a detector atom based scheme was proposed to reconstruct the mechanical state of a nanomechanical oscillator where the atom is directly coupled to the oscillator by a magnetic field. Another proposal for mechanical state reconstruction [40], is based on extracting the information about the mechanical state from the measured emission and scattering spectra of a single photon after decaying outside the optomechancial cavity. Mechanical state tomography scheme [38] employing short optical pulses has also been proposed in an optomechanical system where the position of the mechanical oscillator can be obtained from the phase of the pulse when it exits the cavity.

More recently, we studied a hybrid optomechanical system [92] where a single photon cavity

is simultaneously coupled to a two-level atom and a mechanical mirror. We show that the atomic population inversion dynamics can be modified in such a way that it induces collapses and revivals in the population inversion signal which is known to be periodic when the cavity field is in a Fock state and in the absence of any optomechanical coupling (JC-model). Inspired by the idea of using atoms as tool to measure the quantum state of a cavity field via atom-field coupling [80], here we propose a method to measure the quantum state of a mechanical mirror via polariton-phonon coupling. The motivation behind this idea is that different mechanical states modifies the population inversion of the atom differently. By sending a beam of two-level atoms to interact with the optomechanical cavity field, we showed that the quantum state of the mechanical mirror can be successfully reconstructed by measuring the excited state population of the atoms. In our method, the whole information of a pure mechanical including both the amplitude and phase can be reconstructed and partial information of a mixed mechanical state can be also reconstructed.

This chapter is organized as follows: In Sec. 4.2, we describe the model used to reconstruct the full density matrix of the initial mechanical state. In Sec. 4.3, we give the derivation of the atomic population inversion when the mirror is in a mixed state. In Sec. 4.4, we explain the mathematical method of using the population inversion to measure the initial state of the mirror. In Sec. 4.5, we summarize our results.

4.2 Model

The schematic setup for measuring the quantum state of the mechanical mirror is shown in Fig. 4.1. The system is composed of an optical cavity with an oscillating mirror on one side of the cavity. The cavity field interacts with the mechanical mode through the radiation-pressure coupling. To detect the quantum state of the mechanical mirror, a beam of two-level atoms is sent to pass through the cavity. The atoms can interact with the cavity field and effectively couple to the mechanical phonon through polariton-phonon coupling. The population dynamics of the atoms exciting the cavity can therefore encode the information of the mechanical state.

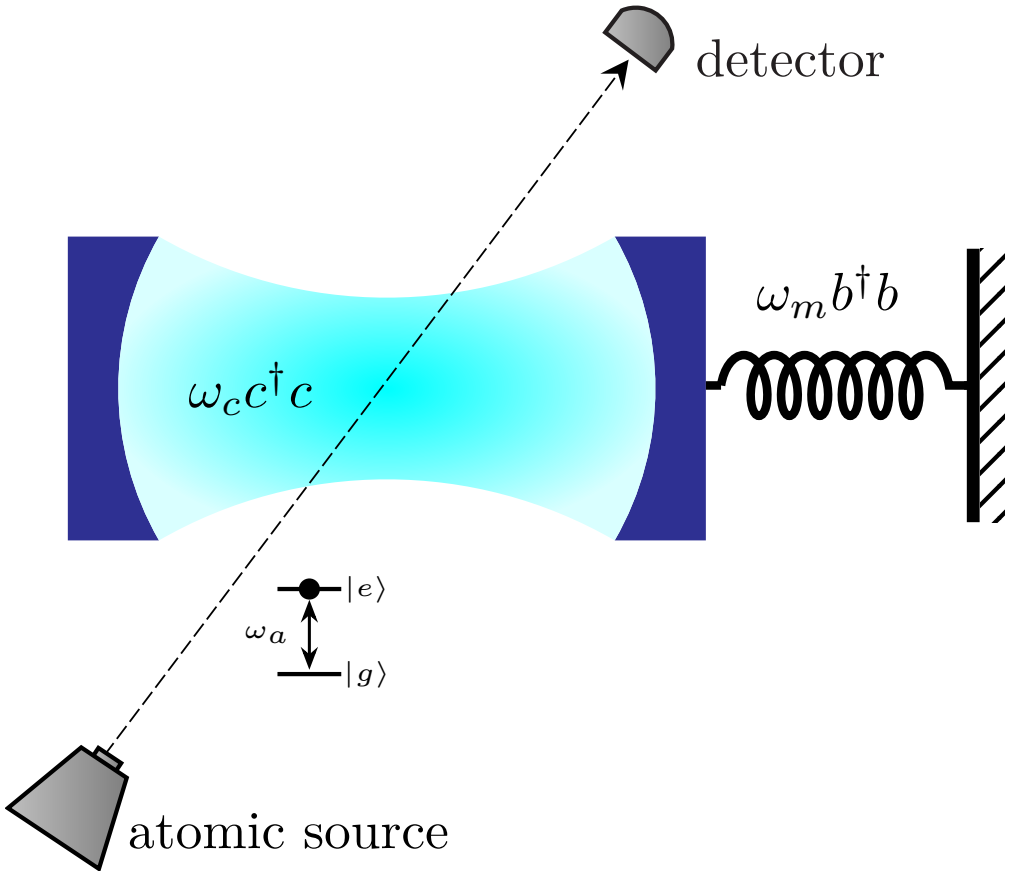

Figure 4.1: Schematic of the mechanical state reconstruction model. Two level atoms in their excited states are sent to interact with the cavity field and the probability of finding the atoms in the excited state $P_e(t)$ is measured when the atoms are exciting the cavity.

The Hamiltonian of the hybrid system is given by

$$\mathcal{H} = \mathcal{H}_0 + \mathcal{H}_I, \tag{4.1}$$

where $\mathcal{H}_0$ is the free Hamiltonian and $\mathcal{H}_I$ is the interaction Hamiltonian. The free Hamiltonian includes three parts which is given by

$$\mathcal{H}_0 = \hbar\omega_c c^\dagger c + \hbar\frac{\omega_a}{2}\sigma_z + \hbar\omega_m b^\dagger b, \tag{4.2}$$

where the first term is the cavity field Hamiltonian, the second term is the atom Hamiltonian, and

the third term is the mechanical mirror Hamiltonian. $c(c^\dagger)$ is the annihilation (creation) operator of the cavity field with cavity field frequency ω_c. σ_z is the z component of the Pauli matrix and the atomic transition frequency is ω_a. $b(b^\dagger)$ is the mechanical mirror annihilation (creation) operator. In the linear regime, the position of the mechanical mirror is given by $x = x_0(b + b^\dagger)$ where $x_0 = \sqrt{\hbar/2m\omega_m}$ is the zero point position of the mechanical mirror with m and ω_m being the mass and frequency of the mechanical mirror, respectively. The interaction part of the Hamiltonian is given by

$$\mathcal{H}_I = -i\hbar g_c(\sigma_+ c - c^\dagger \sigma_-) - \hbar g_m c^\dagger c(b^\dagger + b), \tag{4.3}$$

where the first term in (4.3) is the interaction energy operator between both the two-level atom and the cavity field with coupling strength g_c, and the second term is the interaction energy operator between the cavity field and the mechanical mirror with coupling strength g_m. $\sigma_+ = |e\rangle\langle g|$ ($\sigma_- = |g\rangle\langle e|$) is the raising (lowering) operator of the atom. The coupling strength g_m is defined as $g_m = (\omega_c/L)\sqrt{\hbar/2m\omega_m}$ where L is the length of the cavity. In fact, the form of the Hamiltonian given in Eq. (4.3) does not allow for analytical treatment of the dynamics of the system. However, the Hamiltonian Eq. (4.3) can be simplified in the weak-optomechnical coupling limit such that an approximate version of Eq. (4.3) can be obtained [67, 92] which allows us to analyze the system's evolution analytically. To make this chapter self contained, we briefly discuss the mathematical steps to get an approximation of the Hamiltonian as they have been given in details in [92].

In the interaction picture of the atom and cavity field, the free parts of the atom and cavity field Hamiltonian can be eliminated and the new interaction Hamiltonian is given as

$$\mathcal{H}_I^{'} = -i\hbar g_c(\sigma_+ c - c^\dagger \sigma_-) + \hbar\omega_m b^\dagger b - \hbar g_m c^\dagger c(b^\dagger + b), \tag{4.4}$$

where we assume that the cavity field is in resonance with the atom, i. e., $\delta = \omega_c - \omega_a = 0$ for simplicity. Using the unitary transformation $\mathcal{T} = e^{-\beta c^\dagger c(b^\dagger - b)}$, the transformed Hamiltonian

$\mathcal{H}_{\mathcal{T}} = \mathcal{T}\mathcal{H}_I^{'}\mathcal{T}^{\dagger}$ reduces to

$$\mathcal{H}_{\mathcal{T}} \approx -i\hbar g_c(\sigma_+ c - c^{\dagger}\sigma_-) + \hbar\omega_m b^{\dagger}b - i\hbar\beta g_c(\sigma_+ c + c^{\dagger}\sigma_-)(b^{\dagger} - b), \tag{4.5}$$

Here, only the linear terms are kept in Eq. (4.5) which is a valid approxiamtion in the case of weak optomechanical coupling, i.e., $\beta = g_m/\omega_m \ll 1$.

We can further simplify the transformed Hamiltonian in Eq. (4.5) by transforming the bare bases to the atom-field dressed state bases or the polariton bases. We define the polariton states of the atom-field subsystem as $|+, n\rangle = 1/\sqrt{2}\big(\,|e, n\rangle + i\,|g, n+1\rangle\,\big)$ and $|-, n\rangle = 1/\sqrt{2}\big(\,|e, n\rangle - i\,|g, n+1\rangle\,\big)$. Under these new polariton state bases, the first term of Eq. (4.5) can be diagonalized because $\mathcal{H}_{ac}\,|\pm, n\rangle = \pm\hbar\Omega_n/2\,|\pm, n\rangle$ where $\mathcal{H}_{ac} = -i\hbar g_c(\sigma_+ c - c^{\dagger}\sigma_-)$ and $\Omega_n = 2g_c\sqrt{n+1}$ is the spliting between two polariton branches. We can then define the new Pauli matrices for the polariton states such that $\sigma_z^{(n)}\,|\pm, n\rangle = \pm\,|\pm, n\rangle$ and $\sigma_{\mp}^{(n)}\,|\pm, n\rangle = |\mp, n\rangle$. Under these new polariton Pauli matrixes, the Hamiltonian in Eq. (4.5) after applying the rotating-wave approximation becomes [67, 92]

$$\mathcal{H}_{\mathcal{T}}^{'} = \sum_{n=1}^{\infty}\left[\hbar\frac{\Omega_n}{2}\sigma_z^{(n)} + \hbar g_{pn}\Big(\sigma_-^{(n)}b^{\dagger} + \sigma_+^{(n)}b\Big)\right] + \hbar\omega_m b^{\dagger}b, \tag{4.6}$$

where we assume $\omega_m + \Omega_n \gg g_{pn} \gg |\omega_m - \Omega_n|$ and $g_{pn} = \beta g_c\sqrt{n+1}$ is the effective coupling between the polariton and phonon. The Hamiltonian shown in Eq. (4.6) is a JC-like Hamiltonian where the polariton and the phonon couples to each other effectively.

4.3 Population inversion of the atom

We consider that the atom is initially in the excited state $|e\rangle$ and the cavity field is in a Fock state $|n\rangle$. The mechanical mirror is initially assumed to be in a mixed state $\rho^m(0)$. The density operator for the initial state of the total system is given by [92]

$$\rho(0) = \rho^p(0) \otimes \rho^m(0), \tag{4.7}$$

where $\rho^p(0)$ describes the density operator of the polariton. We use the equation of motion for the density matrix to study the dynamics of the system which is given by

$$\dot{\rho} = -\frac{i}{\hbar}[\mathcal{V}, \rho], \tag{4.8}$$

where the system's interaction picture Hamiltonian $\mathcal{V}$ is the rotating wave approximation of Eq. (4.6) and it is given by [92]

$$\mathcal{V} = \sum_{n=1}^{\infty} \hbar g_{pn} \left[\sigma_-^{(n)} b^\dagger e^{i(\omega_m - \Omega_n)t} - \sigma_+^{(n)} b e^{-i(\omega_m - \Omega_n)t}\right]. \tag{4.9}$$

The solution of Eq. (B.3) can be written using the time evolution operator $U(t)$ as

$$\rho(t) = U(t)\rho(0)U^\dagger(t). \tag{4.10}$$

Tracing over the mirror states directly yields the density operator of polariton state [92] and the density matrix elements of the polariton state can be expressed as

$$\rho_{ij}^p(t) = \sum_{k=0}^{\infty} \langle k, n, i| \, \rho(t) \, |j, n, k\rangle \,, \tag{4.11}$$

where $i, j \equiv +, -$. The probability to find the atom in its excited state is given by [92]

$$P_e(t) = \frac{1}{2}\Big[\rho_{++}^p(t) + \rho_{--}^p(t) + e^{i\omega_m t}\, \rho_{+-}^p(t) + e^{-i\omega_m t}\, \rho_{-+}^p(t)\Big]. \tag{4.12}$$

The density matrix elements $\rho_{++}^p(t)$, $\rho_{--}^p(t)$, $\rho_{+-}^p(t)$, and $\rho_{-+}^p(t)$ in Eq. (4.12) can be calculated using Eq. (E.1) and they are explicitly given by Eq. (E.3) (see appendix A) for an initial mixed state of the mechanical mirror $\rho^m(0)$. By substituting Eq. (E.3) into Eq. (4.12), the atomic population

inversion is given by

$$
\begin{aligned}
W(t) = \sum_{l=0}^{\infty} \Bigg[& \cos\left(g_{pn}\sqrt{l}t\right)\cos\left(g_{pn}\sqrt{l+1}t\right)\cos\left(\omega_m t\right)\rho_{l,l}^{m}(0) + \sin\left(g_{pn}\sqrt{l+1}t\right) \\
& \times \left(\cos\left(g_{pn}\sqrt{l+2}t\right) - \cos\left(g_{pn}\sqrt{l}t\right)\right)\Big(\cos\left(\omega_m t\right)\mathrm{Im}\left(\rho_{l+1,l}^{m}(0)\right) \\
& - \sin\left(\omega_m t\right)\mathrm{Re}\left(\rho_{l+1,l}^{m}(0)\right)\Big) + \sin\left(g_{pn}\sqrt{l+1}t\right)\sin\left(g_{pn}\sqrt{l+2}t\right) \\
& \times \Big(\cos\left(\omega_m t\right)\mathrm{Re}\left(\rho_{l,l+2}^{m}(0)\right) + \sin\left(\omega_m t\right)\mathrm{Im}\left(\rho_{l+2,l}^{m}(0)\right)\Big)\Bigg],
\end{aligned}
\tag{4.13}
$$

where the population inversion is defined as $W(t) = 2P_e(t) - 1$, and $\rho_{i,j}^{m}(0) = \langle i|\,\rho^{m}(0)\,|j\rangle$ is the density matrix elements of the mechanical mirror with $i, j \equiv \{l, l+1, l+2\}$ and l is the phonon number. It is clearly seen that the population of the atom after the interaction depends on the mechanical quantum state. This property can be used to reconstruct the mechanical state.

Let us first consider the simplest case when the mechanical mirror is initially in a Fock state i.e., $\rho^{m}(0) = |l\rangle\langle l|$. In this case, the population inversion shown in Eq. (4.13) reduces to

$$
W(t) = \cos\left(\omega_m t\right)\cos\left(g_{pn}\sqrt{l}t\right)\cos\left(g_{pn}\sqrt{l+1}t\right). \tag{4.14}
$$

In the absence of the optomechanical coupling, i.e., $g_m = 0$, we have $g_{pn} = 0$ and the population inversion Eq. (4.14) goes back to the result of JC-model, i.e., $W(t) = \cos\left(\omega_m t\right)$. In Eq. (4.14), we see that the periodic oscillations of the atomic population inversion (JC-model) when the cavity field is in a Fock state is modified by the cosine functions $\cos\left(g_{pn}\sqrt{l}t\right)$ and $\cos\left(g_{pn}\sqrt{l+1}t\right)$ due to the optomechanical coupling. In Fig. 4.2(a) and 4.2(b), the population inversion is shown for the cases when the mechanical states are $|0\rangle$ and $|2\rangle$, respectively. It is obviously seen that different mechanical states yield different signals of the population inversion although the optomechanical coupling is weak. When the mechanical mirror is in a lower Fock state, the period of the collapse and revival is longer.

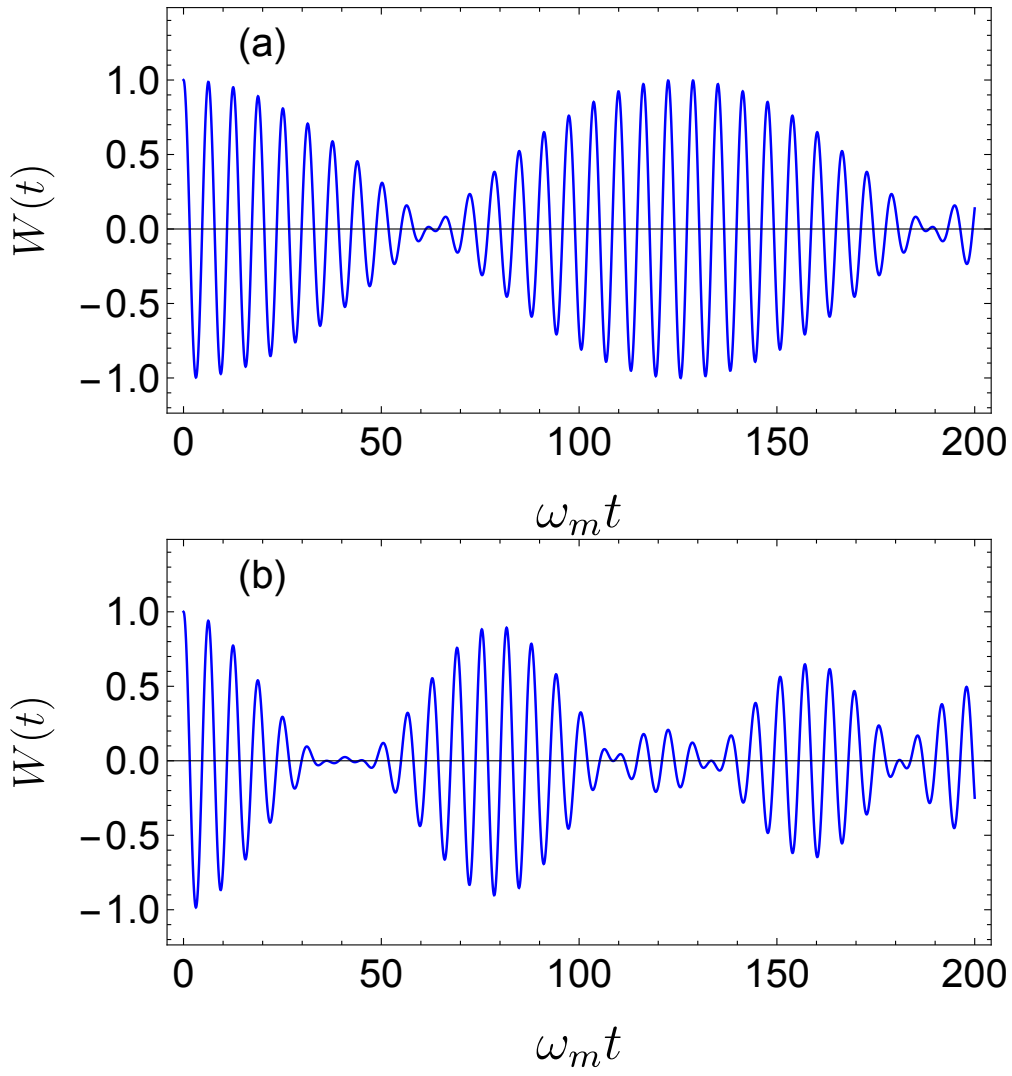

Figure 4.2: Atomic population inversion as a function of time for initial mechanical Fock state (a) $\rho^m(0) = |0\rangle\langle 0|$ and (b) $\rho^m(0) = |2\rangle\langle 2|$. We considered resonant atom-field interaction ($\delta = 0$), $g_c = \omega_m/2$, and $g_m = 0.05\omega_m$.

When the mechanical mirror is initially in a thermal state which is the usual case ($\rho^m_{l,l}(0) = \sum_{l=0}^{\infty} \frac{\bar{l}^l}{(\bar{l}+1)^{l+1}} |l\rangle\langle l|$), the atomic population inversion Eq. (4.13) becomes

$$W(t) = \sum_{l=0}^{\infty} \frac{\bar{l}^l}{(\bar{l}+1)^{l+1}} \cos\left(g_{pn}\sqrt{l}t\right) \cos\left(g_{pn}\sqrt{l+1}t\right) \cos\left(\omega_m t\right), \tag{4.15}$$

where $\bar{l}$ is the average number of thermal phonons of the mechanical state. In Fig. 4.3(a) and

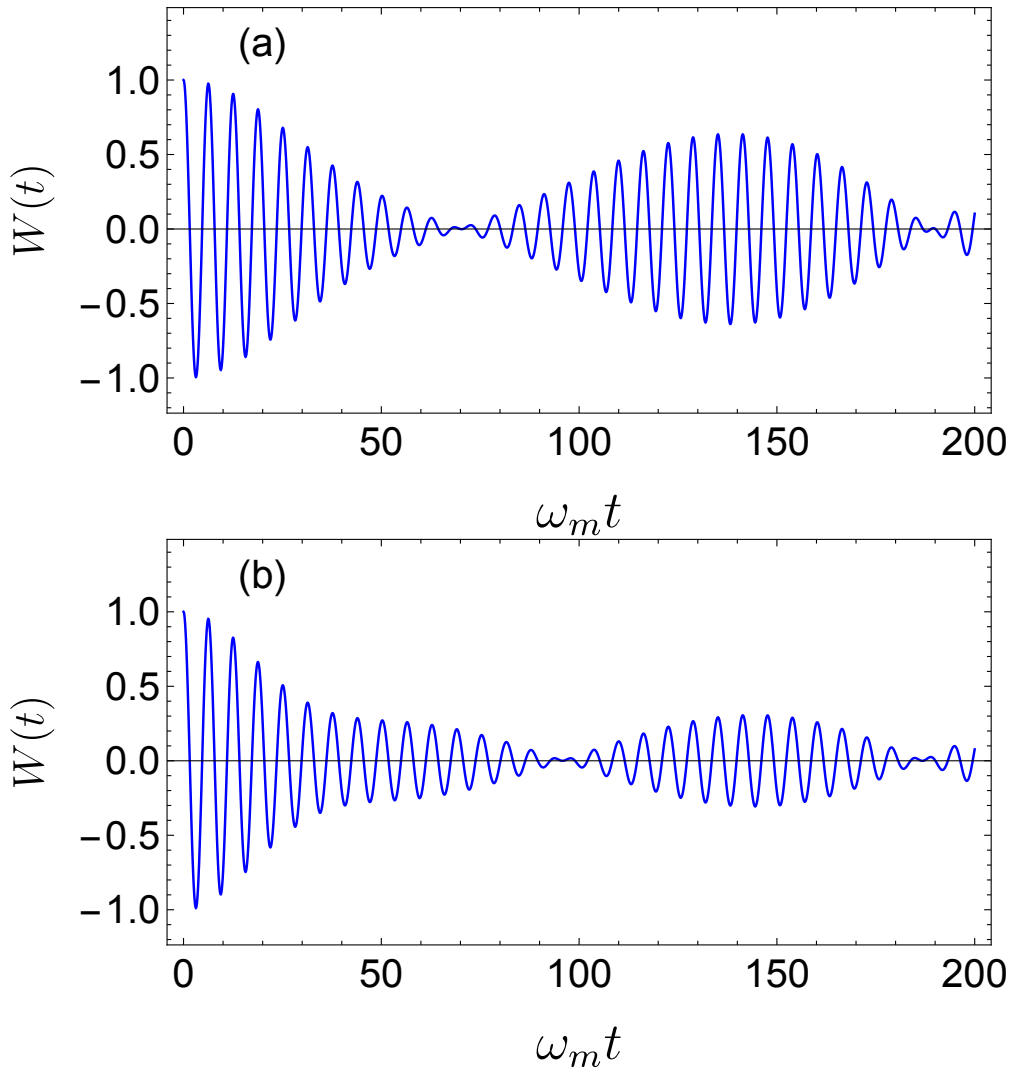

Figure 4.3: Atomic population inversion as a function of time for initial mechanical thermal state for two different mean number of thermal phonons (a) $\bar{l} = 0.5$ and (b) $\bar{l} = 1.5$. We considered resonant atom-field interaction ($\delta = 0$), $g_c = \omega_m/2$, and $g_m = 0.05\omega_m$.

4.3(b), we show the result of Eq. (4.15) for different average number of thermal phonons, i.e., $\bar{l} = 0.5$ and 1.5, respectively. Similar to the mechanical Fock states, mechanical thermal states apparently yield different oscillations of the population inversion which correspond to different average number of thermal phonons. The population inversion decays more quickly with larger average phonon number.

The fact of having different population inversion signals for different mechanical states where the mechanical mirror and the cavity field are weakly coupled motivate the idea of using the atomic

population inversion to extract the initial state of the mechanical mirror. The population inversion can be obtained by measuring the probability of finding the atom in the excited state $P_e(t)$. In the next section, we show how the result Eq. (4.13) can be used to measure the state of the mechanical mirror and we give several examples of mechanical states that can be reconstructed using Eq. (4.13).

4.4 Reconstruction of mechanical mixed state

It is obvious from Eq. (13) that the population inversion (4.13) depends on the density matrix elements $\rho^m_{l,l}(0)$, $\rho^m_{l,l+1}(0)$, $\rho^m_{l+1,l}(0)$, $\rho^m_{l,l+2}(0)$, $\rho^m_{l+2,l}(0)$. Thus, by just measuring $W(t)$ for different interaction times, we are in principle able to determine all the diagonal terms and some off-diagonal terms of the initial density matrix.

Since $W(t)$ depends on infinite summation of the density matrix elements, in practice to reconstruct the quantum state we have to choose a maximum number of phonons l_{max} and this maximum number is much larger than the mean number of phonons $\bar{l}$ i.e., $l_{max} \gg \bar{l}$. For the chosen maximum number of phonons l_{max}, there are a total of $5(l_{max}+1)$ unknown variables to be determined. This apparently requires at least $5(l_{max}+1)$ total number of measurements of the population inversion $W(t)$ in order to find all the $5(l_{max}+1)$ unknown variables. For this purpose, we rewrite Eq. (4.13) as

$$\begin{aligned} W(t_k) = \sum_{l=0}^{l_{max}} \Big[& A_l(t_k)\, \rho^m_{l,l}(0) + B_l(t_k)\, \mathrm{Re}\left(\rho^m_{l,l+1}(0)\right) + C_l(t_k)\, \mathrm{Im}\left(\rho^m_{l+1,l}(0)\right) \\ & + D_l(t_k)\, \mathrm{Re}\left(\rho^m_{l,l+2}(0)\right) + E_l(t_k)\, \mathrm{Im}\left(\rho^m_{l+2,l}(0)\right) \Big], \end{aligned} \tag{4.16}$$

where $k = 1, 2, ..., 5(l_{max}+1)$. Equation (4.16) can be rewritten as a linear system of equations such that

$$\mathbf{W} = \mathbf{M}\, \boldsymbol{\rho}, \tag{4.17}$$

where the vectors $\mathbf{W}$ and $\boldsymbol{\rho}$ are both $5(l_{max}+1)$-dimensional vectors. The vector $\mathbf{W}$ holds the measured data of the population inversion for $5(l_{max}+1)$ different interaction times. The vector $\boldsymbol{\rho}$ contains $5(l_{max}+1)$ density matrix elements to be determined where for each l, there are five density

matrix elements i.e., $\boldsymbol{\rho_l} = \Big(\rho^m_{l,l}(0), \mathrm{Re}\left(\rho^m_{l,l+1}(0)\right), \mathrm{Im}\left(\rho^m_{l+1,l}(0)\right), \mathrm{Re}\left(\rho^m_{l,l+2}(0)\right), \mathrm{Im}\left(\rho^m_{l+2,l}(0)\right)\Big)^T$. The matrix $\mathbf{M}$ is a square matrix defined as

$$\mathbf{M}_{k\,l} = A_l(t_k) + B_l(t_k) + C_l(t_k) + D_l(t_k) + E_l(t_k), \tag{4.18}$$

where the elements of the matrix $\mathbf{M}$ are given by

$$A_l(t_k) = \cos\left(g_{p0}\sqrt{l}t_k\right)\cos\left(g_{p0}\sqrt{l+1}t_k\right)\cos\left(\omega_m t_k\right) \tag{4.19a}$$

$$B_l(t_k) = \sin\left(g_{p0}\sqrt{l+1}t_k\right)\sin\left(g_{p0}\sqrt{l+2}t_k\right)\cos(\omega_m t_k) \tag{4.19b}$$

$$C_l(t_k) = -\sin\left(g_{p0}\sqrt{l+1}t_k\right)\sin\left(g_{p0}\sqrt{l+2}t_k\right)\sin(\omega_m t_k) \tag{4.19c}$$

$$D_l(t_k) = \Big[\cos\left(g_{p0}\sqrt{l+2}t_k\right) - \cos\left(g_{p0}\sqrt{l}t_k\right)\Big]\sin\left(g_{p0}\sqrt{l+1}t_k\right)\sin(\omega_m t_k) \tag{4.19d}$$

$$E_l(t_k) = \Big[\cos\left(g_{p0}\sqrt{l+2}t_k\right) - \cos\left(g_{p0}\sqrt{l}t_k\right)\Big]\sin\left(g_{p0}\sqrt{l+1}t_k\right)\cos(\omega_m t_k). \tag{4.19e}$$

Having the measured data, we can then use the least square fitting method to solve Eq. (4.17) and reconstruct the quantum state of the mechanical mirror. In the next subsections, we give several examples to show how the method described here can be used to reconstruct the initial state of the mechanical mirror.

4.4.1 Reconstruction of mechanical pure state

In this subsection, we give examples when the mechanical mirror is in a pure state and we show that Eq. (4.17) can be used to reconstruct such states with very good agreement to the exact initial states of the mechanical mirror.

In reality, there is a certain uncertainty in the velocity of atoms when they pass through the cavity. In Fig. 4.4, we consider two states, vacuum state $\psi(0) = |0\rangle$ and superposition of Fock states $\psi(0) = 1/\sqrt{2}\big(\,|1\rangle + |2\rangle\,\big)$, and compare the reconstructed states to the exact states.

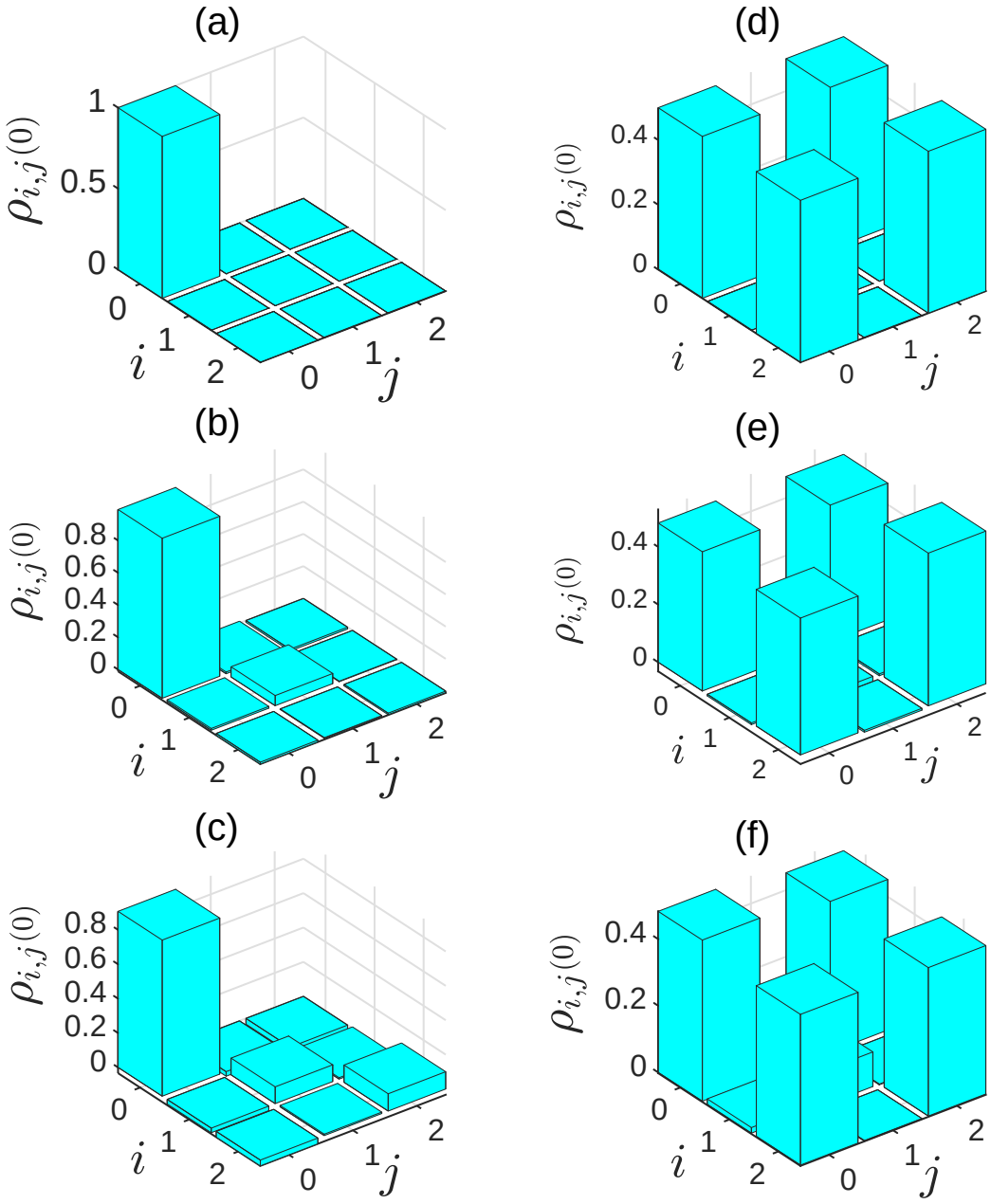

Figure 4.4: Reconstruction of the density matrix elements for initially pure mechanical states. (a-c) Initial mechanical state is $\psi(0) = |0\rangle$ state. (d-f) Initial mechanical state is $\psi(0) = 1/\sqrt{2}\big(|1\rangle + |2\rangle\big)$ state. (a) and (d) Exact density matrix elements. (b) and (e) The reconstructed density matrix elements when the interaction time has 2% fluctuation. (f) and (g) The reconstructed density matrix elements when the interaction time has 4% fluctuation. Other parameters are $g_m/\omega_m = 0.05$ and $N_{runs} = 30$.

In both figures, we compare the reconstructed results the atom velocity has 2% and 4% uncer-

tainties with the exact mechanical state. We randomly choose the sampling points of time between $t_k - 0.01\Delta t$ and $t_k + 0.01\Delta t$ in Figs. 4(b) and 4(e) and between $t_k - 0.02\Delta t$ and $t_k + 0.02\Delta t$ in Fig. 4.4(c) and 4.4(f) where $\Delta t = t_{k+1} - t_k$. At each t_k, the population inversion $W(t_k)$ is measured $N_{runs} = 30$ times and then the average of the population inversion is taken.

Figures. 4(a) and 4(d) shows the exact density matrices for the mechanical states $\psi(0) = |0\rangle$ and $\psi(0) = 1/\sqrt{2}\big(\,|1\rangle + |2\rangle\,\big)$, respectively. In Figs. 4(b) and 4(e), we show the reconstructed density matrix elements when the interaction time has 2% fluctuation, and Figs. 4(c) and 4(f) are the reconstructed density matrix elements when the interaction time has 4% fluctuation. It is clearly seen that in both examples the reconstructed density matrices are very close to their corresponding exact density matrices. When the interaction time has 2% fluctuation, the fidelity between the reconstructed density matrix and the exact density matrix when the mechanical state is $\psi(0) = |0\rangle$ and $\psi(0) = 1/\sqrt{2}\big(\,|1\rangle + |2\rangle\,\big)$ are 0.996% and 0.99%, respectively. When the interaction time has 4% fluctuation, the fidelity in both cases are 0.952% and 0.957%.

4.4.2 Reconstruction of mechanical thermal state

An interesting and more practical example to consider is the case when the mechanical mirror is initially in a thermal state. The initial state of the mechanical mirror in this case is given by

$$\rho^m(0) = \sum_{l=0}^{\infty} \frac{\bar{l}^l}{(\bar{l}+1)^{l+1}} \,|l\rangle\,\langle l|\,, \tag{4.20}$$

where $\bar{l}$ is the average number of phonons. It is clearly seen that the density matrix has only diagonal terms in the thermal state. Eq. (16) then becomes

$$W(t_k) = \sum_{l=0}^{l_{max}} A_l(t_k)\rho_{ll}^m(0) \tag{4.21}$$

from which we can reconstruct the thermal phonon distribution.

The numerical results are shown in Fig. 4.5. In Fig. 4.5(a), we compare the reconstructed and the exact phonon-number distributions for two different cutoffs l_{max} (i.e., $l_{max} = 10$ and $l_{max=14}$)

with $\bar{l} = 3$. It is shown that larger l_{max} yields better reconstructed phonon-number distribution. Thus, in practice l_{max} should be large enough to give a good reconstruction. We also consider the effect of velocity fluctuation and the result is shown in Fig. 4.5(b). Here, we also chose $\bar{l} = 3$ and fix $l_{max} = 15$ and compare the reconstructed phonon-number distribution to the exact one using different interaction time fluctuation, i.e., 2% and 4% uncertainties in the velocities of the atoms passing the cavity. We find that even if the interaction time has 4% fluctuation the reconstructed phonon distribution can still be very close to the exact thermal phonon distribution. It again shows that our method can still work even if the velocity of the atoms has certain fluctuations.

4.4.3 Reconstruction of general density matrix

In addition to the pure states and the thermal states, we can also reconstruct partial information of a general mixed state. In particularly, we can reconstruct the diagonal terms and the non-diagonal terms like $\rho_{l,l+1}$ and $\rho_{l,l+2}$. For example, in Fig. 4.6 we consider reconstruction of the following density matrix

$$\rho^m(0) = \begin{pmatrix} 0.2 & 0.1 & 0.2 \\ 0.1 & 0.3 & 0.1 \\ 0.2 & 0.1 & 0.5 \end{pmatrix}. \tag{4.22}$$

In Figs. 4.6(b) and 4.6(c), we show the reconstructed density matrix elements when the interaction time has 2% and 4% fluctuation, respectively. The fidelity between the reconstructed density matrix and the exact density matrix in Fig. 4.6(b) is 0.99 and in Fig. 4.6(c) is 0.957.

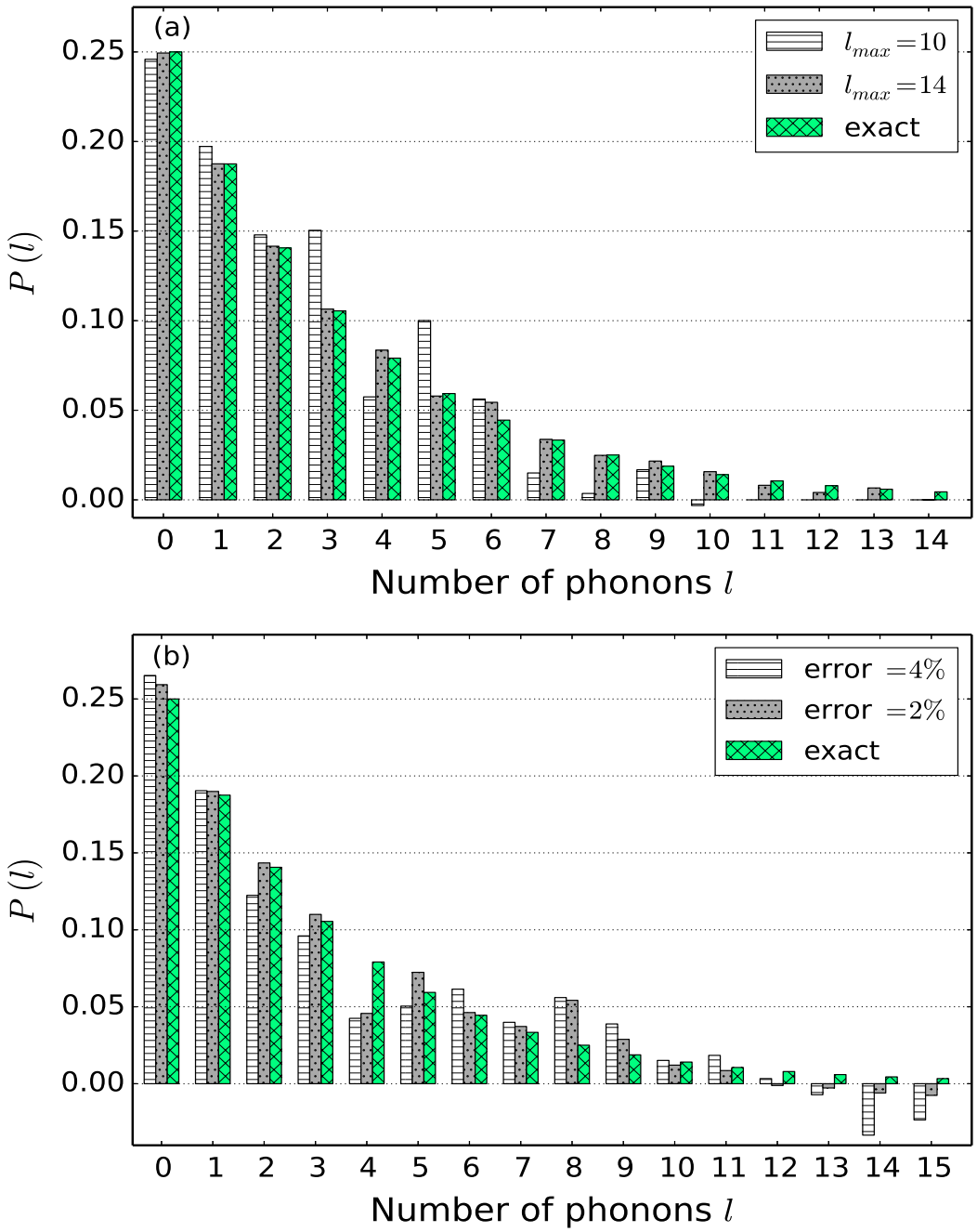

Figure 4.5: Comparison between the exact and reconstructed phonon-number distributions for initially mechanical thermal state. (a) The comparison is made using $l_{max} = 10$ and $l_{max} = 14$ with $g_m/\omega_m = 0.06$. (b) The comparison is made using two different values for the fluctuation in the interaction time, 4% and 2% with $g_m/\omega_m = 0.09$ and $l_{max} = 15$. Mean number of phonons is $\bar{l} = 3$ in both subfigures.

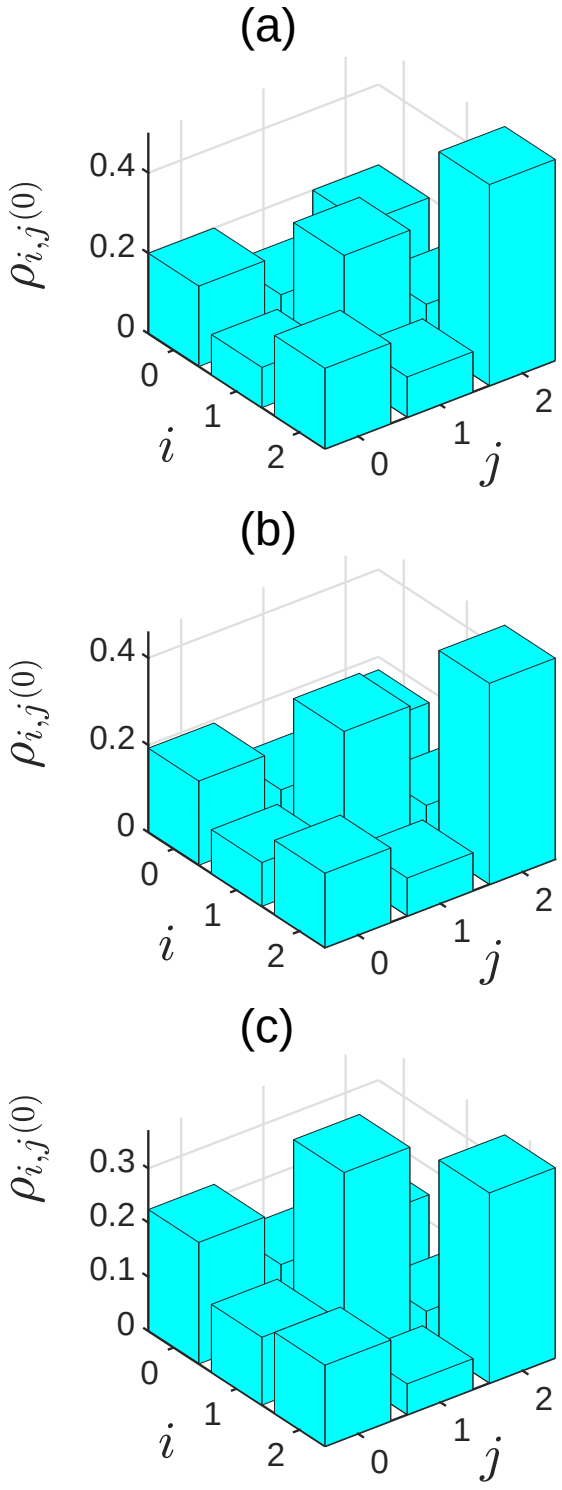

Figure 4.6: Reconstruction of a general density matrix. (a) The exact density matrix elements to be reconstructed. (b) Reconstruction of the density matrix elements when the interaction time has 2% fluctuation. (c) Reconstruction of the density matrix elements when the interaction time has 4% fluctuation.

4.5 Conclusion

In summary, we consider an optomechanical system where a beam of two-level atoms can pass through an optomechanical cavity to interact with a quantized field. The atomic population inversion is modified due to the radiation-pressure coupling between the mechanical mirror and the cavity field. Therefore, the atomic population inversion reflects certain information about the mechanical quantum state. We derive an analytical solution of the atomic population inversion in the limit of weak optomechanical coupling where the mechanical mirror is initially assumed to be in a mixed state. We show that by measuring the atomic population in the excited state at different interaction times, we can reconstruct the full information of the mechanical quantum state. We numerically demonstrate that both pure and mixed mechanical state can be successfully reconstructed using our model even if the interaction time has certain fluctuation.

5. SUMMARY

In summary, we studied the population inversion of a two-level atom placed inside an optomechanical cavity. The atom is coupled to the cavity field via the JC-coupling while the mechanical mirror is coupled to the cavity field via the radiation-pressure coupling. Initially, the two-level atom is considered to be in the excited state while we assumed several initial conditions for the cavity field and the mechanical mirror. Generally, the optomechanical-coupling results in collapses and revivals in the signal of the population inversion when the cavity field and the mechanical mirror are initially considered in Fock states. On the other hand, when the cavity field is initially prepared in a coherent state while the mechanical mirror is in a Fock state, the optomechanical-coupling results in small oscillations in the region where the population inversion collapses in the original JC-model. The results of the population inversion indicates that the signal of the population inversion can be used to infer the quantum state of the mechanical mirror.

To measure the quantum mechanical state of the oscillating mirror using this system, we considered a beam of two level atoms that enter the optomechanical cavity while they are in the excited state when entering the cavity. The atoms can then interact with the cavity field which is initially prepared in the vacuum state. The population inversion of the atoms can be measured after passing through the cavity. The measured population inversion is affected due to the coupling between the cavity field and the mechanical mirror. Since each mechanical state causes different modification on the signal of the population inversion, the measure data of the population inversion can be used to extract the full state of the mechanical mirror. Our reconstruction scheme can be used to determine both pure and mixed mechanical states.

REFERENCES

[1] E. T. Jaynes and F. W. Cummings, "Comparison of quantum and semiclassical radiation theories with application to the beam maser," *Proceedings of the IEEE*, vol. 51, pp. 89–109, Jan 1963.

[2] J. H. Eberly, N. B. Narozhny, and J. J. Sanchez-Mondragon, "Periodic spontaneous collapse and revival in a simple quantum model," *Phys. Rev. Lett.*, vol. 44, pp. 1323–1326, May 1980.

[3] G. Rempe, H. Walther, and N. Klein, "Observation of quantum collapse and revival in a one-atom maser," *Phys. Rev. Lett.*, vol. 58, pp. 353–356, Jan 1987.

[4] D. Leibfried, R. Blatt, C. Monroe, and D. Wineland, "Quantum dynamics of single trapped ions," *Rev. Mod. Phys.*, vol. 75, pp. 281–324, Mar 2003.

[5] P. Meystre and M. Zubairy, "Squeezed states in the jaynes-cummings model," *Physics Letters A*, vol. 89, no. 8, pp. 390 – 392, 1982.

[6] K. Zaheer and M. S. Zubairy, "Phase sensitivity in atom-field interaction via coherent superposition," *Phys. Rev. A*, vol. 39, pp. 2000–2004, Feb 1989.

[7] D. A. Cardimona, "Effect of atomic-state coherence and spontaneous emission on three-level dynamics," *Phys. Rev. A*, vol. 41, pp. 5016–5025, May 1990.

[8] Y. Yang, J. Xu, G. Li, and H. Chen, "Interactions of a two-level atom and a field with a time-varying frequency," *Phys. Rev. A*, vol. 69, p. 053406, May 2004.

[9] S.-Y. Xie, F. Jia, and Y.-P. Yang, "Interactions of a two-level atom and a field with a time-varying frequency without rotating-wave approximation," *Optics Communications*, vol. 273, no. 2, pp. 451 – 459, 2007.

[10] M. Aspelmeyer, T. J. Kippenberg, and F. Marquardt, "Cavity optomechanics," *Rev. Mod. Phys.*, vol. 86, pp. 1391–1452, Dec 2014.

[11] K. Stannigel, P. Komar, S. J. M. Habraken, S. D. Bennett, M. D. Lukin, P. Zoller, and P. Rabl, "Optomechanical quantum information processing with photons and phonons," *Phys. Rev. Lett.*, vol. 109, p. 013603, Jul 2012.

[12] J. D. Teufel, T. Donner, M. A. Castellanos-Beltran, J. W. Harlow, and K. W. Lehnert, "Nanomechanical motion measured with an imprecision below that at the standard quantum limit," *Nature Nanotechnology*, vol. 4, pp. 820 EP –, 11 2009.

[13] I. Wilson-Rae, N. Nooshi, W. Zwerger, and T. J. Kippenberg, "Theory of ground state cooling of a mechanical oscillator using dynamical backaction," *Phys. Rev. Lett.*, vol. 99, p. 093901, Aug 2007.

[14] F. Marquardt, J. P. Chen, A. A. Clerk, and S. M. Girvin, "Quantum theory of cavity-assisted sideband cooling of mechanical motion," *Phys. Rev. Lett.*, vol. 99, p. 093902, Aug 2007.

[15] A. D. O'Connell, M. Hofheinz, M. Ansmann, R. C. Bialczak, M. Lenander, E. Lucero, M. Neeley, D. Sank, H. Wang, M. Weides, J. Wenner, J. M. Martinis, and A. N. Cleland, "Quantum ground state and single-phonon control of a mechanical resonator," *Nature*, vol. 464, pp. 697 EP –, 03 2010.

[16] J. Chan, T. P. M. Alegre, A. H. Safavi-Naeini, J. T. Hill, A. Krause, S. Gröblacher, M. Aspelmeyer, and O. Painter, "Laser cooling of a nanomechanical oscillator into its quantum ground state," *Nature*, vol. 478, pp. 89 EP –, 10 2011.

[17] J. D. Teufel, T. Donner, D. Li, J. W. Harlow, M. S. Allman, K. Cicak, A. J. Sirois, J. D. Whittaker, K. W. Lehnert, and R. W. Simmonds, "Sideband cooling of micromechanical motion to the quantum ground state," *Nature*, vol. 475, pp. 359 EP –, 07 2011.

[18] T. Rocheleau, T. Ndukum, C. Macklin, J. B. Hertzberg, A. A. Clerk, and K. C. Schwab, "Preparation and detection of a mechanical resonator near the ground state of motion," *Nature*, vol. 463, p. 72, 2009.

[19] E. Verhagen, S. Deléglise, S. Weis, A. Schliesser, and T. J. Kippenberg, "Quantum-coherent coupling of a mechanical oscillator to an optical cavity mode," *Nature*, vol. 482, pp. 63 EP –, 02 2012.

[20] M. Karuza, C. Molinelli, M. Galassi, C. Biancofiore, R. Natali, P. Tombesi, G. D. Giuseppe, and D. Vitali, "Optomechanical sideband cooling of a thin membrane within a cavity," *New Journal of Physics*, vol. 14, no. 9, p. 095015, 2012.

[21] S. Machnes, J. Cerrillo, M. Aspelmeyer, W. Wieczorek, M. B. Plenio, and A. Retzker, "Pulsed laser cooling for cavity optomechanical resonators," *Phys. Rev. Lett.*, vol. 108, p. 153601, Apr 2012.

[22] D. Kleckner, I. Pikovski, E. Jeffrey, L. Ament, E. Eliel, J. van den Brink, and D. Bouwmeester, "Creating and verifying a quantum superposition in a micro-optomechanical system," *New Journal of Physics*, vol. 10, no. 9, p. 095020, 2008.

[23] W. Marshall, C. Simon, R. Penrose, and D. Bouwmeester, "Towards quantum superpositions of a mirror," *Phys. Rev. Lett.*, vol. 91, p. 130401, Sep 2003.

[24] J.-Q. Liao and L. Tian, "Macroscopic quantum superposition in cavity optomechanics," *Phys. Rev. Lett.*, vol. 116, p. 163602, Apr 2016.

[25] W. Ge and M. S. Zubairy, "Macroscopic optomechanical superposition via periodic qubit flipping," *Phys. Rev. A*, vol. 91, p. 013842, Jan 2015.

[26] S. Mancini, V. Giovannetti, D. Vitali, and P. Tombesi, "Entangling macroscopic oscillators exploiting radiation pressure," *Phys. Rev. Lett.*, vol. 88, p. 120401, Mar 2002.

[27] Pinard, M., Dantan, A., Vitali, D., Arcizet, O., Briant, T., and Heidmann, A., "Entangling movable mirrors in a double-cavity system," *Europhys. Lett.*, vol. 72, no. 5, pp. 747–753, 2005.

[28] D. Vitali, S. Gigan, A. Ferreira, H. R. Böhm, P. Tombesi, A. Guerreiro, V. Vedral, A. Zeilinger, and M. Aspelmeyer, "Optomechanical entanglement between a movable mirror and a cavity field," *Phys. Rev. Lett.*, vol. 98, p. 030405, Jan 2007.

[29] K. Børkje, A. Nunnenkamp, and S. M. Girvin, "Proposal for entangling remote micromechanical oscillators via optical measurements," *Phys. Rev. Lett.*, vol. 107, p. 123601, Sep 2011.

[30] C. Genes, D. Vitali, and P. Tombesi, "Emergence of atom-light-mirror entanglement inside an optical cavity," *Phys. Rev. A*, vol. 77, p. 050307, May 2008.

[31] W. Ge, M. Al-Amri, H. Nha, and M. S. Zubairy, "Entanglement of movable mirrors in a correlated-emission laser," *Phys. Rev. A*, vol. 88, p. 022338, Aug 2013.

[32] W. Ge, M. Al-Amri, H. Nha, and M. S. Zubairy, "Entanglement of movable mirrors in a correlated emission laser via cascade-driven coherence," *Phys. Rev. A*, vol. 88, p. 052301, Nov 2013.

[33] W. Ge and M. S. Zubairy, "Entanglement of two movable mirrors with a single photon superposition state," *Physica Scripta*, vol. 90, no. 7, p. 074015, 2015.

[34] Y.-D. Wang and A. A. Clerk, "Reservoir-engineered entanglement in optomechanical systems," *Phys. Rev. Lett.*, vol. 110, p. 253601, Jun 2013.

[35] M. J. Woolley and A. A. Clerk, "Two-mode squeezed states in cavity optomechanics via engineering of a single reservoir," *Phys. Rev. A*, vol. 89, p. 063805, Jun 2014.

[36] J. Li, I. M. Haghighi, N. Malossi, S. Zippilli, and D. Vitali, "Generation and detection of large and robust entanglement between two different mechanical resonators in cavity optomechanics," *New Journal of Physics*, vol. 17, no. 10, p. 103037, 2015.

[37] C. F. Ockeloen-Korppi, E. Damskägg, J. M. Pirkkalainen, M. Asjad, A. A. Clerk, F. Massel, M. J. Woolley, and M. A. Sillanpää, "Stabilized entanglement of massive mechanical oscillators," *Nature*, vol. 556, pp. 478–482, 2018.

[38] M. R. Vanner, I. Pikovski, G. D. Cole, M. S. Kim, Č. Brukner, K. Hammerer, G. J. Milburn, and M. Aspelmeyer, "Pulsed quantum optomechanics," *Proceedings of the National Academy of Sciences*, vol. 108, no. 39, pp. 16182–16187, 2011.

[39] M. R. Vanner, J. Hofer, G. D. Cole, M. Aspelmeyer, A. A. Clerk, and K. C. Schwab, "Preparation and detection of a mechanical resonator near the ground state of motion," *Nat. Commun.*, vol. 2295, p. 4, 2013.

[40] J.-Q. Liao and F. Nori, "Spectrometric reconstruction of mechanical-motional states in optomechanics," *Phys. Rev. A*, vol. 90, p. 023851, Aug 2014.

[41] S. Singh and P. Meystre, "Atomic probe wigner tomography of a nanomechanical system," *Phys. Rev. A*, vol. 81, p. 041804, Apr 2010.

[42] M. O. Scully and M. S. Zubairy, *Quantum Optics*. Cambridge University Press, New York, 1997.

[43] A. Joshi and S. V. Lawande, "Generalized jaynes-cummings models with a time-dependent atom-field coupling," *Phys. Rev. A*, vol. 48, pp. 2276–2284, Sep 1993.

[44] S. Singh, C. H. R. Ooi, and Amrita, "Dynamics for two atoms interacting with intensity-dependent two-mode quantized cavity fields in the ladder configuration," *Phys. Rev. A*, vol. 86, p. 023810, Aug 2012.

[45] S. M. Barnett and P. L. Knight, "Dissipation in a fundamental model of quantum optical resonance," *Phys. Rev. A*, vol. 33, pp. 2444–2448, Apr 1986.

[46] S. M. Barnett, P. Filipowicz, and J. e. a. Javanainen, "Dissipation in a fundamental model of quantum optical resonance," *Frontiers in Quantum Optics*, 1986.

[47] S. M. Barnett and J. Jeffers, "The damped jaynesâĂŞcummings model," *Journal of Modern Optics*, vol. 54, no. 13-15, pp. 2033–2048, 2007.

[48] L.-M. Kuang, X. Chen, G.-H. Chen, and M.-L. Ge, "Jaynes-cummings model with phase damping," *Phys. Rev. A*, vol. 56, pp. 3139–3149, Oct 1997.

[49] O. Romero-Isart, A. C. Pflanzer, F. Blaser, R. Kaltenbaek, N. Kiesel, M. Aspelmeyer, and J. I. Cirac, "Large quantum superpositions and interference of massive nanometer-sized objects," *Phys. Rev. Lett.*, vol. 107, p. 020405, Jul 2011.

[50] A. Kronwald, F. Marquardt, and A. A. Clerk, "Arbitrarily large steady-state bosonic squeezing via dissipation," *Phys. Rev. A*, vol. 88, p. 063833, Dec 2013.

[51] E. E. Wollman, C. U. Lei, A. J. Weinstein, J. Suh, A. Kronwald, F. Marquardt, A. A. Clerk, and K. C. Schwab, "Quantum squeezing of motion in a mechanical resonator," *Science*, vol. 349, no. 6251, pp. 952–955, 2015.

[52] J.-M. Pirkkalainen, E. Damskägg, M. Brandt, F. Massel, and M. A. Sillanpää, "Squeezing of quantum noise of motion in a micromechanical resonator," *Phys. Rev. Lett.*, vol. 115, p. 243601, Dec 2015.

[53] F. Lecocq, J. B. Clark, R. W. Simmonds, J. Aumentado, and J. D. Teufel, "Quantum nondemolition measurement of a nonclassical state of a massive object," *Phys. Rev. X*, vol. 5, p. 041037, Dec 2015.

[54] C. U. Lei, A. J. Weinstein, J. Suh, E. E. Wollman, A. Kronwald, F. Marquardt, A. A. Clerk, and K. C. Schwab, "Quantum nondemolition measurement of a quantum squeezed state beyond the 3 db limit," *Phys. Rev. Lett.*, vol. 117, p. 100801, Aug 2016.

[55] Z.-L. Xiang, S. Ashhab, J. Q. You, and F. Nori, "Hybrid quantum circuits: Superconducting circuits interacting with other quantum systems," *Rev. Mod. Phys.*, vol. 85, pp. 623–653, Apr 2013.

[56] L. Zhou, Y. Han, J. Jing, and W. Zhang, "Entanglement of nanomechanical oscillators and two-mode fields induced by atomic coherence," *Phys. Rev. A*, vol. 83, p. 052117, May 2011.

[57] C. Genes, H. Ritsch, and D. Vitali, "Micromechanical oscillator ground-state cooling via resonant intracavity optical gain or absorption," *Phys. Rev. A*, vol. 80, p. 061803, Dec 2009.

[58] F. Bariani, S. Singh, L. F. Buchmann, M. Vengalattore, and P. Meystre, "Hybrid optomechanical cooling by atomic Λ systems," *Phys. Rev. A*, vol. 90, p. 033838, Sep 2014.

[59] Z. Yi, G. xiang Li, S. ping Wu, and Y. ping Yang, "Ground-state cooling of an oscillator in a hybrid atom-optomechanical system," *Opt. Express*, vol. 22, pp. 20060–20075, Aug 2014.

[60] R.-P. Zeng, S. Zhang, C.-W. Wu, W. Wu, and P.-X. Chen, "Ground-state cooling of an optomechanical resonator assisted by an atomic ensemble," *J. Opt. Soc. Am. B*, vol. 32, pp. 2314–2320, Nov 2015.

[61] H. Ian, Z. R. Gong, Y.-x. Liu, C. P. Sun, and F. Nori, "Cavity optomechanical coupling assisted by an atomic gas," *Phys. Rev. A*, vol. 78, p. 013824, Jul 2008.

[62] Y. Chang, H. Ian, and C. P. Sun, "Triple coupling and parameter resonance in quantum optomechanics with a single atom," *Journal of Physics B: Atomic, Molecular and Optical Physics*, vol. 42, no. 21, p. 215502, 2009.

[63] K. Hammerer, M. Wallquist, C. Genes, M. Ludwig, F. Marquardt, P. Treutlein, P. Zoller, J. Ye, and H. J. Kimble, "Strong coupling of a mechanical oscillator and a single atom," *Phys. Rev. Lett.*, vol. 103, p. 063005, Aug 2009.

[64] J. M. Pirkkalainen, S. U. Cho, F. Massel, J. Tuorila, T. T. Heikkilä, P. J. Hakonen, and M. A. Sillanpää, "Cavity optomechanics mediated by a quantum two-level system," *Nature Communications*, vol. 6, pp. 6981 EP –, 04 2015.

[65] D. Breyer and M. Bienert, "Light scattering in an optomechanical cavity coupled to a single atom," *Phys. Rev. A*, vol. 86, p. 053819, Nov 2012.

[66] Y. Yan, J. pei Zhu, and G. xiang Li, "Preparation of a nonlinear coherent state of the mechanical resonator in an optomechanical microcavity," *Opt. Express*, vol. 24, pp. 13590–13609, Jun 2016.

[67] J. Restrepo, C. Ciuti, and I. Favero, "Single-polariton optomechanics," *Phys. Rev. Lett.*, vol. 112, p. 013601, Jan 2014.

[68] T. Holz, R. Betzholz, and M. Bienert, "Suppression of rabi oscillations in hybrid optomechanical systems," *Phys. Rev. A*, vol. 92, p. 043822, Oct 2015.

[69] H. Pimenta and D. F. V. James, "Characteristic-function approach to the jaynes-cummings-model revivals," *Phys. Rev. A*, vol. 94, p. 053803, Nov 2016.

[70] F. Lecocq, J. D. Teufel, J. Aumentado, and R. W. Simmonds, "Resolving the vacuum fluctuations of an optomechanical system using an artificial atom," *Nature Physics*, vol. 11, pp. 635 EP –, 06 2015.

[71] I. Buluta, S. Ashhab, and F. Nori, "Natural and artificial atoms for quantum computation," *Reports on Progress in Physics*, vol. 74, no. 10, p. 104401, 2011.

[72] C. K. Law, "Interaction between a moving mirror and radiation pressure: A hamiltonian formulation," *Phys. Rev. A*, vol. 51, pp. 2537–2541, Mar 1995.

[73] C. Ventura-Velázquez, B. M. Rodríguez-Lara, and H. M. Moya-Cessa, "Operator approach to quantum optomechanics," *Physica Scripta*, vol. 90, no. 6, p. 068010, 2015.

[74] Z. Yang, C. Bai, X. Meng, and M. Wang, "Sinusoidally modulated vacuum rabi oscillation of a two-level atom in an optomechanical cavity," *arXiv:1507.05448*, 2015.

[75] T. J. Kippenberg and K. J. Vahala, "Cavity optomechanics: Back-action at the mesoscale," *Science*, vol. 321, no. 5893, pp. 1172–1176, 2008.

[76] S. Bose, K. Jacobs, and P. L. Knight, "Preparation of nonclassical states in cavities with a moving mirror," *Phys. Rev. A*, vol. 56, pp. 4175–4186, Nov 1997.

[77] V. M. R., P. Igor, and K. M. S., "Towards optomechanical quantum state reconstruction of mechanical motion," *Annalen der Physik*, vol. 527, no. 1-2, pp. 15–26.

[78] J.-Q. Liao, H. K. Cheung, and C. K. Law, "Spectrum of single-photon emission and scattering in cavity optomechanics," *Phys. Rev. A*, vol. 85, p. 025803, Feb 2012.

[79] M. Brune, S. Haroche, J. M. Raimond, L. Davidovich, and N. Zagury, "Manipulation of photons in a cavity by dispersive atom-field coupling: Quantum-nondemolition measurements and generation of "schrödinger cat" states," *Phys. Rev. A*, vol. 45, pp. 5193–5214, Apr 1992.

[80] P. J. Bardroff, E. Mayr, and W. P. Schleich, "Quantum state endoscopy: Measurement of the quantum state in a cavity," *Phys. Rev. A*, vol. 51, pp. 4963–4966, Jun 1995.

[81] M. Wilkens and P. Meystre, "Nonlinear atomic homodyne detection: A technique to detect macroscopic superpositions in a micromaser," *Phys. Rev. A*, vol. 43, pp. 3832–3835, Apr 1991.

[82] M. S. Zubairy, "Quantum state measurement via autler-townes spectroscopy," *Phys. Lett. A*, vol. 222, p. 91, 1996.

[83] P. J. Bardroff, E. Mayr, and W. P. Schleich, "Simulation of quantum-state endoscopy," *Phys. Rev. A*, vol. 53, pp. 2736–2741, Apr 1996.

[84] M. Freyberger and A. M. Herkommer, "Probing a quantum state via atomic deflection," *Phys. Rev. Lett.*, vol. 72, pp. 1952–1955, Mar 1994.

[85] M. Brune, F. Schmidt-Kaler, A. Maali, J. Dreyer, E. Hagley, J. M. Raimond, and S. Haroche, "Quantum rabi oscillation: A direct test of field quantization in a cavity," *Phys. Rev. Lett.*, vol. 76, pp. 1800–1803, Mar 1996.

[86] K. Jacobs, P. L. Knight, and V. Vedral, "Determining the state of a single cavity mode from photon statistics," *Journal of Modern Optics*, vol. 44, no. 11-12, pp. 2427–2439, 1997.

[87] M. S. Zubairy, "Direct measurement of the quantum state of radiation field from the resonance fluorescence spectrum," *Phys. Rev. A*, vol. 57, pp. 2066–2071, Mar 1998.

[88] T. Azim and M. S. Zubairy, "Measurement of photon statistics via electromagnetically induced transparency," *Physics Letters A*, vol. 250, no. 4, pp. 344 – 348, 1998.

[89] M. Mahmoudi, H. Tajalli, and M. S. Zubairy, "Measurement of the wigner function of a cavity field via autler-townes spectroscopy," *Journal of Optics B: Quantum and Semiclassical Optics*, vol. 2, no. 3, p. 315, 2000.

[90] M. Ahmad, S. Qamar, and M. Suhail Zubairy, "Quantum state measurement using phase-sensitive amplification in a driven three-level atomic system," *Phys. Rev. A*, vol. 64, p. 023811, Jul 2001.

[91] X. Zou, K. Pahlke, and W. Mathis, "Scheme for direct measurement of the wigner characteristic function in cavity qed," *Phys. Rev. A*, vol. 69, p. 015802, Jan 2004.

[92] S. Asiri, W. Ge, and M. S. Zubairy, "Optomechanically induced anomalous population inversion in a hybrid system," *Accepted in J. Phys. A*, 2018.

[93] M. Aspelmeyer, S. Gröblacher, K. Hammerer, and N. Kiesel, "Quantum optomechanics—throwing a glance [invited]," *J. Opt. Soc. Am. B*, vol. 27, pp. A189–A197, Jun 2010.

[94] C. Genes, D. Vitali, P. Tombesi, S. Gigan, and M. Aspelmeyer, "Ground-state cooling of a micromechanical oscillator: Comparing cold damping and cavity-assisted cooling schemes," *Phys. Rev. A*, vol. 77, p. 033804, Mar 2008.

[95] K. H. Lee, T. G. McRae, G. I. Harris, J. Knittel, and W. P. Bowen, "Cooling and control of a cavity optoelectromechanical system," *Phys. Rev. Lett.*, vol. 104, p. 123604, Mar 2010.

[96] M. H. Schleier-Smith, I. D. Leroux, H. Zhang, M. A. Van Camp, and V. Vuletić, "Optomechanical cavity cooling of an atomic ensemble," *Phys. Rev. Lett.*, vol. 107, p. 143005, Sep 2011.

[97] B. Pepper, R. Ghobadi, E. Jeffrey, C. Simon, and D. Bouwmeester, "Optomechanical superpositions via nested interferometry," *Phys. Rev. Lett.*, vol. 109, p. 023601, Jul 2012.

[98] M. Paternostro, D. Vitali, S. Gigan, M. S. Kim, C. Brukner, J. Eisert, and M. Aspelmeyer, "Creating and probing multipartite macroscopic entanglement with light," *Phys. Rev. Lett.*, vol. 99, p. 250401, Dec 2007.

[99] C. Genes, A. Mari, P. Tombesi, and D. Vitali, "Robust entanglement of a micromechanical resonator with output optical fields," *Phys. Rev. A*, vol. 78, p. 032316, Sep 2008.

[100] S. G. Hofer, W. Wieczorek, M. Aspelmeyer, and K. Hammerer, "Quantum entanglement and teleportation in pulsed cavity optomechanics," *Phys. Rev. A*, vol. 84, p. 052327, Nov 2011.

[101] M. J. Hartmann and M. B. Plenio, "Steady state entanglement in the mechanical vibrations of two dielectric membranes," *Phys. Rev. Lett.*, vol. 101, p. 200503, Nov 2008.

[102] J. D. Jost, J. P. Home, J. M. Amini, D. Hanneke, R. Ozeri, C. Langer, J. J. Bollinger, D. Leibfried, and D. J. Wineland, "Entangled mechanical oscillators," *Nature*, vol. 459, pp. 683 – 685, 2009.

[103] J.-Q. Liao, Q.-Q. Wu, and F. Nori, "Entangling two macroscopic mechanical mirrors in a two-cavity optomechanical system," *Phys. Rev. A*, vol. 89, p. 014302, Jan 2014.

APPENDIX A

EFFECTIVE HAMILTONIAN

To obtain the effective Hamiltonian of the hybrid system, we first adopt the interaction picture of the cavity field and the atom, therefore the total Hamiltonian can be rewritten as

$$\mathcal{H}_I = \hbar\frac{\delta}{2}\sigma_z + i\hbar g_c(c^\dagger\sigma_- - \sigma_+ c) + \hbar\omega_m b^\dagger b - \hbar g_m c^\dagger c(b^\dagger + b), \tag{A.1}$$

where $\delta = \omega_a - \omega_c$.

Second, we perform a unitary transformation $\mathcal{T} = e^{-\beta c^\dagger c(b^\dagger - b)}$ as considered in Ref. [76] such that

$$\begin{aligned}
\mathcal{H}_\mathcal{T} &= \mathcal{T}\mathcal{H}_I\mathcal{T}^\dagger \\
&= \hbar\frac{\delta}{2}\sigma_z + i\hbar g_c\left(c^\dagger\mathcal{D}(-\beta)\sigma_- - \sigma_+ c\mathcal{D}(\beta)\right) + \hbar\omega_m b^\dagger b \\
&\approx \hbar\frac{\delta}{2}\sigma_z + i\hbar g_c(c^\dagger\sigma_- - \sigma_+ c) \\
&\quad +\hbar\omega_m b^\dagger b - i\hbar\beta g_c(\sigma_+ c + c^\dagger\sigma_-)(b^\dagger - b),
\end{aligned} \tag{A.2}$$

where the displacement operator $\mathcal{D}(\beta) = e^{\beta(b^\dagger - b)} \approx 1 + \beta(b^\dagger - b)$ for $\beta = g_m/\omega_m \ll 1$ for most of the current optomechanical systems [10]. Under the unitary transformation $\mathcal{T}$, the mechanical mirror is transformed into a displaced basis depending on the photon number of the cavity field. We define the atom-cavity Hamiltonian as $\mathcal{H}_{ac} = \hbar\frac{\delta}{2}\sigma_z + i\hbar g_c(c^\dagger\sigma_- - \sigma_+ c)$ and the hybrid interaction Hamiltonian as $\mathcal{H}_{hd} = -i\hbar\beta g_c(\sigma_+ c + c^\dagger\sigma_-)(b^\dagger - b)$.

Third, we diagonalize $\mathcal{H}_{ac}$ in the dressed state bases of the atom-field subsystem [42]

$$|+,n\rangle = \cos\left(\frac{\alpha_n}{2}\right)|e\rangle_a|n\rangle_c + i\sin\left(\frac{\alpha_n}{2}\right)|g\rangle_a|n+1\rangle_c\,, \tag{A.3}$$

$$|-,n\rangle = \sin\left(\frac{\alpha_n}{2}\right)|e\rangle_a|n\rangle_c - i\cos\left(\frac{\alpha_n}{2}\right)|g\rangle_a|n+1\rangle_c\,, \tag{A.4}$$

where $\tan\alpha_n = 2g_c\sqrt{n+1}/\delta$, $\mathcal{H}_{ac}\,|\pm,n\rangle = \pm\hbar\Omega_n/2\,|\pm,n\rangle$, $\Omega_n = \sqrt{\delta^2 + 4g_c^2(n+1)}$, and $(\sigma_+ c + c^\dagger\sigma_-)\,|\pm,n\rangle = \pm i\sqrt{n+1}\,|\mp,n\rangle$.

We define a new set of Pauli matrices for the polariton states as $\sigma_z^{(n)}\,|\pm,n\rangle = \pm\,|\pm,n\rangle$ and $\sigma_\mp^{(n)}\,|\pm,n\rangle = |\mp,n\rangle$. Therefore, the above Hamiltonian is then given by

$$\begin{aligned}\mathcal{H}_\mathcal{T} &= \sum_{n=1}^{\infty}\left(\hbar\frac{\Omega_n}{2}\sigma_z^{(n)} + \hbar g_{pn}(\sigma_-^{(n)} - \sigma_+^{(n)})(b^\dagger - b)\right) \\ &+ \hbar\omega_m b^\dagger b, \end{aligned} \tag{A.5}$$

where $g_{pn} = \beta g_c\sqrt{n+1}$ is the effective polariton-phonon coupling strength.

APPENDIX B

EQUATIONS OF MOTION FOR THE DENSITY MATRIX ELEMENTS

Here we derive the equations of motion for the density matrix elements. The total Hamiltonian of the hybrid optomechanical system is

$$\mathcal{H}_I = \hbar\frac{\delta}{2}\sigma_z + i\hbar g_c(c^\dagger\sigma_- - \sigma_+ c) + \hbar\omega_m b^\dagger b - \hbar g_m c^\dagger c(b^\dagger + b), \tag{B.1}$$

where $\delta = \omega_a - \omega_c$. The density matrix of the hybrid optomechanical system is given by

$$\hat{\rho}(t) = \sum_{i,j,k,l=0}^{\infty} \rho_{ij,kl}^{i'j'}(t)\left|i'\right\rangle_a \left\langle j'\right|_a \otimes \left|i\right\rangle_c \left\langle k\right|_c \otimes \left|j\right\rangle_m \left\langle l\right|_m, \tag{B.2}$$

where $\left|i'(j')\right\rangle_a$ is the state of the two-level atom with $i', j' \equiv \{g, e\}$. $\left|i(k)\right\rangle_c$ and $\left|j(l)\right\rangle_m$ denote the Fock states of the cavity and the mechanical mirror. We derive the equations of motion for the density matrix elements using the Markovian master equation given by

$$\dot{\rho} = -\frac{i}{\hbar}[\mathcal{H}_I, \rho] + \mathcal{L}_a\rho + \mathcal{L}_c\rho + \mathcal{L}_m\rho, \tag{B.3}$$

where $\mathcal{L}_a\rho$, $\mathcal{L}_c\rho$ and $\mathcal{L}_m\rho$ are the dissipation of the atom, the cavity field and the mechanical mirror. These dissipation terms are given by

$$\mathcal{L}_a\rho = \gamma_a(2\sigma_-\rho\sigma_+ - \sigma_+\sigma_-\rho - \rho\sigma_+\sigma_-), \tag{B.4a}$$

$$\mathcal{L}_c\rho = \gamma_c(2c\rho c^\dagger - c^\dagger c\rho - \rho c^\dagger c), \tag{B.4b}$$

$$\mathcal{L}_m\rho = \gamma_m\bar{n}_{th}(2b^\dagger\rho b - bb^\dagger\rho - \rho bb^\dagger) + \gamma_m(1+\bar{n}_{th})(2b\rho b^\dagger - b^\dagger b\rho - \rho b^\dagger b).$$

Where γ_a, γ_c and γ_m are the dissipation rates for the atom, the cavity field and the mechanical mirror, respectively. The equations of motion are then given by

$$\begin{aligned}
\dot{\rho}^{gg}_{ij,kl}(t) &= g_c\sqrt{i}\,\rho^{eg}_{i-1\,j,k\,l} + i\omega_m(l-j)\rho^{gg}_{i\,j,k\,l} + ig_m i\left(\sqrt{j}\,\rho^{gg}_{i\,j-1,k\,l} + \sqrt{j+1}\,\rho^{gg}_{i\,j+1,k\,l}\right) \\
&+ g_c\sqrt{k}\,\rho^{ge}_{i\,j,k-1\,l} - ig_m k\left(\sqrt{l+1}\,\rho^{gg}_{i\,j,k\,l+1} + \sqrt{l}\,\rho^{gg}_{i\,j,k\,l-1}\right) + 2\gamma_a\,\rho^{ee}_{i\,j,k\,l} \\
&+ \gamma_c\left[2\sqrt{(i+1)(k+1)}\,\rho^{gg}_{i+1\,j,k+1\,l} - (i+k)\,\rho^{gg}_{i\,j,k\,l}\right] \\
&+ \gamma_m\,\bar{n}_{th}\left[2\sqrt{jl}\,\rho^{gg}_{i\,j-1,k\,l-1} - (j+l+2)\,\rho^{gg}_{i\,j,k\,l}\right] \\
&+ \gamma_m(1+\bar{n}_{th})\left[2\sqrt{(j+1)(l+1)}\,\rho^{gg}_{i\,j+1,k\,l+1} - (j+l)\,\rho^{gg}_{i\,j,k\,l}\right], \qquad \text{(B.5a)}
\end{aligned}$$

$$\begin{aligned}
\dot{\rho}^{ee}_{ij,kl}(t) &= -g_c\sqrt{i+1}\,\rho^{ge}_{i+1\,j,k\,l} + i\omega_m(l-j)\,\rho^{ee}_{i\,j,k\,l} + ig_m i\left(\sqrt{j}\,\rho^{ee}_{i\,j-1,k\,l} + \sqrt{j+1}\,\rho^{gg}_{i\,j+1,k\,l}\right) \\
&- g_c\sqrt{k+1}\,\rho^{eg}_{i\,j,k+1\,l} - ig_m k\left(\sqrt{l+1}\,\rho^{ee}_{i\,j,k\,l+1} + \sqrt{l}\,\rho^{ee}_{i\,j,k\,l-1}\right) - 2\gamma_a\,\rho^{ee}_{i\,j,k\,l} \\
&+ \gamma_c\left[2\sqrt{(i+1)(k+1)}\,\rho^{ee}_{i+1\,j,k+1\,l} - (i+k)\,\rho^{ee}_{i\,j,k\,l}\right] \\
&+ \gamma_m\bar{n}_{th}\left[2\sqrt{jl}\,\rho^{ee}_{i\,j-1,k\,l-1} - (j+l+2)\,\rho^{ee}_{i\,j,k\,l}\right] \\
&+ \gamma_m(1+\bar{n}_{th})\left[2\sqrt{(j+1)(l+1)}\,\rho^{ee}_{i\,j+1,k\,l+1} - (j+l)\,\rho^{ee}_{i\,j,k\,l}\right], \qquad \text{(B.5b)}
\end{aligned}$$

$$\begin{aligned}
\dot{\rho}^{ge}_{ij,kl}(t) &= i\delta\rho^{ge}_{i\,j,k\,l} + g_c\sqrt{i}\,\rho^{ee}_{i-1\,j,k\,l} + i\omega_m(l-j)\,\rho^{ge}_{i\,j,k\,l} + ig_m i\left(\sqrt{j}\,\rho^{ge}_{i\,j-1,k\,l} + \sqrt{j+1}\,\rho^{ge}_{i\,j+1,k\,l}\right) \\
&- g_c\sqrt{k+1}\,\rho^{gg}_{i\,j,k+1\,l} - ig_m k\left(\sqrt{l+1}\,\rho^{ge}_{i\,j,k\,l+1} + \sqrt{l}\,\rho^{ge}_{i\,j,k\,l-1}\right) - \gamma_a\,\rho^{ge}_{i\,j,k\,l} \\
&+ \gamma_c\left[2\sqrt{(i+1)(k+1)}\,\rho^{ge}_{i+1\,j,k+1\,l} - (i+k)\,\rho^{ge}_{i\,j,k\,l}\right] \\
&+ \gamma_m\bar{n}_{th}\left[2\sqrt{jl}\,\rho^{ge}_{i\,j-1,k\,l-1} - (j+l+2)\,\rho^{ge}_{i\,j,k\,l}\right] \\
&+ \gamma_m(1+\bar{n}_{th})\left[2\sqrt{(j+1)(l+1)}\,\rho^{ge}_{i\,j+1,k\,l+1} - (j+l)\,\rho^{ge}_{i\,j,k\,l}\right]. \qquad \text{(B.5c)}
\end{aligned}$$

Where $\dot{\rho}^{gg}_{ij,kl}(t) = \langle g,i,j|\dot{\rho}|g,k,l\rangle$, $\dot{\rho}^{ee}_{ij,kl}(t) = \langle e,i,j|\dot{\rho}|e,k,l\rangle$, and $\dot{\rho}^{ge}_{ij,kl}(t) = \langle g,i,j|\dot{\rho}|e,k,l\rangle$. To see the effect of the atomic, the cavity field and the mechanical mirror dissipation on the evolution of the population inversion in the hybrid

optomechanical system, we numerically solve the Markovian master equation along with the dissipation terms. We then plot the numerical results of the population inversion using Eq. (B.3) in Figs. (2-5) along with the analytical results. We find the anomalous population inversion is preserved while its amplitude is suppressed when taking the dissipation into account.

APPENDIX C

DERIVATION OF THE EXCITED STATE POPULATION WHEN THE MIRROR IS IN A THERMAL STATE

In this appendix we derive the excited state population of the atom when the mechanical mirror is initially in a mixed state $\rho^m(0)$ while the atom is in the excited state and the cavity field is in a Fock state. Because the mechanical mirror is in a mixed state, we need to analytically solve the Markovian master equation given below in order to get the density operator of the excited state population

$$\dot{\rho} = -\frac{i}{\hbar}[\mathcal{V}, \rho], \tag{C.1}$$

where $\mathcal{V}(t)$ is the Hamiltonian in the interaction picture which can be written as

$$\mathcal{V}(t) = U_0^{\dagger}(t)\mathcal{H}_I U_0(t), \tag{C.2}$$

where

$$U_0(t) = exp\left(-\frac{i}{\hbar}\mathcal{H}_0 t\right) \tag{C.3}$$

and

$$\mathcal{H}_0 = \hbar\omega_m b^{\dagger}b + \sum_{n=1}^{\infty}\hbar\frac{\Omega_n}{2}\sigma_z^{(n)}. \tag{C.4}$$

Applying the same procedure as in [42], the interaction picture Hamiltonain is then given by the following expression

$$\mathcal{V} = \sum_{n=1}^{\infty}\hbar g_{pn}\left[\sigma_-^{(n)}b^{\dagger}e^{i(\omega_m-\Omega_n)t} - \sigma_+^{(n)}be^{-i(\omega_m-\Omega_n)t}\right]. \tag{C.5}$$

The initial state of the system can be written as

$$\rho(0) = \rho^p(0) \otimes \rho^m(0) \tag{C.6}$$

where $\rho^p(0)$ is the initial state of the polariton and it is given by

$$\rho^p(0) = \begin{pmatrix} \rho^p_{++}(0) & \rho^p_{+-}(0) \\ \\ \rho^p_{-+}(0) & \rho^p_{--}(0) \end{pmatrix} = \begin{pmatrix} \cos^2\left(\frac{\alpha_n}{2}\right) & \cos\left(\frac{\alpha_n}{2}\right)\sin\left(\frac{\alpha_n}{2}\right) \\ \\ \cos\left(\frac{\alpha_n}{2}\right)\sin\left(\frac{\alpha_n}{2}\right) & \cos^2\left(\frac{\alpha_n}{2}\right) \end{pmatrix} \tag{C.7}$$

The formal solution of Eq. (C.1) can be written as

$$\rho(t) = U(t)\rho(0)U^\dagger(t), \tag{C.8}$$

where $U(t)$ is the evolution operator of the system and it is given by

$$\begin{aligned} U(t) = A\left|+,n\right\rangle\left\langle+,n\right| + B\left|-,n\right\rangle\left\langle-,n\right| \\ + C\left|+,n\right\rangle\left\langle-,n\right| + D\left|-,n\right\rangle\left\langle+,n\right|, \end{aligned} \tag{C.9}$$

where

$$A = \cos\left(g_{pn}\sqrt{bb^\dagger}\ t\right), \tag{C.10a}$$

$$B = \cos\left(g_{pn}\sqrt{b^\dagger b}\ t\right), \tag{C.10b}$$

$$C = -ib\frac{\cos\left(g_{pn}\sqrt{b^\dagger b}\ t\right)}{\sqrt{b^\dagger b}}, \tag{C.10c}$$

$$D = -ib^\dagger\frac{\cos\left(g_{pn}\sqrt{bb^\dagger}\ t\right)}{\sqrt{bb^\dagger}}. \tag{C.10d}$$

In order to calculate the excited state population $P_e(t)$, we first transform the state $|e,n\rangle$ which is given by

$$\left|e,n\right\rangle = \cos\left(\frac{\alpha_n}{2}\right)\left|+,n\right\rangle + \sin\left(\frac{\alpha_n}{2}\right)\left|-,n\right\rangle, \tag{C.11}$$

to the interaction picture using

$$\left|e,n\right\rangle_I = U_0^\dagger(t)\left|e,n\right\rangle. \tag{C.12}$$

For $\delta = 0$ and $\Omega_n = \omega_m$, the previous transformation gives

$$|e,n\rangle_I = \frac{1}{\sqrt{2}} e^{i\omega_m b^\dagger b t} \left(e^{i\omega_m t/2} |+,n\rangle + e^{-i\omega_m t/2} |-,n\rangle \right). \tag{C.13}$$

From (C.13), the excited state population is given by

$$P_e(t) = \frac{1}{2}\left[\rho^p_{++}(t) + \rho^p_{--}(t) + e^{i\omega_m t}\, \rho^p_{+-}(t) + e^{-i\omega_m t}\, \rho^p_{-+}(t) \right]. \tag{C.14}$$

The density matrix elements of the polariton states in the previous equation can be calculated from the following equations

$$\rho^p_{++}(t) = \frac{1}{2} \sum_{l=1}^{\infty} \langle l| A\rho^m(0)A + C\rho^m(0)A - A\rho^m(0)D - C\rho^m(0)D |l\rangle , \tag{C.15a}$$

$$\rho^p_{--}(t) = \frac{1}{2} \sum_{l=1}^{\infty} \langle l| - D\rho^m(0)C - B\rho^m(0)C + D\rho^m(0)B + B\rho^m(0)B |l\rangle , \tag{C.15b}$$

$$\rho^p_{+-}(t) = \frac{1}{2} \sum_{l=1}^{\infty} \langle l| - A\rho^m(0)C - C\rho^m(0)C + A\rho^m(0)B + C\rho^m(0)B |l\rangle , \tag{C.15c}$$

$$\rho^p_{-+}(t) = \frac{1}{2} \sum_{l=1}^{\infty} \langle l| D\rho^m(0)A + B\rho^m(0)A - D\rho^m(0)D - B\rho^m(0)D |l\rangle . \tag{C.15d}$$

If we consider that the mechanical mirror is initially prepared in incoherent mixture i. e., $\rho^m(0) = \sum_{l=0}^{\infty} p_l |l\rangle \langle l|$, then excited state population when $\Omega_n = \omega_m$ reduces to the following equation

$$P_e(t) = \sum_{l=0}^{\infty} p_l \left[\frac{1}{2} + \frac{1}{2} \cos(\omega_m t) \cos\left(g_{pn}\sqrt{l}t \right) \cos\left(g_{pn}\sqrt{l+1} \right) \right]. \tag{C.16}$$

APPENDIX D

DERIVATION OF THE EXCITED STATE POPULATION FOR THE COHERENT CAVITY FIELD

We consider that the mechanical mirror interacts non-resonantly with a single polariton state $|\pm, n\rangle$. The time-dependent state vector is given by

$$|\psi_T(t)\rangle = \sum_{k=l-1}^{l} c_k^+ |+, n\rangle |k\rangle + \sum_{k=l}^{l+1} c_k^- |-, n\rangle |k\rangle . \tag{D.1}$$

We derive from Schrödinger's equation (2.7) the time evolution of the state vector coefficients as

$$\dot{c}_k^+ = -i\left(\omega_m k + \frac{\Omega_n}{2}\right) c_k^+ - ig_{pn}\sqrt{k+1}c_{k+1}^-, \tag{D.2a}$$

$$\dot{c}_{k+1}^- = -i\left(\omega_m (k+1) - \frac{\Omega_n}{2}\right) c_{k+1}^- - ig_{pn}\sqrt{k+1}c_k^+, \tag{D.2b}$$

The solutions to Eqs. (D.2) are

$$c_k^+(t) = e^{-i\omega_m(k+\frac{1}{2})t}\left[c_k^+(0)\cos\left(\frac{\omega_{nk}}{2}t\right) - i\frac{\Delta_n}{\omega_{nk}}c_k^+(0)\sin\left(\frac{\omega_{nk}}{2}t\right)\right.$$
$$\left. - 2i\frac{g_{pn}\sqrt{k+1}}{\omega_{nk}}c_{k+1}^-(0)\sin\left(\frac{\omega_{nk}}{2}t\right)\right], \tag{D.3a}$$

$$c_{k+1}^-(t) = e^{-i\omega_m(k+\frac{1}{2})t}\left[c_{k+1}^-(0)\cos\left(\frac{\omega_{nk}}{2}t\right) + i\frac{\Delta_n}{\omega_{nk}}c_{k+1}^-(0)\sin\left(\frac{\omega_{nk}}{2}t\right)\right.$$
$$\left. - 2i\frac{g_{pn}\sqrt{k+1}}{\omega_{nk}}c_k^+(0)\sin\left(\frac{\omega_{nk}}{2}t\right)\right]. \tag{D.3b}$$

Where $\Delta_n = \Omega_n - \omega_m$ and $\omega_{nk} = \sqrt{\Delta_n^2 + 4g_{pn}^2(k+1)}$. The population of the excited states can then be calculated using

$$P_e(t) = \sum_{n=0}^{\infty}\sum_{k=l-1}^{l+1}\left|c_k^+(t)\cos\left(\frac{\alpha_n}{2}\right) + c_k^-(t)\sin\left(\frac{\alpha_n}{2}\right)\right|^2, \tag{D.4}$$

which gives the expression of the nonresonant case in Eq. (2.33) using the initial conditions $c_{l-1}^{+}(0) = C_n^c \cos\left(\frac{\alpha_n}{2}\right) \beta n\sqrt{l}, c_{l-1}^{-}(0) = C_n^c \sin\left(\frac{\alpha_n}{2}\right) \beta n\sqrt{l}, c_l^{-}(0) = C_n^c \sin\left(\frac{\alpha_n}{2}\right), c_l^{+}(0) = C_n^c \cos\left(\frac{\alpha_n}{2}\right)$, $c_{l+1}^{-}(0) = -C_n^c \sin\left(\frac{\alpha_n}{2}\right) \beta n\sqrt{l+1}$, and $c_{l+1}^{+}(0) = -C_n^c \cos\left(\frac{\alpha_n}{2}\right) \beta n\sqrt{l+1}$. The contribution due to the resonant interaction between the mechanical mirror and the polariton states $|\pm, s\rangle$ is given by

$$P_e^s(t) = \frac{1}{2}\left[1 + \cos\left(\Omega_s t\right) \cos\left(g_{ps}\sqrt{l}t\right) \cos\left(g_{ps}\sqrt{l+1}t\right)\right]. \tag{D.5}$$

The contribution due to the non-resonant interaction between the mechanical mirror and the other atom-field polariton states $|\pm, n \neq s\rangle$ is given by

$$\begin{aligned} P_e^n(t) =& \frac{1}{2}\left\{\frac{1}{2}\cos^2\left(\frac{\omega_{nl}}{2}t\right) + \frac{1}{2}\left(\frac{\Delta_n}{\omega_{nl}}\right)^2 \sin^2\left(\frac{\omega_{nl}}{2}t\right) + \frac{1}{2}\cos^2\left(\frac{\omega_{nl-1}}{2}t\right) + \frac{1}{2}\left(\frac{\Delta_n}{\omega_{nl-1}}\right)^2 \sin^2\left(\frac{\omega_{nl-1}}{2}t\right)\right. \\ &+ \cos\left(\omega_m t\right)\left[\cos\left(\frac{\omega_{nl}}{2}t\right)\cos\left(\frac{\omega_{nl-1}}{2}t\right) - \frac{\Delta_n^2}{\omega_{nl}\omega_{nl-1}}\sin\left(\frac{\omega_{nl}}{2}t\right)\sin\left(\frac{\omega_{nl-1}}{2}t\right)\right] \\ &- \sin\left(\omega_m t\right)\left[\frac{\Delta_n}{\omega_{nl-1}}\cos\left(\frac{\omega_{nl}}{2}t\right)\sin\left(\frac{\omega_{nl-1}}{2}t\right) + \frac{\Delta_n}{\omega_{nl}}\sin\left(\frac{\omega_{nl}}{2}t\right)\cos\left(\frac{\omega_{nl-1}}{2}t\right)\right] \\ &\left. + 2g_{pn}^2\left[\frac{l}{\omega_{nl-1}^2}\sin^2\left(\frac{\omega_{nl-1}}{2}t\right) + \frac{(l+1)}{\omega_{nl}^2}\sin^2\left(\frac{\omega_{nl}}{2}t\right)\right]\right\}, \end{aligned} \tag{D.6}$$

where $\delta = 0$ is assumed for simplicity, $\Delta_n \equiv \Omega_n - \omega_m$ represents the detuning between the mechanical frequency and the polariton state $|\pm, n\rangle$, and $\omega_{nl} = \sqrt{\Delta_n^2 + 4g_{pn}^2(l+1)}$.

APPENDIX E

DERIVATION OF THE EXCITED STATE POPULATION WHEN THE MIRROR IS IN A THERMAL STATE

It can be shown using (4.11) that the density matrix elements of the polariton states in (4.12) can be calculated using the following equations [92]

$$\rho^p_{++}(t) = \frac{1}{2}\sum_{l=1}^{\infty} \langle l| A\rho^m(0)A + C\rho^m(0)A - A\rho^m(0)D - C\rho^m(0)D |l\rangle , \tag{E.1a}$$

$$\rho^p_{--}(t) = \frac{1}{2}\sum_{l=1}^{\infty} \langle l| - D\rho^m(0)C - B\rho^m(0)C + D\rho^m(0)B + B\rho^m(0)B |l\rangle , \tag{E.1b}$$

$$\rho^p_{+-}(t) = \frac{1}{2}\sum_{l=1}^{\infty} \langle l| - A\rho^m(0)C - C\rho^m(0)C + A\rho^m(0)B + C\rho^m(0)B |l\rangle , \tag{E.1c}$$

$$\rho^p_{-+}(t) = \frac{1}{2}\sum_{l=1}^{\infty} \langle l| D\rho^m(0)A + B\rho^m(0)A - D\rho^m(0)D - B\rho^m(0)D |l\rangle , \tag{E.1d}$$

Where the operators A, B, C, and D are given by [92]

$$A = \cos\left(g_{pn}\sqrt{bb^\dagger}\; t\right), \tag{E.2a}$$

$$B = \cos\left(g_{pn}\sqrt{b^\dagger b}\; t\right), \tag{E.2b}$$

$$C = -ib\frac{\cos\left(g_{pn}\sqrt{b^\dagger b}\; t\right)}{\sqrt{b^\dagger b}}, \tag{E.2c}$$

$$D = -ib^\dagger\frac{\cos\left(g_{pn}\sqrt{bb^\dagger}\; t\right)}{\sqrt{bb^\dagger}}. \tag{E.2d}$$

It follows that the density matrix elements of the polariton states are given by

$$\rho^p_{++}(t) = \frac{1}{2}\sum_{l=0}^{\infty}\Bigg[\cos^2\Big(g_{pn}\sqrt{l+1}t\Big)\,\langle l|\,\rho^m(0)\,|l\rangle + i\sin\Big(g_{pn}\sqrt{l+1}t\Big)\cos\Big(g_{pn}\sqrt{l+1}t\Big) \times\Big(\,\langle l|\,\rho^m(0)\,|l+1\rangle - \langle l+1|\,\rho^m(0)\,|l\rangle\,\Big) + \sin^2\Big(g_{pn}\sqrt{l+1}t\Big)\,\langle l+1|\,\rho^m(0)\,|l+1\rangle\Bigg], \tag{E.3a}$$

$$\rho^p_{--}(t) = \frac{1}{2}\sum_{l=0}^{\infty}\Bigg[\Big(\sin^2\Big(g_{pn}\sqrt{l+1}t\Big) + \cos^2\Big(g_{pn}\sqrt{l}t\Big)\Big)\,\langle l|\,\rho^m(0)\,|l\rangle - i\sin\Big(g_{pn}\sqrt{l+1}t\Big)\cos\Big(g_{pn}\sqrt{l+1}t\Big)\Big(\,\langle l|\,\rho^m(0)\,|l+1\rangle - \langle l+1|\,\rho^m(0)\,|l\rangle\,\Big)\Bigg], \tag{E.3b}$$

$$\begin{aligned}\rho^p_{+-}(t) =& \frac{1}{2}\sum_{l=0}^{\infty}\Bigg[i\cos\Big(g_{pn}\sqrt{l+2}t\Big)\sin\Big(g_{pn}\sqrt{l+1}t\Big)\,\langle l+1|\,\rho^m(0)\,|l\rangle \\ &+ \sin\Big(g_{pn}\sqrt{l+2}t\Big)\sin\Big(g_{pn}\sqrt{l+1}t\Big)\,\langle l+2|\,\rho^m(0)\,|l\rangle \\ &+ \cos\Big(g_{pn}\sqrt{l+1}t\Big)\cos\Big(g_{pn}\sqrt{l}t\Big)\,\langle l|\,\rho^m(0)\,|l\rangle \\ &- i\sin\Big(g_{pn}\sqrt{l+1}t\Big)\cos\Big(g_{pn}\sqrt{l}t\Big)\,\langle l+1|\,\rho^m(0)\,|l\rangle\Bigg],\end{aligned} \tag{E.3c}$$

$$\begin{aligned}\rho^p_{-+}(t) =& \frac{1}{2}\sum_{l=0}^{\infty}\Bigg[-i\cos\Big(g_{pn}\sqrt{l+2}t\Big)\sin\Big(g_{pn}\sqrt{l+1}t\Big)\,\langle l|\,\rho^m(0)\,|l+1\rangle \\ &+ \cos\Big(g_{pn}\sqrt{l}t\Big)\cos\Big(g_{pn}\sqrt{l+1}t\Big)\,\langle l|\,\rho^m(0)\,|l\rangle \\ &+ \sin\Big(g_{pn}\sqrt{l+2}t\Big)\sin\Big(g_{pn}\sqrt{l+1}t\Big)\,\langle l|\,\rho^m(0)\,|l+2\rangle \\ &+ i\sin\Big(g_{pn}\sqrt{l+1}t\Big)\cos\Big(g_{pn}\sqrt{l}t\Big)\,\langle l|\,\rho^m(0)\,|l+1\rangle\Bigg].\end{aligned} \tag{E.3d}$$